2013

THE ULTRASONIC PULSE-ECHO IMMERSION TECHNIQUE AND ATTENUATION COEFFICIENT OF PARTICULATE COMPOSITES

Miguel Angel Goni Rodrigo
University of Rhode Island, mgoni@my.uri.edu

THE ULTRASONIC PULSE-ECHO IMMERSION TECHNIQUE AND ATTENUATION COEFFICIENT OF PARTICULATE COMPOSITES

BY

MIGUEL ANGEL GOÑI RODRIGO

A THESIS SUBMITTED IN PARTIAL FULFILLMENT OF THE

REQUIREMENTS FOR THE DEGREE OF

MASTER OF SCIENCE

IN

MECHANICAL ENGINEERING AND APPLIED MECHANICS

UNIVERSITY OF RHODE ISLAND

2013

MASTER OF SCIENCE THESIS

OF

MIGUEL ANGEL GOÑI RODRIGO

APPROVED:

Thesis Committee:

Major Professor Carl-Ernst Rousseau

David Taggart

Arun Shukla

Michael Greenfield

Nasser H. Zawia
DEAN OF THE GRADUATE SCHOOL

UNIVERSITY OF RHODE ISLAND
2013

ABSTRACT

This thesis comprises two main sections, namely a critical evaluation of the use of the Ultrasonic pulse echo immersion technique to measure attenuation and an application of the same to particulate composites. The former consisted of testing the main assumptions adopted by the different approaches developed to carry out the attenuation coefficient measurement. The first assumption states that a perfectly bonded interface between water and specimen exists. A second assumption requires consistent reflection coefficients every time the specimen is immersed. Finally, some existing methods assume equal reflection coefficients on either side of any specimen during a particular immersion. Herein, it is experimentally shown that while these conditions hold true for some materials (i.e. Polycarbonate), they are nevertheless violated for others (some hydrophobic materials). The materials that violate all three assumptions are more likely to be those that present hydrophobic surfaces. Due to their hydrophobicity the bond between water and the specimen is very weak and random distributions of air molecules can be trapped and retained over the surfaces during the immersion. In these cases, all current techniques would provide erroneous values for the attenuation coefficient. Therefore, a new method was proposed, tested and validated to measure the attenuation coefficient of these special materials and any others. A new methodology having been derived, it was then applied to glass/epoxy particulate composites where longitudinal wave speeds and attenuation coefficients were measured for several specimens with different solid glass microspheres and different volume fractions. Contrary to expectations, it was observed that the presence

of microspheres is not always beneficial, if an increase in the attenuation coefficient is desired, and often adversely affects the behavior of the matrix.

ACKNOWLEDGMENTS

I would like to strongly thank my major advisor, Dr. Carl-Ernst Rousseau, for the opportunity, freedom, constant support and sincere belief he provided me during all the research. His natural honesty and willingness to help on any type of matter is sincerely appreciated, recognized and encouraged to stay the same way, since those values are excellent sources of happiness for everyone. It has been a very rich experience to work with him in his lab and I have much to thank him for. I would also like to thank all the other people who have contributed towards the completion of this work. In the first place, I want to thank all the different faculty members that have enormously extended my knowledge in this wonderful major field known as mechanical engineering. In special, I would like to thank Dr. Martin Sadd for all the knowledge provided on Theory of Elasticity and Wave Motion and for the great moments shared while working with him as a Teaching Assistant. In addition, I would like to thank Dr. Arun Shukla and Dr. Hamouda Ghonem for sharing some of their vast knowledge and for the interaction with their respective labs. In the second place, I would like to thank the department staff that was so helpful at many moments and certainly contributed to the development of this thesis: the technicians, Jim Byrnes and Rob D'Ambrosca, the machinists Joe Gomez and David Ferreira for their valuable instructions on the machining field and also Jen Cerullo, Nancy Dubee and Brittany Mathews for their help and sympathy. In addition, I want to greatly thank my labmate Gifford Plume for all the help, ideas and shock wave lectures he provided me and my colleagues Will and Justin for all their suggestions and great moments. Before

figuratively leaving the university world, I want to express special gratitude to Dr. Jin-Yeon Kim from Georgia Institute of Technology for all his time and all the lessons on ultrasonic transducers and attenuation, which were crucial at some stages of this thesis.

Also, I want to thank my family for especially having allowed me to spend as much time as I needed on my studies from an early age and for all the support received during my university years.

Finally, I would like to specially thank my best friend, Helen, for her huge mental and emotional support throughout my entire time at University, including this thesis, and for being responsible for much of what I am today. I can say I have learned from her as much as what I have learned in University and it is an absolute privilege to know somebody like her.

TABLE OF CONTENTS

LIST OF FIGURES

FIGURE **PAGE**

CHAPTER 1

INTRODUCTION

Ultrasonic Testing (UT) is one of the most widely used techniques in Non Destructive Testing (NDT). Non destructive testing, alternatively known as Non Destructive Evaluation (NDE), is a technique used to detect and evaluate defects in components, systems and materials as well as to carry out dimensional measurements and material characterization without causing damage. For example, NDT is used to detect surface and internal cracks, cavities, detached layers, material inconsistencies, hardness deviation and is also used to measure material properties such as elastic and viscolelastic moduli, wave speeds and attenuation. It can also be used to measure object and layer thicknesses. NDT encompasses multiple techniques that allow it to fulfill all these functions. Among them are: Acoustic Emission Testing (AET), Electromagnetic Testing (ET), Acoustic Resonance Testing (ART), Infrared Testing (IT), Leak Testing (LT), Magnetic Particle Testing (MPT), Ultrasonic Testing (UT) and Radiographic Testing (RT). The technique treated in this thesis falls within ultrasonic testing group. UT is an interesting engineering tool because of its wide range of capabilities, ease of use and an absence of damage to the system or material under study.

The fundamental physics behind UT consist on sending a finite mechanical pulse into an object or material and measuring the pulses that come out of the object or material as a consequence of the interaction between the initial pulse and the object or

material. This mechanical pulse is merely a stress wave, a mechanical perturbation of the medium that propagates within it. This is easily comparable with sound. For instance, when an animal issues a call its vocal cords vibrate and perturb the surrounding air. This perturbation propagating through air is known as sound and the speed at which it propagates is known as sound speed. Likewise, everyone has experienced the phenomenon called echo, wherein sound reflects as it reaches a wall. The physics behind this phenomenon are very similar to those of UT. The only difference is that the media in which the mechanical pulse from UT propagates will be mostly solid materials as opposed to air. As it happens with the sound when it bumps into a wall, when the mechanical pulse travelling in a solid material bumps into a crack it will be reflected. This is the basic principle for the flaw detection application of UT [1-8]. In a similar manner reflected pulses off exterior walls can be measured and analyzed in flawless materials to calculate mechanical properties of that material, such as material moduli, wave speeds or attenuation [9-16].

Having accurate values of the parameters that define an engineering system is crucial to the success of the final stage of any design. For instance, having an accurate value of the yield strength of a given material allows for efficient designs and safe structures. Knowledge of the precise value of the thermal conductivity of an insulating material allows engineers to calculate the amount of insulation required to keep buildings warm longer during the winter. Also, having the correct value of the lift coefficient will result on the construction of efficient wings for airplanes and windmills. Thus, developing techniques and methods that can accurately measure

parameters involved in physical systems such as the above mentioned is extremely important.

In the case of viscoelastic materials like polymers, the attenuation coefficient is one of the main parameters that characterize such materials. Therefore, it will very likely be present in any design involving viscoelasticity.

The attenuation coefficient as perceived in this study is a property of matter that describes the amplitude decrease rate with distance of a wave as it travels through a material. Its dimensions are, indeed, dB/unit length or Np/unit length. It can also be interpreted as the energy loss in a wave with propagation distance.

It is typically shown how the attenuation coefficient concept is born after trying harmonic solutions of the type

$$u(\bar{x},t) = u_0 e^{i(k\bar{x}-wt)} \tag{1.1}$$

as solutions to the governing equation of a wave propagation problem in a viscoelastic material [17, 18]. The procedure in these cases consists of introducing the harmonic Equation (1.1) in the governing equation and solving for parameter *k*. In a viscoelastic material this parameter *k* will be an imaginary number. It is, indeed, the imaginary part of this parameter *k* what composes the attenuation coefficient, since once *k* is substituted in Equation (1.1) its imaginary part will become real after being multiplied

by the imaginary unit *i* already present in Equation (1.1). An example showing this will be presented shortly after an important clarification is made.

The attenuation coefficient property must not be confused with the concept of attenuation. Generally, any type of wave amplitude decrease, energy loss or any property´s magnitude decay with time or distance can be called attenuation. The causes for these phenomena can be diverse. For instance, the general solution to the classical wave equation in spherical coordinates (1.2) is given by Equation (1.3):

$$\nabla^2\Phi = \frac{1}{c^2}\frac{\partial^2\Phi}{\partial t^2} \tag{1.2}$$

$$\phi(r,\theta,\psi,t) = r^{-1/2}\begin{Bmatrix} J_{\gamma+1/2}(\alpha r) \\ Y_{\gamma+1/2}(\alpha r) \end{Bmatrix}\left\{P_\gamma^\beta(\cos\theta)\right\}\begin{Bmatrix} \sin(\beta\psi) \\ \cos(\beta\psi) \end{Bmatrix}\begin{Bmatrix} \sin(c\alpha t) \\ \cos(c\alpha t) \end{Bmatrix} \tag{1.3}$$

where *c* is the wave speed, *t* represents time, *r*, θ and Ψ are the spherical coordinates, *J* and *Y* are Bessel functions of order $\gamma + 1/2$, P_γ^β is the associated Legendre function of degree β and order γ and γ, β and α are constants.

As it can be seen, the initial terms of the solution originate a decrease in amplitude of the wave as it travels along coordinate *r*. This decrease in wave amplitude can be called attenuation but is unrelated to the previously defined attenuation coefficient.

The attenuation observed in Equation (1.3) is a characteristic of the problem under study but it does not depend on the medium in which the wave is propagating.

The attenuation coefficient analyzed in this thesis refers to a property of a material that causes a wave amplitude decrease (or energy loss) with distance through different mechanisms specific to that material. The two main mechanisms that form the attenuation coefficient are called absorption and scattering. The absorption term has also been named internal friction in the past. It refers to the energy absorbed by the material that is usually converted to heat. The scattering phenomenon will appear and will be significant in this study with particulate composites, in which the particles embedded inside the matrix will deflect and locally trap the wave causing additional attenuation.

Consider a simple one dimensional problem that will further clarify the concept of the attenuation coefficient. Let a rod be made of a viscoelastic material and at the same time consider one dimensional motion in the x direction and no externally applied forces. Using Newton's second law with these conditions provides,

$$\rho \frac{\partial^2 u}{\partial t^2} = \frac{\partial \sigma}{\partial x} \tag{1.4}$$

where ρ is the density, u the displacement in the x-dir and σ is the stress.

The stress-strain relation for a viscoelastic material can be written as

$$\sigma = E^* \varepsilon = E^* \frac{\partial u}{\partial x} \tag{1.5}$$

where $E^* = E' + iE''$ is a complex number called the dynamic modulus composed of the storage modulus E' and the loss modulus E''.

Introducing the stress-strain relation in Equation (1.4) gives

$$\frac{\partial^2 u}{\partial t^2} = \frac{E^*}{\rho}\frac{\partial^2 u}{\partial x^2} \tag{1.6}$$

Equation (1.6) is called the governing equation.

Now consider the trial solution of the type,

$$u(x,t) = u_0 e^{i(kx-wt)} \tag{1.7}$$

Using this trial solution in the governing equation results in

$$\omega^2 u_0 = k^2 u_0 \frac{E^*}{\rho} \rightarrow k = \frac{\omega}{\sqrt{\frac{E^*}{\rho}}} = \frac{\omega}{\sqrt{\frac{E' + iE''}{\rho}}} = \frac{\omega}{\sqrt{\frac{E'}{\rho}(1 + i\tan\delta)}} \tag{1.8}$$

where $\tan\delta = \frac{E''}{E'}$ by definition.

Suppose tan δ is small. Next expand the square root using Taylor series and only retain the lowest order terms

$$k \approx \frac{\omega}{\sqrt{\frac{E'}{\rho}}}\left(1 + i\frac{1}{2}\tan\delta\right) \tag{1.9}$$

Bringing this solution of k back to trial solution (1.7) it can be seen how its imaginary part will become a real exponential of the type

$$e^{-\alpha x} \quad \text{where } \alpha \approx \frac{\omega}{\sqrt{\frac{E'}{\rho}}}\frac{1}{2}\tan\delta \tag{1.10}$$

The variable α is the attenuation coefficient. One of the main characteristics that can be seen from this expression is its dependence on the frequency (ω) of the wave. This dependence of the attenuation coefficient on frequency will be experimentally shown throughout this thesis. In addition to this, the attenuation coefficient also depends on other variables such as temperature or microstructure. However, these latter factors will not be considered in this work.

Now that the concept of attenuation coefficient is elucidated, it is time to find out how it can be obtained for a particular material so that it can later be used in the final stage of a specific engineering design. First, one could think of a classic engineering method consisting of applying a dynamic load to a specific material´s specimen and measuring the stress and the strain. In fact, materials that present viscoelasticity will show a delay between the applied stress and the corresponding strain. This delay is directly related to the attenuation coefficient [17]. Therefore, applying a dynamic load of a certain frequency could be used to measure the attenuation coefficient corresponding to that frequency. This method could be of practical use for low frequencies. However, if there is interest in measuring the attenuation coefficient for high frequencies of the order of MHz, the suggested method would become impractical.

A very common group of solutions used to solve this problem at high frequencies is ultrasonic techniques. Ultrasonic transducers can generate high frequency (order of MHz) mechanical pulses that are introduced into the material. These pulses are

received back into the transducer after they have travelled through the material and changes in those pulses can be analyzed to calculate the attenuation coefficient. One of the most popular techniques within this group of ultrasonic techniques is the Ultrasonic Pulse-Echo Immersion Technique. This technique will be thoroughly examined in this thesis and is explained with full detail in the Theory section.

An interesting application for the attenuation coefficient measurement at high frequencies is particulate composites. Particulate composites are relatively recent materials that consist of particles of a material A (typically ceramics or metals) embedded in a matrix of a material B (typically a polymer). Regarding the present study, the particulate composites under investigation consist of solid spherical glass particles embedded in an epoxy matrix. As it happens in all other composites, the goal of the particles is to improve the properties of the epoxy matrix with respect to aspects that are weaker than desired. Thus, the solid glass microspheres increase the mechanical strength and stiffness of the matrix. At the same time the matrix complements the properties of the glass by providing the ductility, toughness and low density of a polymer like epoxy. Another interesting characteristic of these particulate composites is the effect of the particles on the attenuation coefficient of the composite material. In this thesis, an experimental study of these effects will be performed by means of the ultrasonic pulse echo immersion technique. Different particle sizes and particle volume fractions will be tested and analyzed with the purpose of finding the most adequate particle size and volume fraction to obtain high attenuation coefficients.

1.1 Review of Literature

Below a historical review of the ultrasonic immersion techniques will be presented.

As a brief introduction, it can be mentioned that these techniques require immersing the specimen in a certain liquid (typically water) and immersion transducers will communicate with the specimen through the liquid, which acts as a coupling agent. The mechanical pulse generated by the transducers travels through the liquid into the specimen. This incident pulse will break into several reflected pulses that will come back to the transducer and several transmitted pulses that will travel away from the transducer on the other side of the specimen. All of these reflected and transmitted pulses can be measured. In practice, either the reflected or the transmitted portions are measured since there is no need to measure both. If the reflected portions are measured, the ultrasonic immersion technique is known to be working in the pulse echo mode whereas if the transmitted portions are measure then it is known to be working in the through transmission mode. In the pulse echo mode only one transducer is necessary while in the through transmission mode two transducers are required.

It is important to highlight at this point that these ultrasonic techniques are much more commonly used to measure wave speeds of materials by using the time lapse between echoes and the thickness of the specimen. This feature will be constantly used in later sections.

The interest in wave propagation in solid samples goes back to 1948 with Nolle and Mowry [19] who carried out measurements of the attenuation coefficient in High Polymers by an acoustic pulse immersion technique to finally obtain velocity and attenuation of longitudinal waves. Their apparatus consisted of a single transducer working both as a pulse generator and pulse receiver and a tank filled with water. The sample was totally immersed in water and the transducer was located at a certain distance from the sample, transmitting the ultrasonic pulses through water towards the sample, as shown in Figure 1.

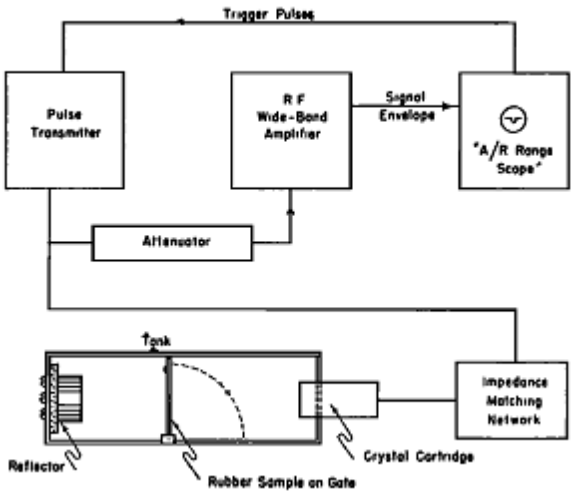

Figure 1. Attenuation measurement set up by Nolle and Mowry [19].

The procedure to calculate the wave speed and attenuation was the following: First, the test was run without the specimen (Gate laying down horizontally). For this case, the value indicated by the attenuator setting in the pulser/receiver unit was recorded. Next, the specimen was placed under water perpendicular to the transducer beam (Gate standing vertically). At this point, they would change the attenuator

setting in the pulser/receiver until this second signal also coming from the reflector was superimposed (in amplitude) to the first signal for which there was no specimen. The magnitude of decibels by which the attenuator setting was changed was interpreted as the apparent attenuation in the specimen. In order to obtain the real attenuation coefficient, calculations were performed that relied on the perfectly bonded interface condition. This assumption will be examined in this thesis. The main characteristic of this procedure is the change of the settings of the pulser/receiver unit to measure attenuation, which limits the accuracy of the measurement to the resolution of the attenuator setting. Nowadays, the settings are not modified during the test and the difference in amplitude between signals is analyzed to provide better accuracy.

In the 1960s and 1970s, McSkimin [20] did much work in the ultrasonic measurement field. He explained numerous ultrasonic methods for measuring mechanical properties of liquids and solids. He suggested a method to measure the attenuation coefficient at high frequencies that is somewhat similar to the one used by Nolle and Mowry [19]with the difference that it uses transmitted pulses instead of reflected ones and it does not modify the settings of the signal processing unit for the two different test scenarios (with and without sample). In other words, McSkimin used a transmitting transducer and a receiving transducer on opposite sides of the sample and recorded two signals, one without a sample in the tank and the other one with the sample fully immersed in the tank. Eventually, he proceeds with the respective signal analysis again assuming the perfectly bonded interface condition.

Another example of ultrasonic attenuation study is provided by Kline [21] (1984) who used the first front wall reflection (A_0) and first back wall echo (A_1) as illustrated in Figure 2. He also relied on the perfectly bonded interface condition to calculate attenuation.

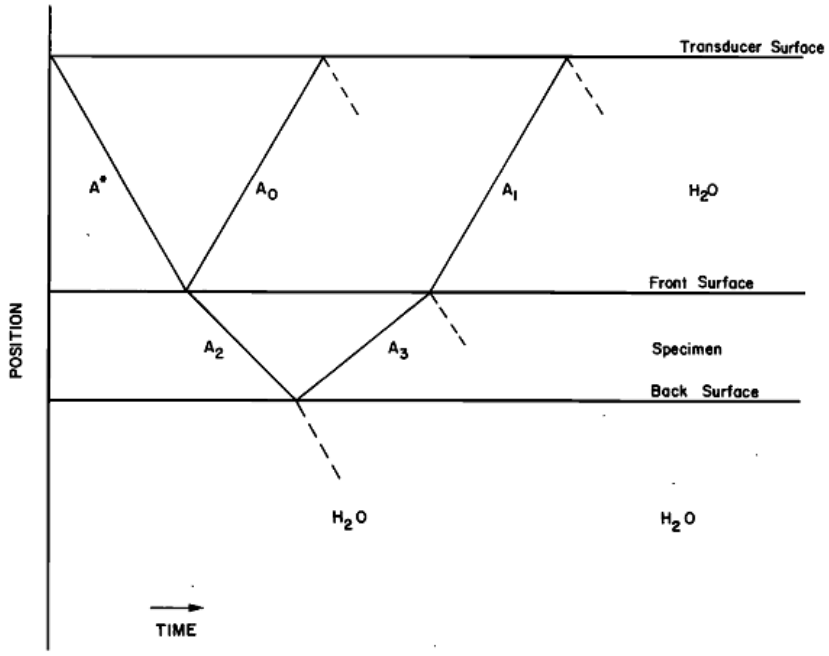

Figure 2. Attenuation measurement by Kline [21].

More recent studies show some alternatives for measuring materials attenuation. An intuitive study is carried out by Umchid [22] (2008) in which he compares the signals from specimens with different thicknesses using the through transmission mode. By always locating the transducer at the same distance from the specimen's faces, the only difference in the signal between tests is the higher attenuation introduced by the thicker specimens. An example with just two specimens of different thicknesses is illustrated in Figure 3:

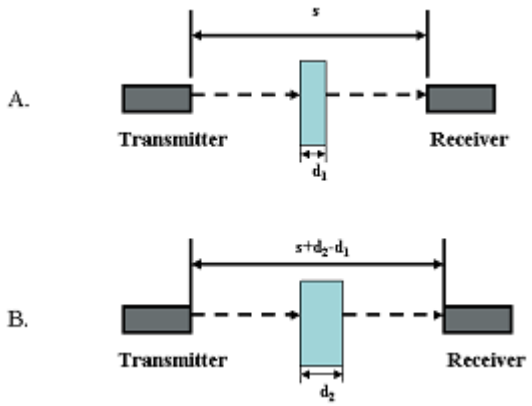

Figure 3. Version utilized by Umchid [22].

Another recent alternative is the one proposed by Youssef and Gobran [23] which consists of adding one more signal to the method developed by Nolle and Mowry [19]. The additional signal is the first front wall reflection, as illustrated in Figure 4.

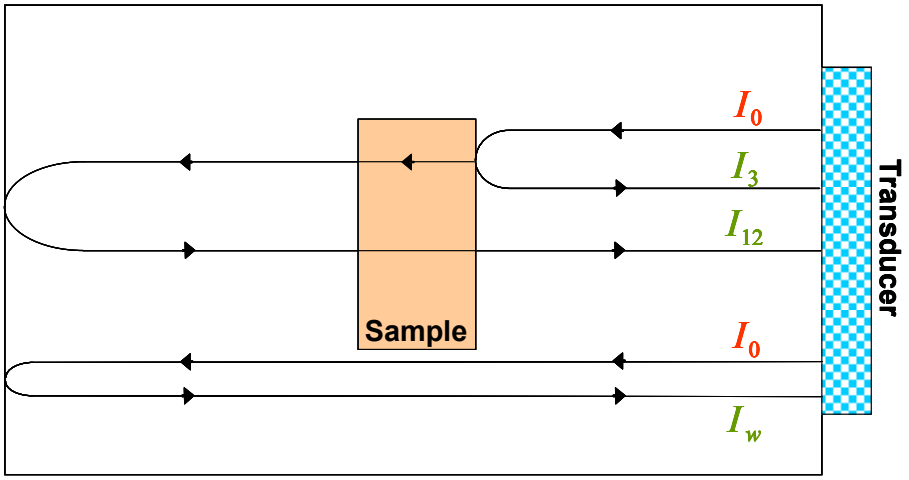

Figure 4. Approach developed by Youssef and Gobran.

This procedure presents some advantages over the ones mentioned so far in that one does not need to know the density of the specimen and does not need to assume a

perfectly bonded interface. However, it does assume that the interface conditions on both sides of the specimen are equal.

Another recent study that presents an improved version of the classic ultrasonic immersion technique was executed by He and Zheng [24] in 2000. In this method two transducers are used, one acting as transmitter and the other as receiver. Again two tests are carried out featuring two different scenarios: the first scenario has no sample within the tank while the second scenario includes an immersed sample. Several signals are recorded as seen in Figure 5.

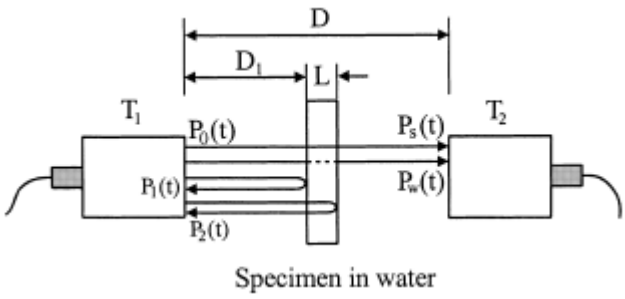

Figure 5. Modern version developed by He and Zheng [24].

This method can calculate the attenuation coefficient very accurately even when the density of the specimen is unknown and when the perfectly bonded interface condition is not satisfied. However, as it happens with Youssef and Gobran's method, it is required that the interface conditions on both sides of the specimen be equal.

Summarizing all the previously explored ultrasonic immersion techniques to measure attenuation leads to the following conclusions: in all cases there exists a

signal analysis and calculation stage after the measurements have been done. These calculations rely on different assumptions. On the one hand, there is a perfectly bonded interface assumption and on the other hand, when the perfectly bonded interface condition is not necessary, there is another assumption that requires interface conditions on both sides of the specimen to be equal. The main goal of the first part of this thesis is to carefully examine these assumptions and to discover whether they hold for every test and material. Validating these assumptions will provide much robustness to the ultrasonic immersion techniques to measure the attenuation coefficient. Nevertheless, if cases are found for which the assumptions do not hold, a new method that can accurately measure attenuation for those and all the other cases will be needed, or otherwise, erroneous values for the attenuation coefficient will be obtained.

Regarding the attenuation study on particulate composites, the main interest is related to the effect of the particles on the attenuation coefficient of the effective composite material. The effective composite material or effective medium is a virtual homogeneous material that has the same macroscopic properties as the composite. Back in the 1960s Waterman and Truell [25] were among the first developers of theoretical studies of multiple scattering of waves using a previously introduced concept of "configurational" averaging of the wave fields within the scattering medium. They found a criterion that enabled them to obtain approximate integral equations that could be solved for individual quantities of interest. In this manner, their theoretical work could predict wave speeds and attenuation in particulate composites with spherical particles. Yamakawa [26] also pioneered the idea of a close

relation between scattering of elastic waves and wave attenuation. Later in the 1970s Datta [27] studied scattering by a random distribution of inclusions and provided expressions for the averaged propagation constant which seemed to be accurate for small inclusion concentrations. More specifically he studied elastic ellipsoidal inclusions. Continuing with the theoretical models, Beltzer and Brauner [28-31] published several papers in the 1980s, proposing different models based on: 1) combining Kramers-Kronig relations with scattering analysis provided by Waterman and Truell, and Yamakawa; 2) based on a differential scheme, which is well known in the static analysis of composites and can provide better results than the Kramers-Kronig relations based models when dealing with multiple scattering. It is convenient to highlight that the previous models that did not use a differential scheme are adequate for a small scattering density. This is why sometimes they are called dilute concentration models. More recently (2004) Biwa [32] used a differential scheme with an analogous formulation to the works by Beltzer for the specific case of ultrasonic wave attenuation in particle reinforced polymer matrix composites. Another type of theoretical models is the so called self consistent methods. Yeon-Kim, *et al*., [33] followed a self consistent method analogous to the coherent potential approximation used in alloy physics. According to Yeon-Kim, *et al*., the coherent potential approximation is a method developed in the theory of disordered solids to determine the macroscopic mechanical properties of polycrystalline materials. In the self consistent method used by Yeon-Kim, *et al*., three conditions must be satisfied by the elastic properties of the effective medium. By solving these conditions, the dynamic effective density and material moduli can be determined. After this, phase velocities

and attenuation were calculated and compared with Waterman and Truell's theory as well as with the experimental results obtained by Kinra, *et al*. [34], which were in good agreement with the self consistent method predictions. In a similar manner, Bin Yang [35] used a self consistent method called the generalized self consistent method (GSCM) to calculate scattering of longitudinal and shear waves originated by spherical inclusions in an isotropic matrix. Self consistent methods have become quite powerful for particulate composite modeling since unlike the other methods they are able to account for multiple scattering in the presence of a high concentration of scatterers.

The theoretical models mentioned above necessitate experimental validation. Kinra *et al*. [34] performed numerous tests in the 1980s on particulate composites made of glass spheres in an epoxy matrix, in the frequency range of 0.3-5 MHz, measuring longitudinal and shear phase velocities and attenuation of longitudinal waves. They showed how both velocities and the attenuation would increase with particle volume fraction. In the case of the attenuation, it would also increase with frequency. More recent experimental studies have been conducted by Biwa, *et al*., [36] on rubber particles within a PMMA matrix. They measured phase velocities and attenuation spectra to determine the bulk and shear moduli of the particles. They found that the phase velocities would decrease considerably with rubber particle volume fraction whereas attenuation would significantly increase with particle volume fraction. Also, Layman *et al*. [37] measured phase velocities and attenuation as a function of frequency for random particulate composites consisting of spherical glass

particles imbedded in an epoxy matrix. They compared their measurements with results from the Waterman and Truell theory and also with the generalized self consistent model (GSCM). For low particle concentration both models agreed with the experimental measurements of phase velocity and attenuation. However, for high particle concentrations, the Waterman and Truell theory and the GSCM showed significant discrepancies with respect to attenuation. The GSCM model worked well whereas the Waterman and Truell theory overpredicted the attenuation. This is because this latter model does not consider the interaction between particles, which becomes important as the particle concentration increases. Thus the Waterman and Truell theory is only adequate for low scatterer concentration. The conclusions extracted from the work by Layman, *et al*., [37] agree with the conclusions given by Yeon-Kim, *et al*., [33]. In 2008, Mylavarapu and Woldesenbet [38] utilized the ultrasonic pulse-echo technique to calculate longitudinal and shear wave speeds and apparent attenuation on syntactic foams and solid particulate composites. Syntactic foams is the term used for a specific type of particulate composites consisting of hollow particles instead of solid ones. Also, apparent attenuation refers to the amplitude difference between echoes in the raw signal. Apparent attenuation is not the attenuation coefficient of a material and it should be treated very carefully since it can be very misleading. For instance, two materials could show the same apparent attenuation but have totally different attenuation coefficients (real attenuation). Mylavarapu and Woldesenbet showed how both wave speeds increase with particle volume fraction for the solid glass particles. As to attenuation, they showed how the apparent attenuation of solid glass particulate composites is always higher than that of

syntactic foams. In addition, according to their study, the apparent attenuation in the solid particulate composites reached a maximum around the 30% particle volume fraction and it decreased considerably for higher volume fractions. This behavior is somewhat similar to the experimental results published by Layman, *et al*., [37] in which the attenuation also reached a maximum. However, in this latter study the attenuation reached its maximum around the 15% particle volume fraction and after this remained relatively constant. It must be said that these differences could have been entirely originated by the difference between apparent attenuation, which Mylavarapu and Woldesenbet measured, and the real attenuation coefficient shown in Layman's work.

Going back to theoretical models for particulate composites, Biwa [39, 40] conceived a model based on the independent scattering formulated by Beltzer that incorporated absorption losses within the matrix and/or the inclusions, that is, taking into account the viscoelastic nature of the matrix and of the particles, if necessary. He later used this model to predict the attenuation coefficient of shear waves in a fiber reinforced composite as well as the attenuation coefficient of longitudinal waves in a glass/epoxy and rubber/PMMA particulate composite. The predictions provided by Biwa's model show excellent agreement with the experiments for low particle concentrations. This reinforced the need to incorporate the absorption losses of the constituents in the mathematical foundations. If this model is combined with a differential scheme or a self consistent model, it will be able to predict ultrasonic attenuation for higher particle concentrations. Another interesting work is the one

published in 2009 by Mylavarapu and Woldesenbet [41], where they developed a model of the ultrasonic pulse echo technique that could take into account particle size, porosity and radius ratio. The model assumed the ultrasonic incident beam to be a plane longitudinal wave and the medium to be isotropic. The model also incorporated attenuation loss from absorption in the matrix and the particles, scattering and resonance in the particles. However, it did not consider interaction between particles. Results from the model were compared to experiments on glass/epoxy particulate composites showing good agreement for dilute concentrations. Finally, Kanaun, *et al*., [42] developed a version of the effective field method (EFM), which is fundamentally the method employed by Waterman and Truell, in which they derived a dispersion equation that has several solutions for the wave number that depend on the characteristics of the composite, e.g. the particle concentration. In 2012, Liu [43] used a finite element method to study ultrasonic wave propagation in polymer matrix particulate/fibrous composites. In particular, he used a method called the extended finite element method (XFEM) that incorporates the equations of motion in time domain, showing improved agreement between experimentally measured attenuation coefficients of particulate composites, especially at the high particle volume fractions and analytical methods or models. The method represents a very strong and versatile alternative to all the other methods explained so far. It is noteworthy that this method showed that maximum attenuation can be achieved by aligning fibers in the direction of wave propagation for longitudinal waves in fiber reinforced composites.

This historical review has demonstrated the preponderance of theoretical models that describe wave propagation in particulate composites. Several of these models are able to provide accurate results for wave speeds and attenuation at low particle volume fractions (dilute concentrations) as shown experimentally. However, only very few models can provide acceptable predictions for wave speeds and attenuation at moderate and high particle volume fractions. Therefore, there is still much research needed to develop models that contain the necessary information to describe correctly wave propagation for the high concentration cases. On the other hand, there is a tremendously large amount of experimental measurements that could be performed based on different criteria such as particle/matrix materials, particle size, frequency of incident wave, particle volume fraction, etc. This thesis will contribute to providing accurate experimental results for specific cases so that the existing theoretical models can find additional cases that can help support their validity and hence, improve the understanding of wave propagation in the field of particulate composites.

1.2 Motivation.

In the first place, there is an evident need for a solid and robust method of measuring a parameter of such importance in viscoelasticity as the attenuation coefficient. As it has been shown, the existing methods based on ultrasonic transducers rely on several assumptions. The more robust, reliable and better a measuring method, the least number of assumptions it needs. Therefore, focusing on the specific case developed in this work, proving the existing assumptions pertaining

to the ultrasonic immersion technique are true, would eliminate the associated uncertainty and provide great robustness to this attenuation measuring method. However, were these existing assumptions shown to be wrong, the development of a new method that can function correctly under the conditions that violate the already existing assumptions would become necessary.

On the second place, a review of the work done so far on particulate composites highlights the necessity of theoretical research to find models that can describe wave propagation within those materials for high particle concentrations and more experimental work is also necessary to provide validation of these theoretical models. Since the combination of parameters such as particle/matrix materials, particle size, frequency of incident wave, particle volume fraction, etc. is very large, this study was narrowed to provide valid attenuation measurements for specific cases based on the previously reviewed ultrasonic immersion technique so that the results can be used to provide sound validation for theoretical models.

References

[1] Batra, N. K., and Chaskelis, H. H. "Determination of Minimum Flaw Size Detectable by Ultrasonics in Titanium Alloy Plates." *NDT International.* Vol. 18, (5) pp. 261-264. (1985).

[2] Cerri, M., and Cusolito, R. "Experiences in Capability Assessment of Manual Ultrasonic Examination Techniques for Planar Flaw Detection and Sizing in Austenitic Stainless Steel Joints." *NDT International.* Vol. 22, (4) pp. 229-239. (1989).

[3] Hislop, J. D. "Flaw Size Evaluation in Immersed Ultrasonic Testing." *Non-Destructive Testing.* Vol. 2, (3) pp. 183-192. (1969).

[4] Lavender, J. D. "Methods for Non-Destructive Testing of Steel Forgings Part 1.—Ultrasonic Flaw Detection: British Standard BS 4124 (Part 1)." *Non-Destructive Testing.* Vol. 1, (4) pp. 251. (1968).

[5] Marianeschi, E., and Tili, T. "A Note on the Smallest Defect that can be Detected using Ultrasonics." *NDT International.* Vol. 16, (2) pp. 75-77. (1983).

[6] Rodríguez, M. A., Ramos, A., and San Emeterio, J. L. "Location of Multiple Proximate Flaws using Perpendicular NDT Ultrasonic Arrays." *Ultrasonics.* Vol. 44, Supplement, (0) pp. e1105-e1109. (2006).

[7] Ruiz-Reyes, N., Vera-Candeas, P., Curpián-Alonso, J., Cuevas-Martínez, J. C., and Blanco-Claraco, J. L. "High-Resolution Pursuit for Detecting Flaw Echoes Close to the Material Surface in Ultrasonic NDT." *NDT & E International.* Vol. 39, (6) pp. 487-492. (2006).

[8] Turó, A., Chávez, J. A., García-Hernández, M. J., Bulkai, A., Tomek, P., Tóth, G., Gironés, A., and Salazar, J. "Ultrasonic Inspection System for Powder Metallurgy Parts." *Measurement.* Vol. 46, (3) pp. 1101-1108. (2013).

[9] "46876 the Pulsed Ultrasonic Velocity Method for Determining Material Dynamic Elastic Moduli : Blessing, G.V. Dynamic Elastic Modulus Measurements in Materials, ASTM STP 1045. Edited by A. Wolfenden. Pp. 47–57. American Society for Testing and Materials, Philadelphia, Pennsylvania (United States)." " " *NDT & E International.* Vol. 27, (1) pp. 50. (1994).

[10] "52971 Determination of the Elastic Constants of Composite Materials from Ultrasonic Group Velocity Measurements : Niu, Lin Dissertation Abstracts International, Vol. 53, no. 7, p. 3584 (Jan. 1993) (DA9236006)." " " *NDT & E International.* Vol. 27, (1) pp. 45. (1994).

[11] Freitas, V. L. d. A., Albuquerque, V. H. C. d., Silva, E. d. M., Silva, A. A., and Tavares, J. M. R. S. "Nondestructive Characterization of Microstructures and Determination of Elastic Properties in Plain Carbon Steel using Ultrasonic Measurements." *Materials Science and Engineering: A.* Vol. 527, (16–17) pp. 4431-4437. (2010).

[12] Papadakis, E. P., Patton, T., Tsai, Y., Thompson, D. O., and Thompson, R. B. "The Elastic Moduli of a Thick Composite as Measured by Ultrasonic Bulk Wave Pulse Velocity." *The Journal of the Acoustical Society of America.* Vol. 89, (6) pp. 2753-2757. (1991).

[13] Rokhlin, S. I., and Wang, W. "Double through-Transmission Bulk Wave Method for Ultrasonic Phase Velocity Measurement and Determination of Elastic Constants of Composite Materials." *The Journal of the Acoustical Society of America.* Vol. 91, (6) pp. 3303-3312. (1992).

[14] Smith, R. E. "Ultrasonic Elastic Constants of Carbon Fibers and their Composites." *Journal of Applied Physics.* Vol. 43, (6) pp. 2555-2561. (1972).

[15] Tauchert, T. R., and Güzelsu, A. N. "Measurements of the Elastic Moduli of Laminated Composites using an Ultrasonic Technique." *Journal of Composite Materials.* Vol. 5, (4) pp. 549-552. (1971).

[16] Zimmer, J. E., and Cost, J. R. "Determination of the Elastic Constants of a Unidirectional Fiber Composite using Ultrasonic Velocity Measurements." *The Journal of the Acoustical Society of America.* Vol. 47, (3B) pp. 795-803. (1970).

[17] Lakes, Roderic S. *Viscoelastic Solids.* CRC Press, 1998.

[18] Davis, Julian L. *Mathematics of Wave Propagation.* Princeton University Press, 1997.

[19] Nolle, A. W. "Measurement of Ultrasonic Bulk-Wave Propagation in High Polymers." *The Journal of the Acoustical Society of America.* Vol. 20, (4) pp. 587. (1948).

[20] McSkimin, H. J. *Physical Acoustics: Principles and Methods.* Vol. 1A, Academic Press, 1964.

[21] Kline, R. A. "Measurement of Attenuation and Dispersion using an Ultrasonic Spectroscopy Technique." *The Journal of the Acoustical Society of America.* Vol. 76, (2) pp. 498-504. (1984).

[22] Umchid, S. "Frequency Dependent Ultrasonic Attenuation Coefficient Measurement." *The 3rd International Symposium on Biomedical Engineering.* Vol. , ( ) pp. 234-238. (2008).

[23] Youssef, M. H., and Gobran, N. K. "Modified Treatment of Ultrasonic Pulse-Echo Immersion Technique." *Ultrasonics.* Vol. 39, (7) pp. 473-477. (2002).

[24] He, P., and Zheng, J. "Acoustic Dispersion and Attenuation Measurement using both Transmitted and Reflected Pulses." *Ultrasonics.* Vol. 39, (1) pp. 27-32. (2001).

[25] Waterman, P. C., and Truell, R. "Multiple Scattering of Waves." *Journal of Mathematical Physics.* Vol. 2, (4) pp. 512-537. (1961).

[26] Yamakawa, N. "Scattering and Attenuation of Elastic Waves." *Geophysical Magazine (Tokyo).* Vol. 31, ( ) pp. 63-103. (1962).

[27] Datta, S. K., ed. *Scattering by a Random Distribution of Inclusions and Effective Elastic Properties,* J. W. Proban ed. Vol. : University of Waterloo press, 1978.

[28] Beltzer, A. I., and Brauner, N. "Acoustic Waves in Random Discrete Media Via a Differential Scheme." *Journal of Applied Physics.* Vol. 60, (2) pp. 538-540. (1986).

[29] Beltzer, A. I., Bert, C. W., and Striz, A. G. "On Wave Propagation in Random Particulate Composites." *International Journal of Solids and Structures.* Vol. 19, (9) pp. 785-791. (1983).

[30] Beltzer, A. I., and Brauner, N. "The Dynamic Response of Random Composites by a Causal Differential Method." *Mechanics of Materials.* Vol. 6, (4) pp. 337-345. (1987).

[31] Brauner, N., and Beltzer, A. I. "High-Frequency Elastic Waves in Random Composites Via the Kramers--Kronig Relations." *Applied Physics Letters.* Vol. 46, (3) pp. 243-245. (1985).

[32] Biwa, S., Watanabe, Y., Motogi, S., and Ohno, N. "Analysis of Ultrasonic Attenuation in Particle-Reinforced Plastics by a Differential Scheme." *Ultrasonics.* Vol. 43, (1) pp. 5-12. (2004).

[33] Kim, J., Ih, J., and Lee, B. "Dispersion of Elastic Waves in Random Particulate Composites." *The Journal of the Acoustical Society of America.* Vol. 97, (3) pp. 1380-1388. (1995).

[34] Kinra, V. K., Petraitis, M. S., and Datta, S. K. "Ultrasonic Wave Propagation in a Random Particulate Composite." *International Journal of Solids and Structures.* Vol. 16, (4) pp. 301-312. (1980).

[35] Yang, R. -. "A Dynamic Generalized Self-Consistent Model for Wave Propagation in Particulate Composites." *Journal of Applied Mechanics.* Vol. 70, (4) pp. 575-582. (2003).

[36] Biwa, S., Ito, N., and Ohno, N. "Elastic Properties of Rubber Particles in Toughened PMMA: Ultrasonic and Micromechanical Evaluation." *Mechanics of Materials.* Vol. 33, (12) pp. 717-728. (2001).

[37] Layman, C., Murthy, N. S., Yang, R., and Wu, J. "The Interaction of Ultrasound with Particulate Composites." *The Journal of the Acoustical Society of America.* Vol. 119, (3) pp. 1449-1456. (2006).

[38] Mylavarapu, P., and Woldesenbet, E. "Ultrasonic Characterization of Sandwich Core Materials." *Journal of Sandwich Structures and Materials.* Vol. 10, (5) pp. 413-428. (2008).

[39] Biwa, S. "Independent Scattering and Wave Attenuation in Viscoelastic Composites." *Mechanics of Materials.* Vol. 33, (11) pp. 635-647. (2001).

[40] Biwa, S., Idekoba, S., and Ohno, N. "Wave Attenuation in Particulate Polymer Composites: Independent scattering/absorption Analysis and Comparison to Measurements." *Mechanics of Materials.* Vol. 34, (10) pp. 671-682. (2002).

[41] Mylavarapu, P., and Woldesenbet, E. "A Predictive Model for Ultrasonic Attenuation Coefficient in Particulate Composites." *Composites Part B: Engineering.* Vol. 41, (1) pp. 42-47. (2010).

[42] Kanaun, S., Levin, V., and Pervago, E. "Acoustical and Optical Branches of Wave Propagation in Random Particulate Composites." *International Journal of Engineering Science.* Vol. 46, (4) pp. 352-373. (2008).

[43] Liu, Z., Oswald, J., and Belytschko, T. "XFEM Modeling of Ultrasonic Wave Propagation in Polymer Matrix particulate/fibrous Composites." *Wave Motion.* Vol. 50, (3) pp. 389-401. (2013).

CHAPTER 2

THEORY

2.1 Wave propagation.

A classical definition of a wave could be phrased as follows: the propagation of a perturbation or disturbance with time and distance through space, carrying energy but not matter. If the perturbation or disturbance needs a physical medium to propagate through space, it is classified under a mechanical wave. For example, sound is a mechanical wave that needs a medium to propagate, e.g. air or water. On the other hand, if that perturbation or disturbance does not need a physical medium in order to propagate it will be classified under an electromagnetic wave. For instance, light is an electromagnetic wave that can travel in vacuum.

From this point forward this thesis will focus on mechanical waves travelling in solid materials. Indeed, when a disturbance like an impact occurs in a solid material, it will travel through the material due to the interaction between the atoms/molecules that form that solid. The field that studies the propagation of mechanical disturbances in solid materials is called elastodynamics. The mathematical foundations of this field will be presented below [1, 2].

In the first place, it is essential to introduce the equations of motion. These equations are based on the application of Newton's Second Law to an infinitesimal volume. Considering a 2D case, the stresses and forces present in the infinitesimal element are shown in Figure 6.

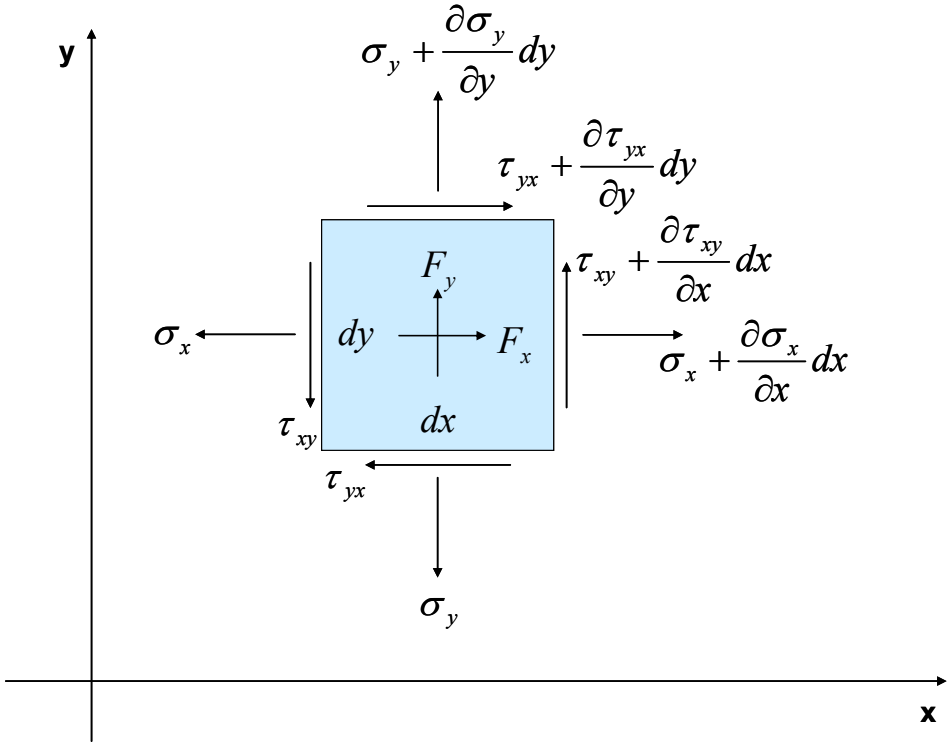

Figure 6. Stress in a two dimensional infinitesimal element.

Here, F_x and F_y represent the body forces per unit volume acting on the element. By simply applying Newton's Second Law in the x and y direction the following two equations are obtained:

$$\frac{\partial \sigma_x}{\partial x} + \frac{\partial \tau_{yx}}{\partial y} + F_x = \rho \frac{\partial^2 u}{\partial t^2}$$
$$\frac{\partial \tau_{xy}}{\partial x} + \frac{\partial \sigma_y}{\partial y} + F_y = \rho \frac{\partial^2 v}{\partial t^2} \qquad (2.1)$$

By extending the problem to the 3-D case, the following equations can be obtained:

$$\begin{aligned}
&\frac{\partial \sigma_x}{\partial x}+\frac{\partial \tau_{yx}}{\partial y}+\frac{\partial \tau_{zx}}{\partial z}+F_x=\rho\frac{\partial^2 u}{\partial t^2}\\
&\frac{\partial \tau_{xy}}{\partial x}+\frac{\partial \sigma_y}{\partial y}+\frac{\partial \tau_{zy}}{\partial z}+F_y=\rho\frac{\partial^2 v}{\partial t^2}\\
&\frac{\partial \tau_{xz}}{\partial x}+\frac{\partial \tau_{yz}}{\partial y}+\frac{\partial \sigma_z}{\partial z}+F_z=\rho\frac{\partial^2 w}{\partial t^2}
\end{aligned} \tag{2.2}$$

It can be seen that setting acceleration terms to zero, these equations of motion become the equilibrium equations used in the Theory of Elasticity. It is important to point out again that these equations of motion are independent of any material properties and therefore can be applied to any case.

In the second place, another important component of the fundamentals of elastodynamics is the strain tensor defined in Theory of Elasticity as well as the Strain-Displacement relations [3], which can be seen below:

Strain tensor:

$$\varepsilon_{ij}=\begin{pmatrix}\varepsilon_x & \gamma_{xy} & \gamma_{xz}\\ \gamma_{yx} & \varepsilon_y & \gamma_{yz}\\ \gamma_{zx} & \gamma_{zy} & \varepsilon_z\end{pmatrix} \tag{2.3}$$

Strain-displacement relations:

$$\begin{aligned}
&\varepsilon_x=\frac{\partial u}{\partial x},\ \varepsilon_y=\frac{\partial v}{\partial y},\ \varepsilon_z=\frac{\partial w}{\partial z}\\
&\gamma_{xy}=\gamma_{yx}=\frac{\partial u}{\partial y}+\frac{\partial v}{\partial x},\ \gamma_{yz}=\gamma_{zy}=\frac{\partial v}{\partial z}+\frac{\partial w}{\partial y},\ \gamma_{xz}=\gamma_{zx}=\frac{\partial u}{\partial z}+\frac{\partial w}{\partial x}
\end{aligned} \tag{2.4}$$

Finally, stress-strain relations are required to balance the number of equations and unknowns. Unlike in the previous equations, in this case, the properties of the material

come into play and therefore information about the wave propagation media is necessary.

Let us consider for now elastic media that obey Hooke's Law. It is also assumed that the media are homogenous and isotropic.

By means of the stress-strain relations and the strain-displacements relations, the previously shown equations of motion can be written in terms of displacement providing the following expression:

$$\mu\nabla^2\overline{u} + (\lambda + \mu)\nabla(\nabla \cdot \overline{u}) = \rho\ddot{\overline{u}} \tag{2.5}$$

where λ and μ the elastic moduli of the material.

Taking the divergence ($\nabla \cdot$) of Equation (2.5) provides

$$(\lambda + 2\mu)\nabla^2\upsilon = \rho\ddot{\upsilon} \tag{2.6}$$

where υ represents the dilatation and is defined by $\upsilon = \frac{\partial u}{\partial x} + \frac{\partial v}{\partial y} + \frac{\partial w}{\partial z}$. Equation (2.6) is the wave equation and it represents a motion called dilatational wave motion. This motion coincides with irrotational wave motion, which would be characterized by $\overline{\nabla} \times \overline{u} = 0$.

In a similar manner, taking the curl ($\nabla \times$) of Equation (2.5) yields,

$$\mu\nabla^2\overline{\omega} = \rho\ddot{\overline{\omega}} \tag{2.7}$$

where $\overline{\omega}$ is the rotation vector. Again, Equation (2.7) is the wave equation and it represents a motion called rotational or shearing motion. This coincides with equivoluminal wave motion, which would be governed by $\upsilon = 0$.

It should be reemphasized that the classical wave equation has been obtained for two different types of motion in elastic media. This is a mathematical proof of the existence of waves propagating in solid materials. In fact, the two previously introduced wave motions are the only two types possible in unbounded elastic media. This can be proved with the use of Helmholtz Decomposition Theorem. From now on, the dilatational wave motion will be called longitudinal waves while the rotational motion will be called shear waves.

Having demonstrated the existence of waves within solid materials, let us consider the problem of a plane longitudinal harmonic displacement wave arriving at a plane interface between two semi-unbounded media *a* and *b*. Figure 7 shows a longitudinal wave (A_1) travelling towards the interface at an angle (φ_1). Since the conditions that follow after the incident wave reaches the interface are unknown, it is appropriate to treat the problem in a general way and therefore include reflections and transmissions of both types of waves. It is expected that the reflected and transmitted waves will be of the same nature as the incident one, i.e., plane and harmonic. The amplitudes and angles of the reflected and transmitted waves are unknown whereas the amplitude and angle of the incident wave are assumed to be known, as well as the properties of both media.

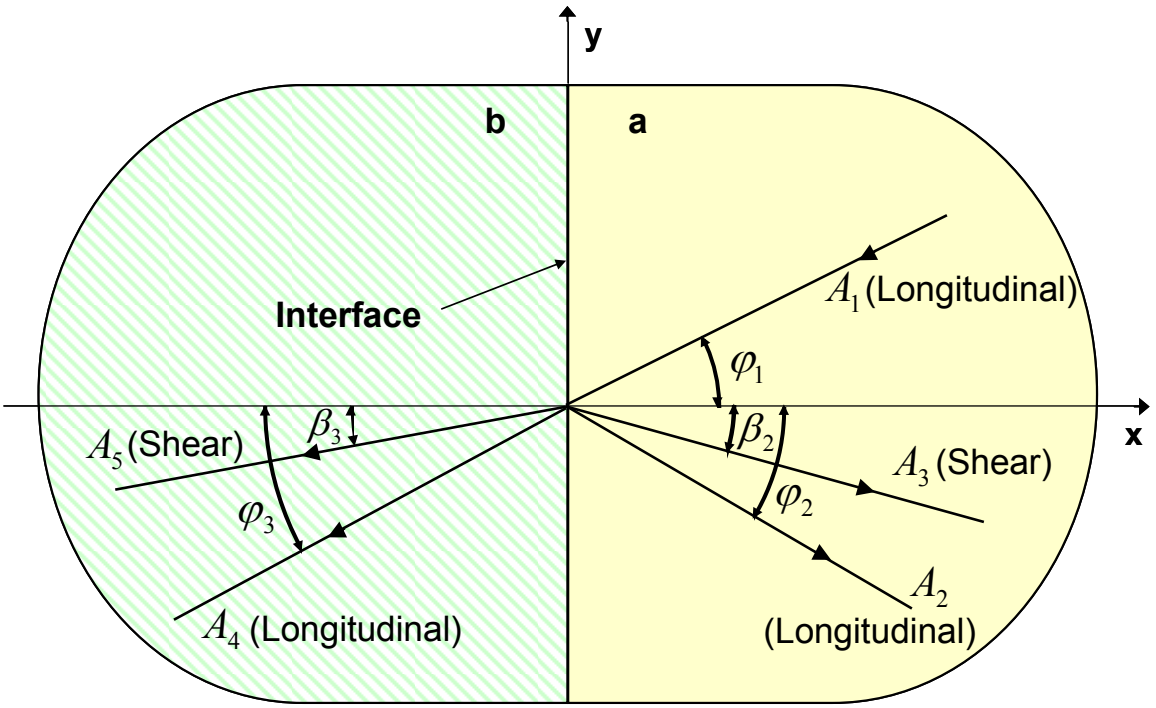

Figure 7. Reflection and transmission of a plane longitudinal wave from a plane interface between two media.

A plane harmonic wave is given by an expression of the type shown below. Note that the variable, ϕ, this expression provides represents displacement.

$$\phi = A\sin(\omega t \pm klx \pm kmy) \tag{2.8}$$

where k is the wave number, $l = \cos\varphi$, $m = \sin\varphi$, φ is the angle of the wave direction with respect to the x axis and the signs + and – depend on the wave direction.

Assuming a perfectly bonded interface yields the following boundary conditions:

$$u_a = u_b \tag{2.9a}$$
$$v_a = v_b \tag{2.9b}$$
$$w_a = w_b \tag{2.9c}$$
$$(\sigma_x)_a = (\sigma_x)_b \tag{2.9d}$$
$$(\tau_{xy})_a = (\tau_{xy})_b \tag{2.9e}$$
$$(\tau_{xz})_a = (\tau_{xz})_b \tag{2.9f}$$

In this case, $w_a = w_b = 0$.

After these conditions are applied, the following equations are derived:

$$\frac{\sin\varphi_1}{(c_l)_a} = \frac{\sin\varphi_2}{(c_l)_a} = \frac{\sin\beta_2}{(c_s)_a} = \frac{\sin\varphi_3}{(c_l)_b} = \frac{\sin\beta_3}{(c_s)_b} \tag{2.10a}$$

$$(A_1 - A_2)\cos\varphi_1 + A_3\sin\beta_2 - A_4\cos\varphi_3 - A_5\sin\beta_3 = 0 \tag{2.10b}$$

$$(A_1 + A_2)\sin\varphi_1 + A_3\cos\beta_2 - A_4\sin\varphi_3 + A_5\cos\beta_3 = 0 \tag{2.10c}$$

$$(A_1 + A_2)(c_l)_a\cos 2\beta_2 - A_3(c_s)_a\sin 2\beta_2 - A_4(c_l)_b\left(\frac{\rho_b}{\rho_a}\right)\cos 2\beta_3 - A_5(c_s)_b\left(\frac{\rho_b}{\rho_a}\right)\sin 2\beta_3 = 0 \tag{2.10d}$$

$$\rho_a(c_s)_a^2\left[(A_1 - A_2)\sin 2\varphi_1 - A_3\left(\frac{c_l}{c_s}\right)_a\cos 2\beta_2\right] - \rho_b(c_s)_b^2\left[A_4\frac{(c_l)_a}{(c_l)_b}\sin 2\varphi_3 - A_5\frac{(c_l)_a}{(c_s)_b}\cos 2\beta_3\right] = 0 \tag{2.10e}$$

where c_l and c_s represents longitudinal and shear wave speeds respectively.

The solution to this problem is especially simple for the case of an incident wave travelling perpendicular to the interface, that is, $\alpha_1 = 0$. In this case, the results would be:

$$A_2 = A_1\frac{\left[\rho_b(c_l)_b - \rho_a(c_l)_a\right]}{\left[\rho_b(c_l)_b + \rho_a(c_l)_a\right]} \tag{2.11a}$$

$$A_3 = 0 \tag{2.11b}$$

$$A_4 = A_1\frac{2\rho_a(c_l)_a}{\left[\rho_b(c_l)_b + \rho_a(c_l)_a\right]} \tag{2.11c}$$

$$A_5 = 0 \tag{2.11d}$$

The ratio between A_2 and A_1 is defined as the reflection coefficient while the ratio between A_4 and A_1 is the transmission coefficient. The term ρc_l present in both coefficients is known as the acoustic impedance of a material. These reflection and transmission coefficients will be the essence of the upcoming study on the ultrasonic pulse echo immersion technique. Note that the reflection and transmission coefficients defined above are based on a displacement wave. In the case of a stress wave, the same procedure is applied and the reflection and transmission coefficients would be given by:

$$R_{ij} = \frac{(\rho c)_j - (\rho c)_i}{(\rho c)_i + (\rho c)_j} \tag{2.12}$$

$$T_{ij} = \frac{2(\rho c)_j}{(\rho c)_i + (\rho c)_j} \tag{2.13}$$

where the incident wave travels in medium *i* towards medium *j*.

The most important conclusion to extract from this analysis is that when a longitudinal wave reaches perpendicularly an interface between two media, a reflected wave as well as a transmitted wave with opposite traveling direction is originated at the interface. Both waves are longitudinal and of identical shape to the incident one. No shear waves are originated in this case.

2.2 Ultrasonic pulse echo immersion technique (U.P.E.I.)

The U.P.E.I. technique is mostly known for measuring the longitudinal wave speed and attenuation coefficient of solid materials. Focusing on the attenuation measurement, the principles behind the technique can be well represented by Figure 8.

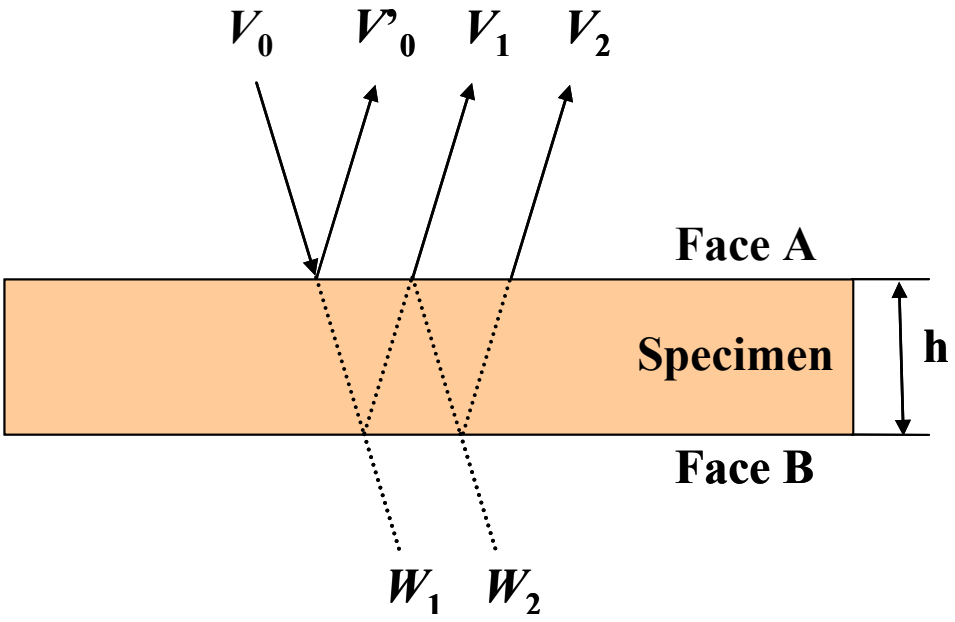

Figure 8. Fundamentals of the ultrasonic pulse echo immersion technique.

Figure 8 must be interpreted as follows: first an ultrasonic pulse of amplitude V_0 arrives perpendicularly at face A of the specimen. (Note that the different pulses have been drawn at an inclination only for visualization purposes). As was concluded in the theory, part of this incident ultrasonic pulse will be reflected back and the rest will be transmitted into the specimen. The exact same phenomenon occurs every time a pulse reaches an interface. The reflected and transmitted portions are dictated by the reflection and transmission coefficients of the interface, respectively. The reflected pulses off face B that go back towards the incident pulse source are denoted as echoes V_1, V_2 and so on. Thus, the first reflected pulse $V_0^{'}$ is not considered an echo but is known as the front wall reflection.

Taking into account the attenuation experienced by the pulse within the specimen and accounting for the beam spreading suffered by the pulse as it travels in 3D space, the amplitudes of the front wall reflection ($V_0^{'}$) and the first and second echoes V_1 and V_2 are calculated as shown below,

$$V_0^{'} = V_0 R_A D\left(s_0^{'}\right) \tag{2.14}$$

$$V_1 = V_0 T_A^2 R_B D\left(s_1\right) e^{-\alpha 2h} \tag{2.15}$$

$$V_2 = V_0 T_A^2 R_B^2 R_A D\left(s_2\right) e^{-\alpha 4h} \tag{2.16}$$

where R_A, R_B, T_A, T_B are the reflection and transmission coefficients of faces A and B respectively. $D(s)$ stands for the beam spreading of the pulse, α is the attenuation coefficient of the specimen and h is the thickness of the specimen. The beam spreading $D(s)$ function is derived by Rogers and Van Buren [4] as:

$$D(s) = \left\{\left[\cos(2\pi/s) - J_0(2\pi/s)\right]^2 + \left[\sin(2\pi/s) - J_1(2\pi/s)\right]^2\right\}^{1/2} \tag{2.17}$$

where J_0 and J_1 are Bessel functions of orders 0 and 1, respectively.

The s variable for each case would be:

$$s_0^{'} = \frac{2L\lambda_w}{a^2} \tag{2.18a}$$

$$s_1 = \frac{2h\lambda_s + 2L\lambda_w}{a^2} \tag{2.18b}$$

$$s_2 = \frac{4h\lambda_s + 2L\lambda_w}{a^2} \tag{2.18c}$$

where a is the radius of the transducer, L is the distance from the transducer to its closest face of the specimen, λ_w is the wavelength of the wave in water for a given

frequency and λ_s is the wavelength of the wave in the specimen material for a given frequency.

Using the first and second echoes, V_1 and V_2, and performing the corresponding operations, an expression for the attenuation coefficient of the specimen can be obtained and it is shown below:

$$\alpha = \frac{1}{2h} \cdot \ln\left(\frac{V_1}{V_2} \cdot R_A \cdot R_B \cdot \frac{D(s_2)}{D(s_1)} \right) \tag{2.19}$$

For this calculation, the thickness h of the specimen is known; V_1 and V_2 are measured values; and $D(s_1)$, $D(s_2)$ can be calculated with Equation (2.17). The key to the attenuation coefficient measurement will be to obtain the reflection coefficients R_A and R_B.

Before starting to analyze the reflection coefficients of the pulse echo technique, it is necessary to clarify that Equation (2.19) does not constitute a unique means for obtaining the attenuation coefficient. As the name of the technique implies, only the echoes have been used so far. However, the transmitted signals into the liquid from face B could also be recorded and utilized to calculate the attenuation. Following the same approach as in Equations (2.14, 2.15, 2.16) the amplitude of the transmitted pulses is given by:

$$W_1 = V_0 T_A T_B D(s_{w1}) e^{-\alpha h} \tag{2.20}$$

$$W_2 = V_0 T_A T_B R_B R_A D(s_{w2}) e^{-\alpha 3h} \tag{2.21}$$

Using the first two transmitted signals W_1 and W_2, an expression to calculate the attenuation coefficient is easily derived and shown below

$$\alpha = \frac{1}{2h} \cdot \ln\left(\frac{W_1}{W_2} \cdot R_A \cdot R_B \cdot \frac{D(s_{w2})}{D(s_{w1})} \right) \tag{2.22}$$

This technique is commonly known as the through transmission mode of the ultrasonic immersion technique. In a similar manner any other echoes and/or transmitted pulses can be combined to find an expression for the attenuation coefficient. In this thesis, the approach explained first involving echoes V_1 and V_2 will be utilized because it only requires one transducer and V_1 and V_2 are the echoes with the best signal to noise ratio. Other echoes could perfectly be used but in our case any echo after the 2nd one (V_2) does not present an acceptable signal to noise ratio.

2.3 Analysis of the reflection coefficients.

As previously mentioned, the validity of the attenuation coefficient provided by the ultrasonic pulse echo immersion technique will rely on obtaining the right value of the reflection coefficient on both faces of the specimen. Thus, the question is clear: how can we obtain the reflection coefficient value?

2.3.1 Classical or conventional approach.

Conventionally the reflection coefficients have been calculated using the elastic wave propagation theory described above. Expressions for the reflection and transmission coefficients were derived under the assumption of a perfectly bonded interface. Recalling Equations (2.12) and (2.13), if the acoustic impedances of the

materials that compose the interface are known, the reflection coefficient can be calculated. Once its value is obtained it can be introduced in the attenuation coefficient Equation (2.19) to complete the measurement.

Works by Nolle and Mowry [5], McSkimin [6] and Kline [7] follow this approach in order to calculate the attenuation coefficient. The physical configurations of their experiments were presented in Chapter 1. Henceforth, below, only the mathematical expressions used by these works will be explained.

In the first place, Nolle and Mowry [5] used the following expression

$$correction = 4\log_{10}\left[\frac{1}{1-p}\right],\ p = \left[\frac{(\rho c)_l - (\rho c)_s}{(\rho c)_l + (\rho c)_s}\right]^2 \tag{2.23}$$

where ρ and c are the density and longitudinal wave speed, respectively, and l and s stand for liquid and specimen, respectively.

Indeed, this is based on the expression derived before for the reflection coefficient (Equation 2.12).

In the second place, McSkimin [6] proceeded as follows,

$$\alpha = \frac{1}{h}\ln\left(\frac{W_1}{W_2}T\right),\ T = \frac{4(\rho c)_l(\rho c)_s}{[(\rho c)_l + (\rho c)_s]^2}, \tag{2.24}$$

Again, this relies on the expression derived before for the transmission coefficient (Equation 2.13).

Finally, Kline [7] performed his calculation as described below,

$$\alpha = \frac{1}{2h}\ln\left(T_{12}T_{21}\frac{R_{21}}{R_{12}}\right)$$
$$R_{ij} = \frac{(\rho c)_i - (\rho c)_j}{(\rho c)_1 + (\rho c)_2},\ T_{ij} = \frac{2(\rho c)_i}{(\rho c)_1 + (\rho c)_2} \tag{2.25}$$

In all these cases, theoretical values for the reflection coefficient were used.

Hence, it can be inferred from these expressions that the previous works based their attenuation coefficient calculation on the perfectly bonded interface assumption.

Summarizing: the classical or conventional approach relies on the assumption of a perfectly bonded interface between the immersion liquid and the specimen. This assumption will be called Assumption 1.

Assumption 1: Perfectly bonded interface between the immersion liquid and the specimen.

2.3.2 Modern versions of the technique.

Recently, some alternative approaches to apply the ultrasonic pulse echo immersion technique have been carried out, providing some advantages beyond those of the classical or conventional approach. Studies conducted by Umchid [8], Youssef and Groban [9] and He and Zheng [10] present themselves as improved procedures to calculate the attenuation coefficient of a material using the ultrasonic pulse

echo/through transmission immersion technique. As the physical description of the tests setups was provided in Chapter 1, only the mathematical basis is now presented.

In the first place, Umchid [8] formulated the attenuation coefficient by comparing the signals from two specimens with different thickness in the following manner,

$$\alpha_f = \frac{20}{d_2 - d_1}\left(\log_{10} V_{d2} - \log_{10} V_{d1}\right) \tag{2.26}$$

It is important to realize that there is no need to calculate reflection or transmission coefficients in this relation.

In the second place, Youssef and Groban [9] used the pulse echo mode in addition to a signal I_w obtained when there is no specimen immersed. Signals I_w, I_3 and I_{12} can be combined to obtain the following two equations:

$$\frac{I_3}{I_w} = R \tag{2.27a}$$

$$\frac{I_{12}}{I_w} = \left(1 - R\right)^4 e^{-\alpha 2h} \tag{2.27b}$$

where I_3, I_{12} and I_w are known (measured by the transducer)

Once again, this procedure does not require the knowledge of the reflection coefficients since their value becomes an unknown of the system of equations that can be solved together with the attenuation coefficient of the specimen.

Finally, He and Zheng [10] provided a third method that utilizes two transducers to record four signals. Signal A_w is recorded without the specimen. Operating with the transmitted signal A_5 on the one hand and with the reflected signals A_1 and A_2 on the other hand, the following two equations are derived,

$$\alpha = \frac{\ln T}{L} + \ln\left(\frac{A_w}{A_s}\right) \tag{2.28a}$$

$$\alpha = \frac{\ln T}{2L} + \frac{1}{2L}\ln\left(\frac{A_1}{A_2}\right) \tag{2.28b}$$

The term ln(T) can be substituted from Equation (2.28a) into Equation (2.28b) to arrive at the following expression for the attenuation coefficient,

$$\alpha = \frac{1}{L}\left[\ln\left(\frac{A_1}{A_2}\right) - \ln\left(\frac{A_w}{A_s}\right)\right] \tag{2.29}$$

Similar to the previous cases, the reflection or transmission coefficients need not be known in order to calculate the attenuation coefficient.

Although not easily perceived, as in the classical approach, there are two assumptions hidden within the calculations associated with the modern versions. First, the procedure proposed by Umchid [8] assumes that the reflection and transmission coefficients of both specimens are equal. In principle, this seems a logical assumption. Another assumption relates to the setups suggested by Youssef and Groban [9] and He and Zheng [10], which supposed the reflection and transmission coefficients of both faces of the specimen to be identical.

Summarizing, the modern versions offer the advantage of providing the attenuation coefficient without needing the values of the reflection or transmission coefficients. Nevertheless, one of the modern approaches requires same reflection and transmission coefficients for the two specimens it uses and the others assume equal reflection and transmission coefficient for both faces of a unique specimen. These assumptions will be referred to as Assumption 2a and 2b, respectively.

Assumption 2a: If two specimens are used, they must have equal reflection coefficients.

Assumption 2b: Reflection coefficients of both faces of a unique specimen must be equal in absolute value.

The question at this point is whether the three previously described assumptions hold true for all materials. If they do, any of the techniques described before would be valid and adequate to measure attenuation coefficients. However, if any of those assumptions falters for certain cases, then the corresponding method would provide an erroneous value of the attenuation coefficient for those cases and therefore that method would be invalid.

Regarding Assumption 1, it is somewhat intuitive to imagine the cases where difficulties could arise. Assumption 1 relies on the idea of a perfectly bonded interface. Since throughout this study all cases will consist of a solid material immersed in water, it is convenient to investigate the nature of the bond between water and a solid material. The physics behind this bond are based on Van der Waals forces and more specifically on what is called dispersive adhesion. Dispersive adhesion is the

force that dominates the wetting phenomenon which is characterized by the contact angle between a water droplet and the solid surface upon which it is sitting. Thus, a small contact angle means a high adhesion force between water and the solid material. On the other hand, a large contact angle implies a low adhesion force and therefore a weak bond between water and the solid material. In these cases, the solid material is called hydrophobic and the attraction between water molecules is stronger than those between water molecules and the solid material atoms/molecules. If a material of this type is considered, it could occur that the force exerted by a tensile stress wave at the interface between the solid material and water could break the interface bond and consequently Assumption 1 would also be broken. This is perfectly possible and so experiments should be conducted to verify this condition. In addition, Assumptions 2a and 2b should be considered for these cases where special behavior is found at this type of interfaces.

The answers to the questions presented above are tied to the technique of measuring the reflection coefficients. Indeed, comparing the reflection coefficient values obtained via measurements with the theoretical values provided by Equation (2.12) under Assumption 1 will determine if the perfectly bonded interface exists or not. A method to conduct these measurements was found and is described in Chapter 3.

References

[1] Kolsky, H. *Stress Waves in Solids.* Dover Publications, 1963.

[2] Graff, Karl F. *Wave Motion in Elastic Solids.* Dover Publications, 1991.

[3] Sadd, Martin H. *Elasticity: Theory, Applications and Numerics.* Academic Press, Ed 2, 2009.

[4] Rogers, P. H., and Van Buren, A. L. "An Exact Expression for the Lommel-Diffraction Correction Integral." *The Journal of the Acoustical Society of America.* Vol. 55, (4) pp. 724-728. (1974).

[5] Nolle, A. W. "Measurement of Ultrasonic Bulk-Wave Propagation in High Polymers." *The Journal of the Acoustical Society of America.* Vol. 20, (4) pp. 587. (1948).

[6] McSkimin, H. J. *Physical Acoustics: Principles and Methods,* W. P. Mason ed. Vol. 1A: Academic Press, 1964.

[7] Kline, R. A. "Measurement of Attenuation and Dispersion using an Ultrasonic Spectroscopy Technique." *The Journal of the Acoustical Society of America.* Vol. 76, (2) pp. 498-504. (1984).

[8] Umchid, S. "Frequency Dependent Ultrasonic Attenuation Coefficient Measurement." *The 3rd International Symposium on Biomedical Engineering.* Vol. , ( ) pp. 234-238. (2008).

[9] Youssef, M. H., and Gobran, N. K. "Modified Treatment of Ultrasonic Pulse-Echo Immersion Technique." *Ultrasonics.* Vol. 39, (7) pp. 473-477. (2002).

[10] He, P., and Zheng, J. "Acoustic Dispersion and Attenuation Measurement using both Transmitted and Reflected Pulses." *Ultrasonics.* Vol. 39, (1) pp. 27-32. (2001).

CHAPTER 3

EXPERIMENTAL METHODS

As concluded in Chapter 2 (Theory), it is desired to measure the reflection coefficient between water and different solid materials. Below a method that can carry out this measurement is described in detail.

3.1 Reflection coefficient measurement.

The goal of these measurements is to challenge the validity of the assumptions adopted by the current ultrasonic techniques. Different procedures to carry out the measurement can be applied for each assumption.

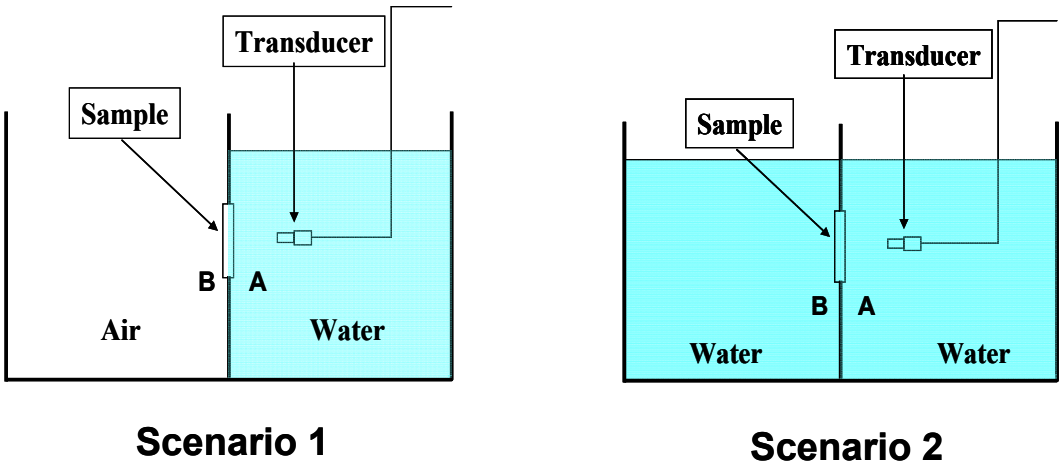

Figure 9. Procedure used to test Assumption 1.

Testing Assumption 1: Perfectly bonded interface.

In order to measure the reflection coefficient a simple procedure can be used. Figure 9 illustrates this procedure where a tank has been divided in two spaces by a middle wall. This middle wall seals one side from the other and also holds the specimen. Two signals are necessary to perform the measurement: the first signal corresponds to a scenario in which only side A of the tank is filled with water. Once the transducer is placed perpendicular to the specimen and at the proper distance, it can not be moved until the test is completed. After the first signal is recorded, side B of the tank is filled with water and the second signal is recorded. The only difference between the two signals is the presence or absence of water on side B, all other parameters remaining constant throughout the entire test. It is assumed that the two pulses generated by the transducer have equal or very similar amplitude. Recalling Equation (2.15) corresponding to the first echo of the signal, let us apply it to the two different scenarios of this test.

Recall: $$V_1 = V_0 T_A^2 R_B D(s_1) e^{-\alpha 2h} \tag{2.15}$$

The first scenario consists of having the specimen backed by air on side B. This implies that the reflection coefficient at that interface is 1. Hence, the amplitude of the first echo for this first scenario is:

$$V_1^{(1)} = V_0 T_A^2 1 D(s_1) e^{-\alpha 2h} \tag{3.1}$$

The second scenario is identical to the first one with the exception that side B is backed by water, i.e., having a water-specimen interface. This is the unknown

reflection coefficient that must be measured and so it will be called R_B. Thus, the amplitude of the first echo in this second scenario is:

$$V_1^{(2)} = V_0 T_A^2 R_B D(s_1) e^{-\alpha 2h} \tag{3.2}$$

As it can be quickly observed, the only difference between the two echoes is the reflection coefficient R_B. Therefore, if the second signal is divided by the first, the result will be the reflection coefficient R_B corresponding to the water-solid material interface.

$$R_B = \frac{V_1^{(2)}}{V_1^{(1)}} \tag{3.3}$$

A similar procedure can be followed to measure the reflection coefficient R_A. Once these measurements have been obtained, they can be compared to the theoretical values of the reflection coefficient given by Equation (2.12). If the values match, it will mean that a perfectly bonded interface exists and therefore Assumption 1 is valid. However, if the values do not match, it will mean that the condition of a perfectly bonded interface is not fulfilled, so Assumption 1 is invalid making the classical approach of measuring attenuation invalid.

Testing Assumptions 2b and 2a: equal reflection coefficients on both faces of the same specimen and equal reflection coefficients every test.

In order to find out if the reflection coefficients on both faces of the specimen are equal when the specimen is fully immersed in water an extension of the procedure used with Assumption 1 can be used. First, that procedure is repeated to provide the reflection coefficient on side B. Now that the specimen is fully immersed, it is desired to know if the reflection coefficient on side A is the same or different from reflection

coefficient B. In order to measure R_A, the transducer is moved to side B. Everything else remains untouched. Once the transducer is moved to side B and placed perpendicular to the specimen, a signal is recorded (signal 3). Next, side A of the tank is emptied and another signal is recorded (signal 4). These two signals will provide the reflection coefficient R_A corresponding to a specimen fully immersed. It is important to realize that the two reflection coefficients of a fully immersed specimen are measured by this procedure and they will reveal whether the reflection coefficients on both sides of the specimen are equal when it is fully immersed in water. If they are equal, Assumption 2b is valid and the techniques based on it will consequently be valid also. However, if the reflection coefficients are different on each side, Assumption 2b will be invalid, also indicating a breakdown in Assumption 1.

Furthermore, if the previously described procedure for Assumption 2b is performed at least twice, causing the specimen to undergo at least one additional immersion, and the reflection coefficients measured in the first immersion are compared to those measured in later immersions, Assumption 2a can be tested. Note that in order for Assumption 2a to be valid, the reflection coefficients do not need to be equal on both faces, but it is enough if they are consistent every time the specimen is fully immersed in water.

After different immersions the specimens were placed in a cabinet to dry at room temperature.

3.2 Materials.

Three different materials were chosen in order to verify Assumptions 1, 2a and 2b by means of the measured reflection coefficients. It was suggested at the end of Chapter 2 that a material that presents a large contact angle for water droplets might violate the conditions presented. Hence, Teflon was chosen. In addition, a typical engineering plastic such as Polycarbonate was also used as well as a hydrophobic substance commercially known as Hydrobead –T. The latter was chosen since, as in the case of Teflon, it is expected that its interface bond with water might not be able to resist the ultrasonic stress pulse at all instants of time.

The specimens tested consisted of: two square plates of Teflon with dimensions 3 x 3 x 0.375 in and two square plates of Polycarbonate with dimensions 4 x 4 x 0.5 in. These dimensions were chosen to avoid lateral wall reflections interacting with the first two echoes. One of the Polycarbonate plates was coated with Hydrobead-T on only one of the faces. Once the coating was applied it was set aside to cure for 24 hours at room temperature.

At this point it is important to remember the general idea behind this work so far. In the first place, the reflection coefficients of these plates with water will be measured and later compared with the theoretical values of the reflection coefficients given by Equation (2.12) in order to examine Assumption 1. This equation requires a perfectly bonded interface between **two** media. Nonetheless, the specimens composed of the Polycarbonate plate with the coating will now have a triple media interface. Therefore,

a new derivation of the reflection coefficient for this new case is required. Research has shown that this case has already been solved, e.g.. Scott and Gordon [1] and also Rose and Meyer, and Vincent [2, 3]. The problem consists of a thin layer embedded between two semi-infinite media and a harmonic pulse reaching that interface perpendicularly. It is assumed that the length of the pulse is larger than the thickness of the thin layer. In this case, there will be multiple reflections and transmissions as it can be seen in Figure 10.

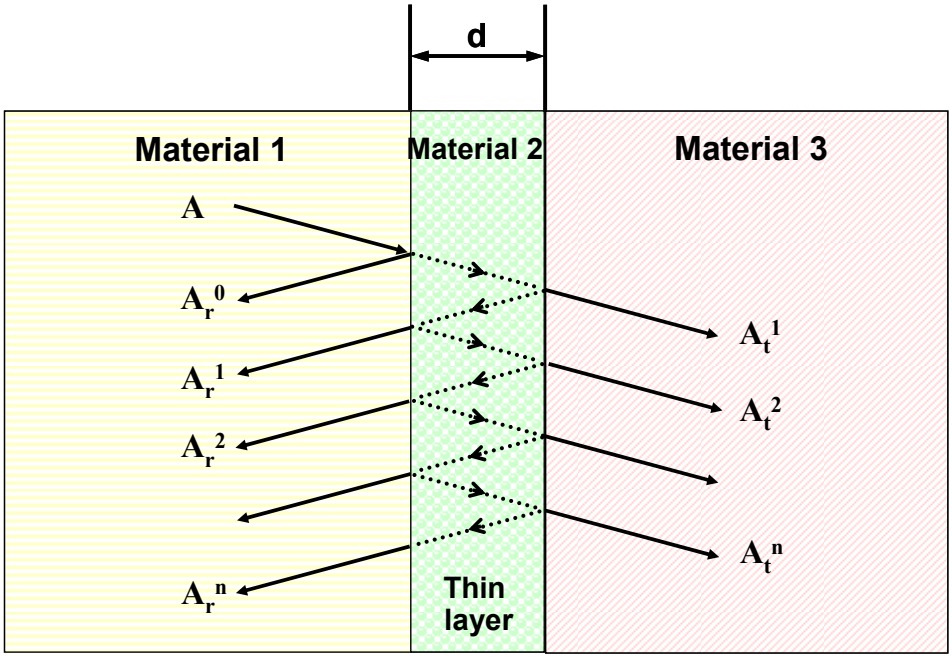

Figure 10. Reflection and transmission of a plane longitudinal wave at three media interface composed of a thin layer embedded between two semi-infinite media.

The general terms for the n^{th} reflected and transmitted pulses would be, respectively:

$$A_r^n = A\left[R_{12} + T_{12}T_{21}R_{21}^{n-1}R_{23}^n e^{-j2nk_2 d}\right], \text{ for } n = 1, 2, 3, \ldots \quad (3.4)$$

where the first reflection, AR_{12}, is considered the 0th (A_r^0), A is the amplitude of the incident pulse, R and T are the reflection and transmission coefficients given by Equations (2.12) and (2.13) respectively, k_2 is the wave number in the thin layer material and d is the thickness of the thin layer.

$$A_t^n = A\left[T_{12}T_{23}e^{jk_3d}\left(R_{21}R_{23}\right)^{n-1}e^{-j(2n-1)k_2d}\right], \text{ for } n = 1, 2, 3, \ldots \tag{3.5}$$

where k_3 is the wave number in the third medium.

Considering an infinite number of reflected and transmitted pulses and summing them, the reflection and transmission coefficients are derived and shown below:

$$R = R_{12} + T_{12}T_{21}R_{23}\frac{e^{-j2k_2d}}{1 - R_{23}R_{21}e^{-j2k_2d}} \tag{3.6}$$

$$T = T_{12}T_{23}\frac{e^{j(k_3-k_2)d}}{1 - R_{23}R_{21}e^{-j2k_2d}} \tag{3.7}$$

Note how in this case the reflection and transmission coefficients depend on the frequency (f) of the incident pulse via the wave number $k = \frac{2\pi}{c}f$, where c is the wave speed. In addition, they are a complex quantity. The only parameter of interest for this study is the magnitude. Therefore, focusing on the reflection coefficient, its magnitude can be calculated as

$$R = R_{12} + \left|\frac{T_{12}T_{21}R_{23}\left(\cos\theta - R_{21}R_{23} - j\sin\theta\right)}{\left(1 - R_{21}R_{23}\cos\theta\right)^2 + \left(R_{21}R_{23}\sin\theta\right)^2}\right| \tag{3.8}$$

where $\theta = \frac{4\pi d}{\lambda_2}$.

Note that by definition the wave number $k_2 = \frac{2\pi}{\lambda_2}$ where λ_2 is the wavelength in medium 2.

For the case in which the thickness of the layer *d* is much smaller than the wavelength of the pulse in the layer´s material, the quantity $4\pi d/\lambda$ becomes negligible. Inserting this condition ($\theta \approx 0$) in Equation (3.8) yields the following result for the reflection coefficient

$$R = \frac{R_{12} + (1 - R_{12})^2 R_{23}}{(1 - R_{21} R_{23}) R_{12}} \tag{3.9}$$

Introducing the acoustic impedances in the transmission and reflection coefficients present in Equation (3.9) and performing the corresponding mathematical operations, it can be demonstrated that the reflection coefficient *R* reduces to:

$$R = \frac{Z_3 - Z_1}{Z_3 + Z_1} \tag{3.10}$$

which is the same expression derived in Chapter 2 for the two media interface. In other words, the presence of a layer that is narrow in comparison to the wavelength impinging upon it does not affect the reflection coefficient.

Regarding the specimens used in this work, the thickness of the hydrophobic coating applied on one of the Polycarbonate plates was measured via an optical microscope (see Figure 11). The average value for the thickness was approximately 25 μm. The wave speed in the coating is unknown, but due to its polymeric nature a range for the wavelength values for this material was assumed to be in the range of 1.5 to 3

mm, corresponding to a thickness that is two orders of magnitude below the value of the wavelength. Introducing these values in Equation (3.8) provides practically the same magnitude for the reflection coefficient as the case for which there is no coating: 0.280130 and 0.280123 respectively. Therefore Equation (2.12) will also be used for the coated Polycarbonate plate.

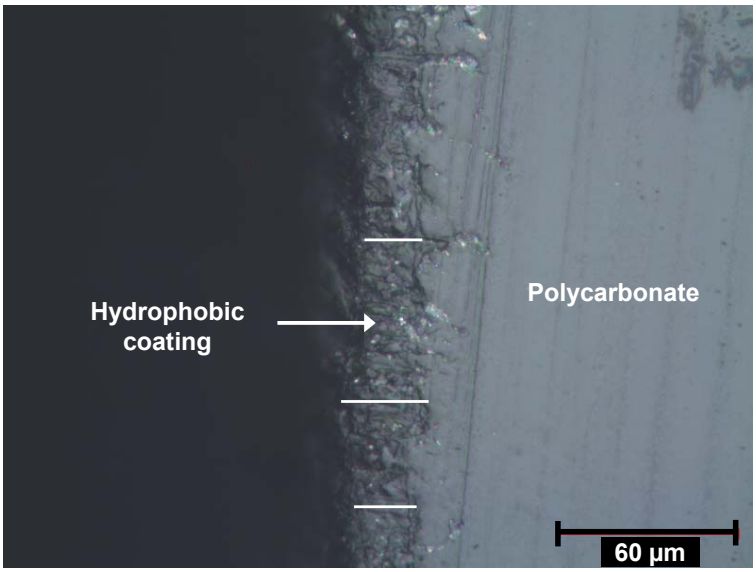

400x

Figure 11. Optical microscope image (400x) of the hydrophobic coat applied to the Polycarbonate specimen.

The specimens just described will be used to test the three assumptions adopted by the different approaches of the ultrasonic pulse echo immersion technique. Once a valid approach for the technique is found, it will be used to measure the attenuation coefficient of particulate composites. The particulate composites tested in this work consist of solid glass microspheres embedded in an epoxy matrix. The specimens have a cylindrical geometry with a diameter of 2.75 in and a thickness of approximately 0.375 in. Two types of solid glass microspheres were purchased from Potter Industries under the category of A-Glass Spheriglass. The first type of microspheres is called

2530 A-Glass and the mean value for the diameter is between 60-70 microns (μm) while the second type is known as 3000 and the mean value for the diameter is between 30-50 microns (μm). More detailed technical information on A-Glass is provided at the end of this thesis in the Appendices. With respect to the epoxy, Epothin Resin and Hardener from Buehler were used.

There will be four specimens composed of 2530 type microspheres and four specimens composed of 3000 type microspheres. For each type of glass microspheres, the specimens will have a 5, 10, 20 and 30 % volume fraction of glass microspheres. In order to calculate the mass of microspheres necessary to obtain the desired volume fractions the following equations were used:

$$m_p = XV\rho_p \tag{3.11}$$

$$m_h = \frac{(1-X)V\rho_{ep}}{1+\frac{5}{1.95}} \tag{3.12}$$

$$m_{res} = m_h \frac{5}{1.95} \tag{3.13}$$

where X is the volume fraction desired, V is the volume of the mold, ρ is density and the subscripts p, ep, h, res stand for particles, epoxy, hardener and resin respectively.

3.3 Manufacturing process.

A few challenges appear at the time of manufacturing these particulate composites. In the first place, the glass microspheres quickly sink at the bottom of the uncured epoxy due to their higher density. Secondly, air bubbles are likely to be

trapped during the molding process and stay inside the specimen once curing is complete. In order to overcome the first challenge a rotating apparatus was built to rotate the molds while the specimen is curing. In this manner, the glass particles will remain in their initial positions ensuring a uniform spatial distribution of the microspheres will be achieved. This process necessitates a fully closed mold, which brings up the possibility of trapping air bubbles. In order to ensure that all the air evacuates the mold while closing, a customized design was implemented. The mold consists of a main body with a cylindrical hole, a removable tap on the bottom firmly held to the main body, a piston with a conically shaped interior cavity and a top piece attached to the main body that contains a spring to hold the piston down. This can be easily visualized in the schematic of Figure 12.

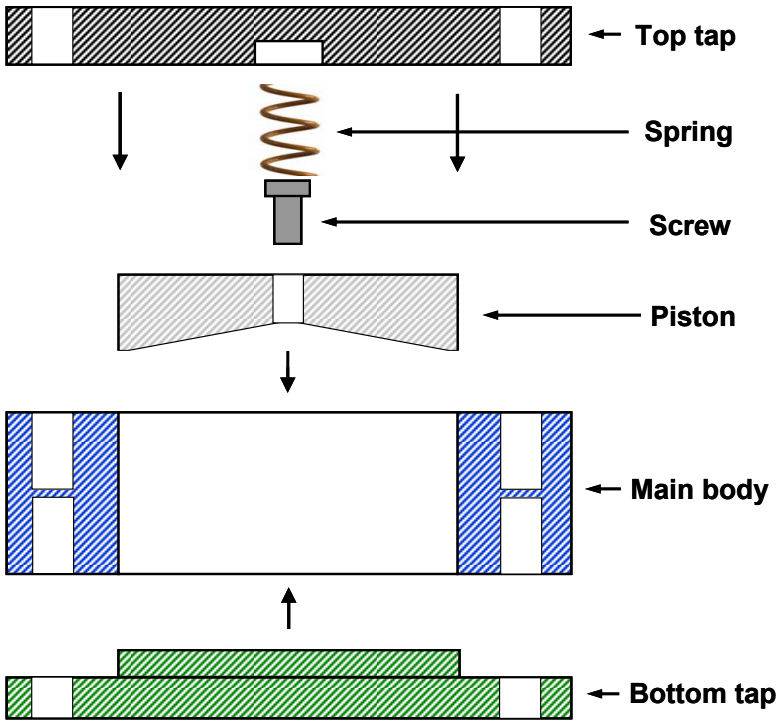

Figure 12. Schematics of the mold components and assembling.

The procedure for using the mold is as follows: first, the bottom tap is inserted in the main body and firmly held with the corresponding screws. Then, the mixture of epoxy and glass microspheres is poured into the main body. Next, the piston is slowly pushed down along the cylindrical hole of the main body. The conically shaped interior surface of the piston drives the air towards the center of the mold while it is being evacuated through the center hole in the piston. As the piston slides down the main body, the air inside comes out of the piston hole. Once the piston has moved a certain distance, all the air inside will have been evacuated and the mixture of epoxy and glass will start exiting. At this point the hole in the piston is plugged by means of a screw. Finally, a spring is compressed between the piston and the top piece, which is fixed to the main body with several screws. The compressed spring keeps the mixture under some pressure so that no air is reintroduced during the rotation process and the mold walls are always kept in contact with the specimen as it cures and contracts.

Prior to this, the mixture of epoxy and glass microspheres was held under vacuum (10 torr) for approximately 15 minutes to remove the air introduced during the mixing process.

Once the mold is sealed, it is placed in the rotating device for at least 2 hours to guarantee a uniform distribution of the microspheres inside the epoxy matrix.

3.4 Equipment.

It is now time to describe the equipment necessary to carry out the experiments planned for this thesis. The ultrasonic testing equipment utilized consists of a

pulser/receiver unit, an ultrasonic transducer and an oscilloscope. Besides this, a tank with a separating wall that seals both sides and is able to hold a specimen will be needed, as well as transducer holders.

The pulser/receiver unit generates the high voltage impulse that excites the transducer and processes all the signals coming from the transducer via several filters and amplifiers to provide an adequate output signal. Nowadays, there exist several variations of this device. In this work, the 5058PR from Panametrics was employed. One of the most important characteristics of this pulser/receiver is that its output is limited to +1.5 V and -1.5 V. If the signal coming from the transducer exceeds that voltage after amplification, the exceeding part of the signal will be cut off at the final stage of the pulser/receiver and it will not appear in the output signal. Therefore, the user must be very careful and use the attenuator setting to ensure that the part of the signal that is of interest is within that voltage range. The excitation voltage used for the transducers was 400 V. The manufacturer warns against using higher voltages to avoid damaging the transducers.

The ultrasonic transducers are responsible for generating the incident ultrasonic wave or pulse and measuring the corresponding reflections or transmissions originated by that incident pulse. There are many different types of ultrasonic transducers specialized in specific applications and based on different frequencies. Their fundamentals lay on the piezoelectric effect, which states that an electric charge is generated in certain materials in response to applied mechanical stress. Reversibly, an

applied electric field generates mechanical deformation or strain in the material. The materials that undergo this phenomenon are called piezoelectric materials. Every transducer has an active element made of a piezoelectric material. This active element receives the excitation signal that causes it to vibrate at a certain frequency and thus generates an ultrasonic pulse that is then transmitted to a coupling agent in contact with the specimen. In a similar manner, an ultrasonic wave travelling through the specimen reaches the coupling agent and is transmitted to the active element of the transducer. This wave deforms the active element, generating an electric voltage according to the piezoelectric effect. This voltage is proportional to the deformation of the active element and therefore to the amplitude of the ultrasonic wave that comes from the specimen. Thus attenuation can be measured using this technology.

Another important concept to take into account when using a transducer is the nearfield concept. The nearfield is the region directly in front of the transducer where the generated pulse amplitude varies widely due to constructive and destructive interference from the vibrating active element. The nearfield is finite in length and its boundary is considered the natural focus of the transducer where the generated pulse amplitude reaches a maximum in a smooth shape that will drop gradually, as it is shown in the work developed by Rogers and Van Buren [4]. In fact, function *D(s)* derived from that work predicts the amplitude of the generated pulse at any radial distance from the transducer including the nearfield. This expression is plotted in Figure 13.

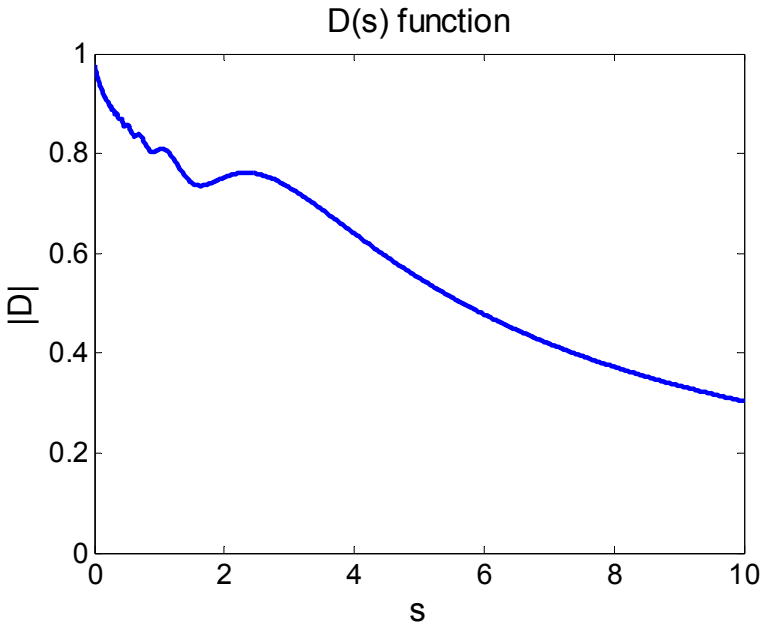

Figure 13. Beam spreading function, D(s).

Every transducer has its own nearfield length since it depends on the radius and frequency as well as on the wave speed of the media in which the pulse is first transmitted (in this case water). In the case of immersion transducers, it is recommended that the transducer be placed at distance beyond its nearfield from the specimen so that a smooth pulse is transmitted into the specimen. The nearfield length, *N*, can be easily calculated with the following formula:

$$N = \frac{D^2 f}{4c} \tag{3.14}$$

where *D* is the diameter of the transducer, *f* is the frequency of the wave and *c* is the wave speed in the material where the nearfield needs to be calculated.

In the present work, the transducers used were immersion transducers. All tests were carried out with a 1 MHz immersion transducer manufactured by Panametrics

whose nearfield is 27 mm. Immersion transducers are high quality transducers that use a liquid (preferably water) as a coupling agent between the transducer and the specimen.

In addition, an oscilloscope is required to visualize and record the output signal coming from the pulser/receiver unit. In this case, a Tektronix TDS 3014B with a sampling rate capability of 1.25GS/s was utilized. The signals were saved on a floppy disk to be analyzed later using a computer.

3.5 Signal Analysis.

As just mentioned, a 1 MHz immersion transducer was used to carry out the experiments in this work. This single value can be misleading since ultrasonic transducers cannot generate single frequency waves. The vibration induced in the active element by a voltage impulse generates a finite spectrum of ultrasonic waves, that is to say, the ultrasonic pulse generated by the transducer is the summation of many single frequency waves. This spectrum possesses a Gaussian shape in which there is a dominant frequency called the center frequency. This center frequency is the one that characterizes the transducer. Therefore, the immersion transducer previously mentioned has a 1 MHz center frequency and its useful spectrum will range between 0.7 and 1.2 MHz.

It is always more useful and interesting to find out how single frequency waves propagate and behave within a material rather than a summation of multiple single

frequency waves with different amplitudes. The signals obtained from the transducer and the pulser/receiver are always in time domain, that is, they provide the amplitude of the signal at different instants of time. As was explained, this signal is the summation of multiple single frequency waves and so the behavior observed in time domain is the behavior of the summation as a whole, but not the behavior of each single wave frequency wave. Hence, if the single frequency waves that compose the signal behave different from each other as they propagate through the material, this will not be appreciated in the time domain analysis. Indeed, time domain is not the appropriate domain to analyze the signal since the behavior of all single frequency waves is desired. Therefore, it is necessary to transform the time domain signal captured during the experiments to the frequency domain where every single frequency wave forming the signal can be analyzed one by one. This transformation is possible by performing the Fast Fourier Transform (FFT), which is an algorithm that computes the discrete Fourier Transform of the discrete time domain signal measured. The FFT can be easily performed with MATLAB with an already built in command.

Throughout this thesis, all the signal analysis calculations are computed in the frequency domain. This is extremely important when calculating the attenuation coefficient of a material since as it was introduced in Chapter 1 it strongly depends on frequency. By working in the frequency domain, the attenuation coefficient is already calculated as a function of frequency.

The procedure followed in this thesis is to analyze every echo within a signal independently. In other words, only the instants of time that belong to a particular echo undergo a FFT. This way, the spectrum of only that particular echo is obtained without being influenced by any other region of the time domain signal. This process can be more easily understood with an example.

Let us consider a time domain signal corresponding to a test conducted on a Polycarbonate plate with a 1 MHz immersion transducer. Figure 14 shows the time domain signal.

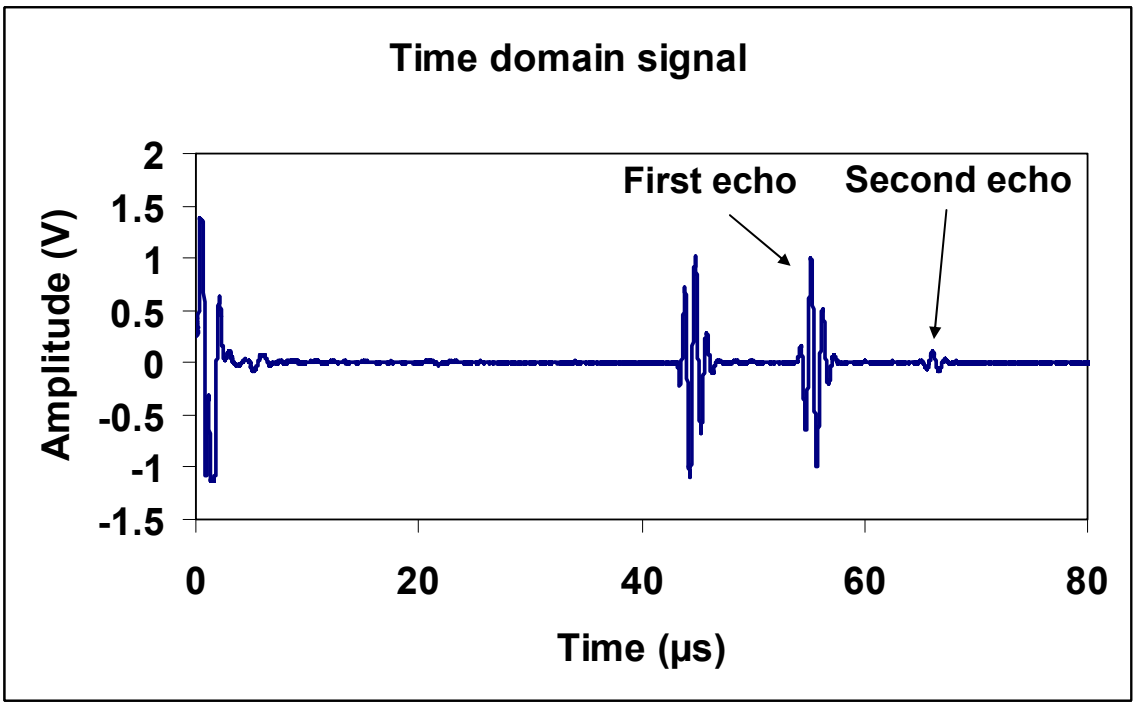

Figure 14. Time domain signal obtained during a test.

The first and second echoes are indicated with an arrow each. The procedure simply consists of zooming on each echo separately. Figure 15 shows a zoom on echoes 1 and 2 respectively.

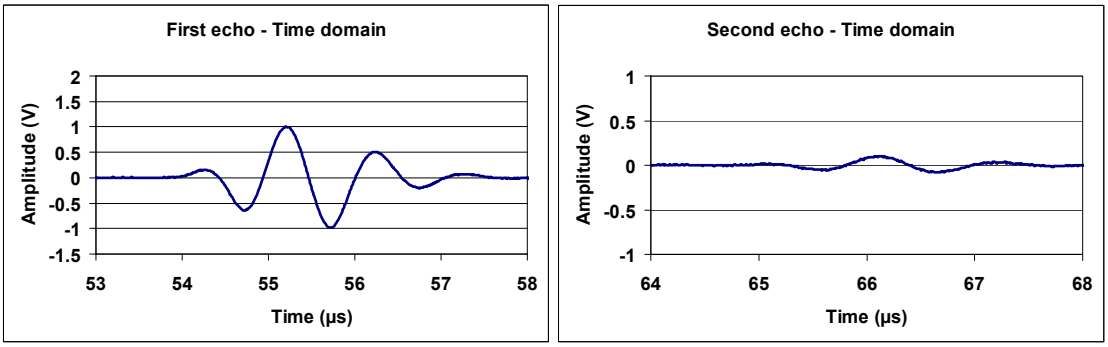

(a) (b)

Figure 15. a): First echo in time domain. b): Second echo in time domain.

Each echo is treated independently in order to obtain its frequency spectrum. Thus, looking at one of the echoes, an FFT is performed on the interval of time shown on the zoomed window. Finally, Figure 16 shows the spectra obtained after performing the FFT for the first and second echoes, respectively.

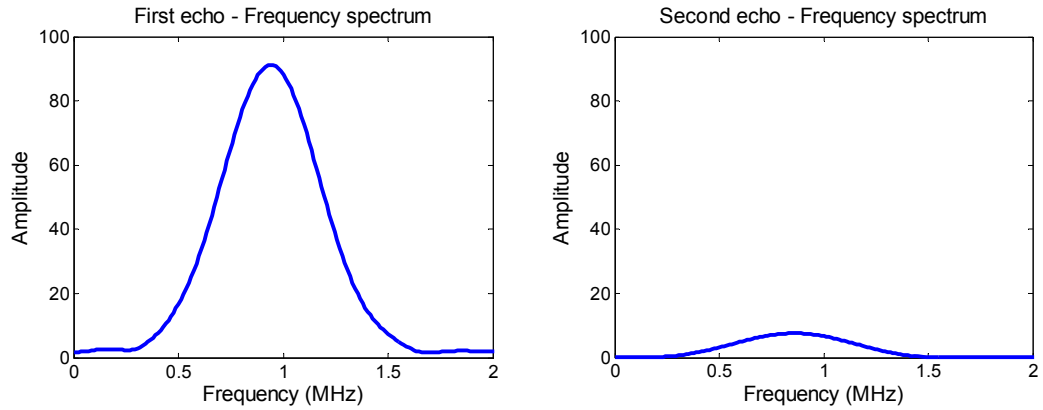

(a) **(b)**

Figure 16. a): First echo frequency spectrum. b): Second echo frequency spectrum

Once the spectra of the echoes are obtained, the corresponding calculations developed in Chapter 2 proceed on a frequency by frequency basis. For example, if the attenuation coefficient at 1 MHz is wanted then the amplitudes of the echo spectra that

correspond to the 1 MHz frequency are used in Equation (2.19) as well as the proper wavelength involved in the D(s) function. The wavelength is easily calculated from the well known relation

$$c = \lambda f \tag{3.15}$$

where c is the longitudinal wave speed on the material and f is the frequency (in this example, 1 MHz). Likewise, if the attenuation coefficient at 0.9 MHz is wanted, then the amplitudes of the echo spectra that correspond to the 0.9 MHz frequency are used in Equation (2.19) with the proper wavelength (λ) for the D(s) function.

In order to perform the calculations for the full spectrum a MATLAB code was developed and it is presented in the Appendix.

References

[1] Scott, W. R., and Gordon, P. F. "Ultrasonic Spectrum Analysis for Nondestructive Testing of Layered Composite Materials." *The Journal of the Acoustical Society of America.* Vol. 62, (1) pp. 108-116. (1977).

[2] Rose, J. L., and Meyer, P. A. "Ultrasonic Signal Processing Concepts for Measuring the Thickness of Thin Layers." *Materials evaluation : ME.* Vol. 32, (12) pp. 249-258. (1974).

[3] Vincent, A. "Influence of Wearplate and Coupling Layer Thickness on Ultrasonic Velocity Measurement." *Ultrasonics.* Vol. 25, (4) pp. 237-243. (1987).

[4] Rogers, P. H., and Van Buren, A. L. "An Exact Expression for the Lommel-Diffraction Correction Integral." *The Journal of the Acoustical Society of America.* Vol. 55, (4) pp. 724-728. (1974).

CHAPTER 4

RESULTS

Now that the experimental procedure, equipment and signal analysis have been explained, it is time to conduct the experiments and tests.

Regarding the investigation on the ultrasonic pulse echo immersion technique assumptions, the Teflon specimens were the first to be tested. As described in Chapter 3, two different procedures can be followed to examine the different assumptions. The first one was responsible for testing Assumption 1. The second one was aimed to test Assumption 2b but was also shown to simultaneously test Assumption 1. Upon repeating this second procedure several times, Assumption 2a can also be assessed. Hence, this second procedure was employed to carry out the experiments. Some of the results are presented below for the different tests conducted. The figures show the measured experimental values in comparison to the theoretical values provided by Equation (2.12) under Assumption 1.

Test 1 – Teflon plate 1

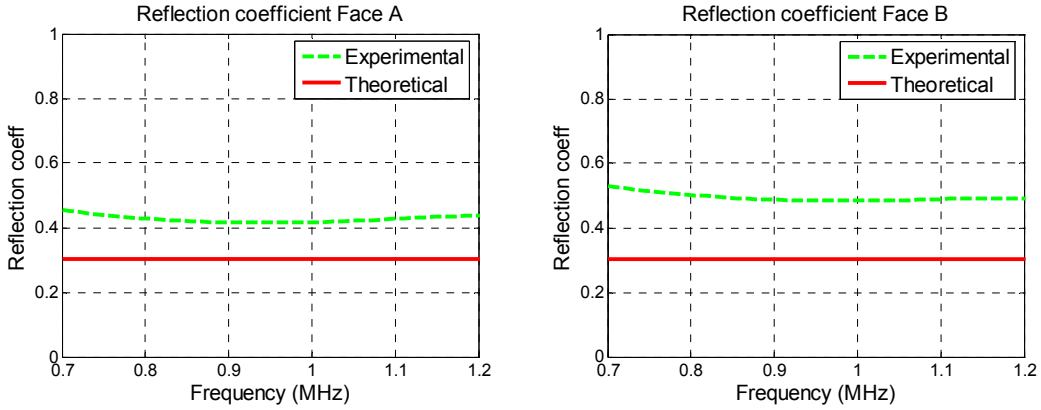

Figure 17. Reflection coefficient measurement for Teflon.

Test 2 – Teflon plate 1

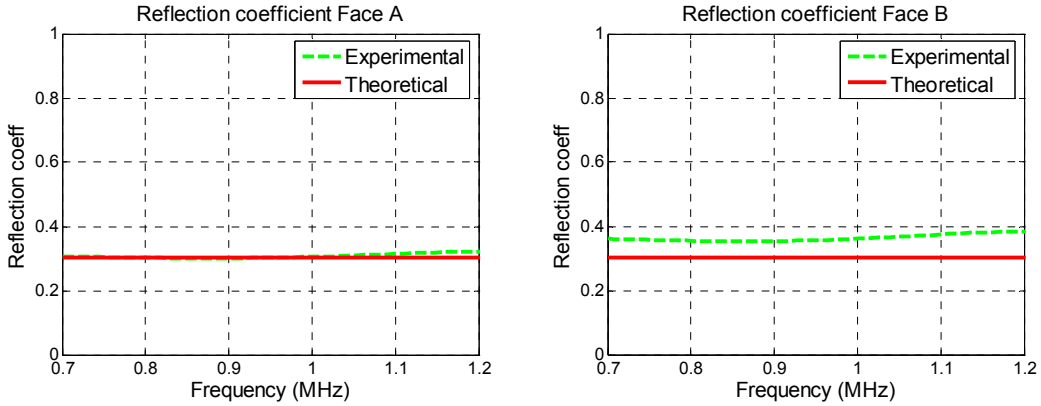

Figure 18. Reflection coefficient measurement for Teflon.

Test 3 – Teflon plate 2

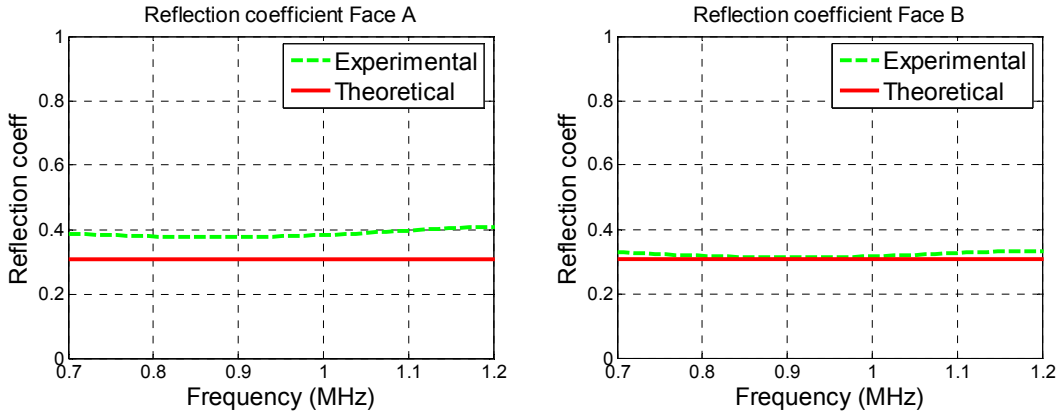

Figure 19. Reflection coefficient measurement for Teflon.

Test 4 – Teflon plate 2

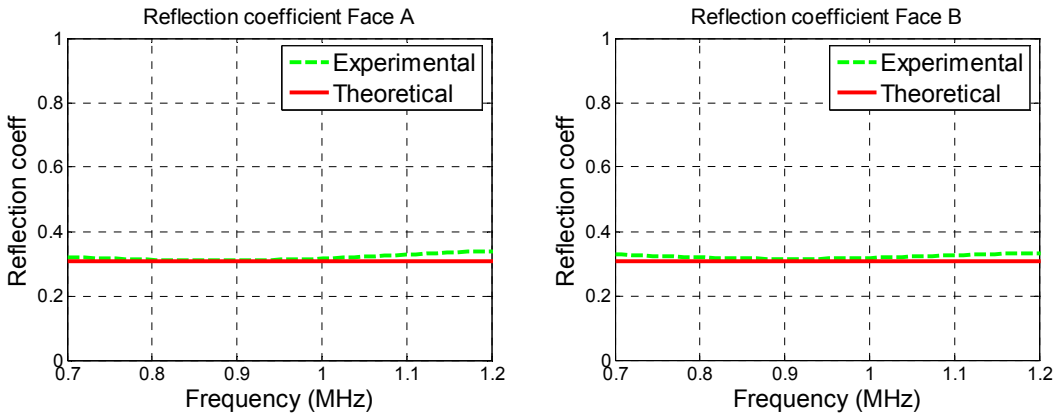

Figure 20. Reflection coefficient measurement for Teflon.

Figures 17 to 20 show results from the tests conducted on Teflon and represent the reflection coefficients on the two faces (A and B). First, it can be clearly seen how most of the times the reflection coefficient is higher than the one predicted by the theory under Assumption 1. In addition, it can be seen how the reflection coefficients can differ on the two faces of the same specimen when fully immersed in water. Finally, it is observed how the reflection coefficients on both faces can easily change in value from one test to another. Therefore, it can be concluded that all three assumptions treated in this study are violated. Let's study them one by one.

Assumption 1: Perfectly bonded interface.

The condition of a perfectly bonded interface is proven erroneous by the fact that many times the reflection coefficient is higher than the value corresponding to a perfectly bonded interface predicted by the theory. A perfectly bonded interface implies reflection coefficient values given by Equation (2.12). Since the measured

values, which represent the real reflection coefficients, differ from the theoretical ones, a perfectly bonded interface does not exist. Therefore, the classical approach should not be used with these specimens since errors from the reflection coefficients would be introduced in the attenuation coefficient calculation through Equation (2.19).

Assumptions 2b and 2a: Equal reflection coefficients at both faces of the same specimen and equal reflection coefficients every test.

Each one of the tests shows more or less different reflection coefficients on the faces of the specimen during the same test. This fact invalidates Assumption 2b, which requires equal reflection coefficients at both faces during the same test. Furthermore, the different tests also show how the reflection coefficients of the different faces of a specific specimen can vary from one test to the next. This implies that Assumption 2a is not valid for these cases. Therefore none of the modern versions of the pulse echo immersion technique can be used to calculate the attenuation of these Teflon specimens because the corresponding equations are based on assumptions that are invalid.

For Polycarbonate specimens, the same procedure was used. It is important to remember that there are two types of Polycarbonate specimens, where only one of them had a hydrophobic coating on one of its faces. For this reason, the specimens were called Polycarbonate Uncoated for the plate with no coating and Polycarbonate Coated for the plate with the coating. Following the same order, first the results from

the experiments conducted on the Uncoated plate are presented and then the experiments corresponding to the Coated plate.

Test 1 – Polycarbonate Uncoated.

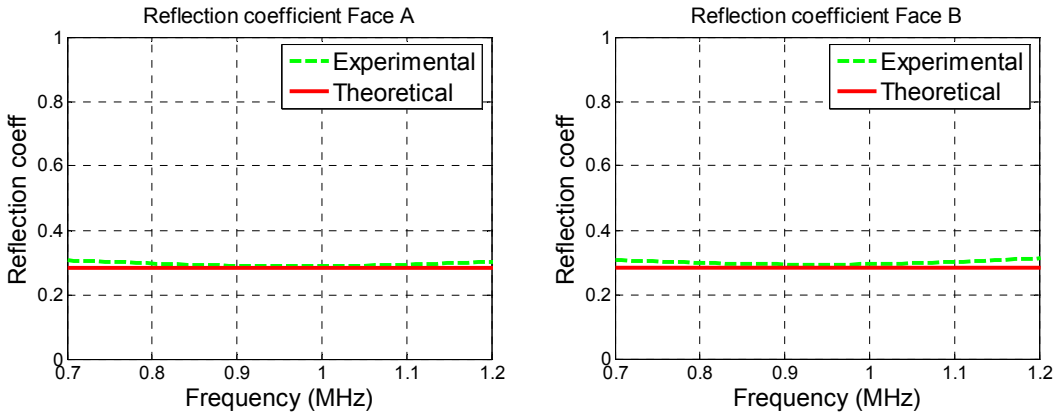

Figure 21. Reflection coefficient measurement for Polycarbonate.

Test 2 – Polycarbonate Uncoated

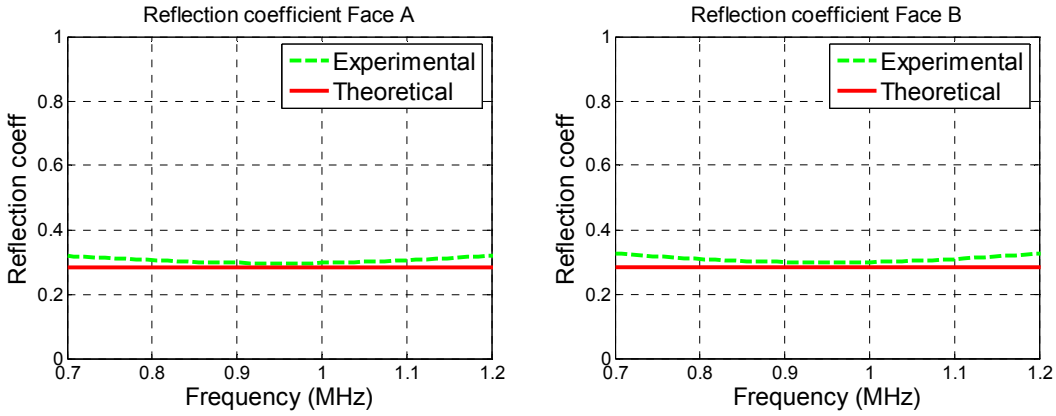

Figure 22. Reflection coefficient measurement for Polycarbonate.

Test 1 – Polycarbonate Coated

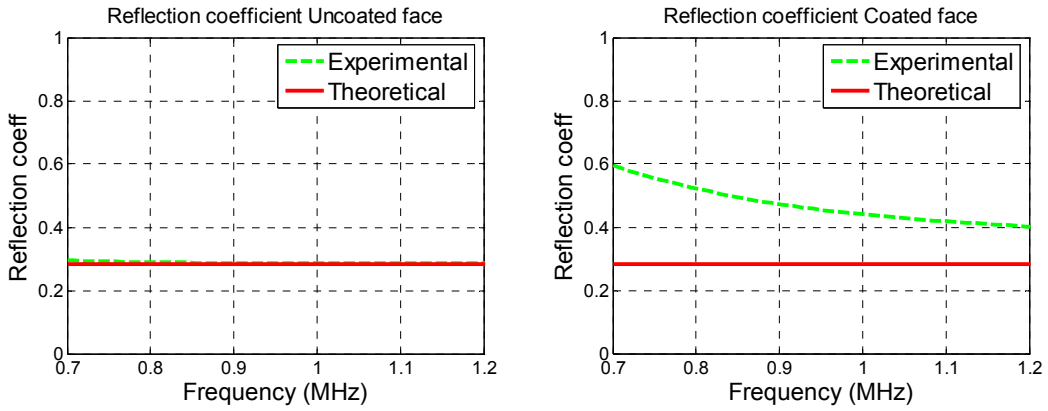

Figure 23. Reflection coefficient measurement on Polycarbonate with coating.

Test 2 – Polycarbonate Coated

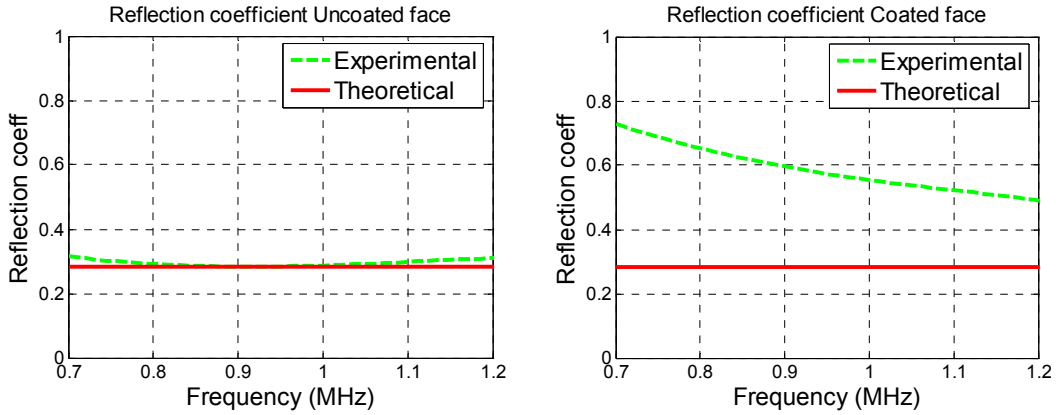

Figure 24. Reflection coefficient measurement on Polycarbonate with coating.

On the one hand, the tests on the Uncoated plate show a very good agreement between the measured reflection coefficient and the one calculated theoretically with Equation (2.12). This implies that a perfectly bonded interface condition exists and that Assumption 1 can be accepted. Therefore, the classical approach is perfectly valid to calculate the attenuation coefficient of this Polycarbonate specimen (Uncoated). It

can also be seen immediately that Assumptions 2a and 2b hold for this case and so, any of the methods presented in Chapter 2 can provide a correct measurement of the attenuation coefficient of this material.

On the other hand, the tests on the Coated plate show a similar behavior to that of Teflon specimens. In this case, it is due to the coated face since the uncoated face of this specimen fulfills Assumption 1, as expected from what was observed for the Uncoated specimen. The hydrophobic coating presents a very large difference with respect to the theoretical value based on Equation (2.12). This means that Assumption 1 does not hold true at this interface and therefore the classical approach cannot be used with this specimen. Also, following the behavior observed in Teflon, the reflection coefficient at this interface varies from test to test violating Assumption 2a and consequently, invalidating the techniques that rely on this assumption. For this case, it is very clear that Assumption 2b does not apply since the reflection coefficients at each interface are totally different for a given test. In conclusion, none of the techniques described in Chapter 2 can be used with this Coated specimen.

The question that arises after seeing these results is why the assumptions deteriorate for the Teflon and Polycarbonate Coated plates and not for the Polycarbonate Uncoated plate. The answer rests on the hydrophobic nature of the surface. This hydrophobicity manifests itself in practice through two mechanisms that are responsible for the results observed in the experiments conducted. These two mechanisms are the weak bond between water and the hydrophobic surface and the

presence of air molecules at this type of interfaces. Let us now integrate these postulates into the experience observed. The Polycarbonate Uncoated plate does not have hydrophobic surfaces. In this case, water molecules have a larger attraction to the Polycarbonate molecules than to the other water molecules. Therefore, when the specimen is immersed, water "sticks" to the specimen surfaces. This interface bond is strong enough to resist the stress applied by the ultrasonic pulses and so the interface behaves as a perfectly bonded interface. In consequence, all three assumptions hold true for this case. When hydrophobic surfaces such as the Teflon specimens and the coated face of the Polycarbonate Coated plate are immersed, the attraction between water molecules is stronger than the attraction between water molecules and those hydrophobic surfaces. A direct consequence of this phenomenon is the existence of a weak bond between these specimens and water. Moreover, since water molecules are more attracted to one another than to the solid surface, when the specimens are immersed, air molecules get trapped at the surface roughness scale throughout the hydrophobic surface. This air that initially (before immersion) was in full contact with the solid surface is not totally vacated by the water when the specimen is being immersed because the attraction of water molecules to the surface is low enough to allow air molecules to stay in equilibrium between the surface and water. This idea can be more easily visualize by means of the schematic of Figure 25.

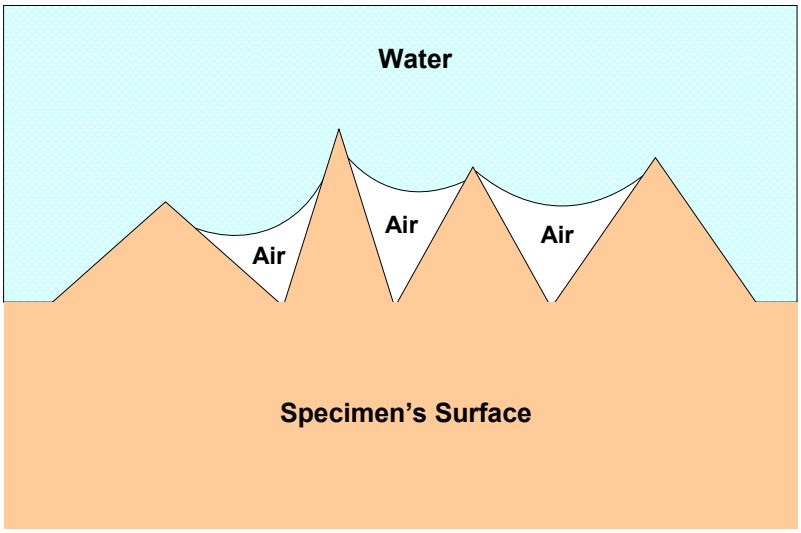

Figure 25. Air molecules trapped at the surface roughness scale for a hydrophobic specimen.

As shown in the figure, air molecules can get trapped inside the valleys of the surface roughness profile. This phenomenon by itself already breaks the condition of a perfectly bonded interface between water and the specimen since now there is air in between. In addition to this, if the bond between water and the specimen is weak enough, the tensile stress induced by the ultrasonic pulse could break the bond and therefore once again break the condition of a perfectly bonded interface.

It is clear at this point that if at least one of these two hydrophobic-based mechanisms is taking place, Assumption 1 will be violated and the real reflection coefficients will not match the ones provided by Equation (2.12). So the fact that Assumption 1 did not hold true for most of the Teflon specimens or the Polycarbonate coated plate can be fully explained by the hydrophobic nature of the specimens. For the few cases of the Teflon tests in which the measured reflection coefficients matched

the theoretical ones, it is likely few air molecules got trapped when the specimen was being immersed and the interface bond was strong enough to resist the ultrasonic pulse. Still focusing on the Teflon and Polycarbonate coated specimens, the fact that the reflection coefficients are different at the two interfaces of a single specimen and also different from test to test can be explained by the trapped air molecules conjecture. The number of air molecules trapped at the surface will depend on the surface roughness. A large surface roughness will tend to trap more air within its valleys than a perfectly flat surface. In addition to this, there is a random component for the interaction between water and the specimen when the latter is being immersed. Also, different types of particles could have adhered surfaces in a different way, adding further differences between the two surfaces of a single specimen. Blending all of this, it is understandable that different reflection coefficients are observed at the two interfaces of the same specimen and also different reflection coefficients are measured from test to test when the specimen undergoes consecutive immersions.

In addition to all this, there is an outstanding feature exhibited by the reflection coefficients of the coated face of the Polycarbonate Coated specimen that contrasts with that of the Teflon specimens. Indeed, a pronounced frequency dependence is shown by the interface of the former. The coating used on this specimen is far more hydrophobic than Teflon. This enables a larger number of air molecules to remain in equilibrium between the specimen surface and the water. In this case, there could be air basins spread over the surface, having significant thickness. This non uniform extra

layer of air is believed to be the cause of that frequency dependence displayed for that specific reflection coefficient.

Before concluding the chapter, there is a need to clarify the reflection coefficients shown in Figures 17, 18, 19 and 20 for the Teflon plates. A cursory look at those figures seems to indicate a tendency that drives the experimental reflection coefficient values towards the theoretical value with successive performance of the tests. However, no such trend was observed. In order to avoid misleading conclusions on this subject Figure 26 is presented, where the measured values for the reflection coefficients of Teflon plates 1 and 2 are shown for the successive tests performed. The values shown in the figure correspond to the peak frequency of 0.9 MHz.

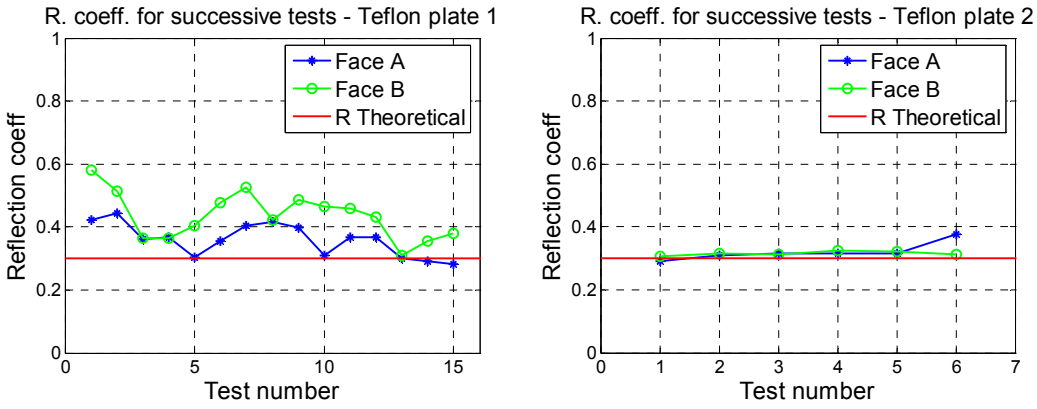

Figure 26. Teflon reflection coefficients for successive tests.

Clearly, a randomness is observed in some experimental values such as Teflon plate 1, with no trend towards the theoretical value. Regarding Teflon plate 1, repeated cycling toward and away from the theoretical reflection coefficients are observed for

Face A. Similarly, reflection coefficients for Plate 1 Face B or those of plate 2 do not show a clear tendency towards a common and specific point. As shown in the next chapter, the new technique presented takes into account the reflection coefficients given at each test and provides a correct measurement of the attenuation coefficient.

A final clarification could also be made about the influence of the storage conditions in the specimens. It was mentioned at the end of Section 3.1 that the specimens were kept in a cabinet. One could wonder if any particles in the air could have landed on the upward face of the specimens and consequently be a potential cause of the different reflection coefficients measured for the faces of single specimens, like in the case of the Teflon plates. This hypothesis has been disregarded since the Uncoated Polycarbonate specimen was stored under the same conditions as all other specimens and both its faces behaved identically.

In conclusion, non-hydrophobic materials seem to establish a perfectly bonded interface with water and therefore satisfy all three assumptions tested in this study. Because of this, any of the immersion techniques presented in Chapter 2 are valid as means of calculating the attenuation coefficient. However, hydrophobic materials will almost always violate all three assumptions and consequently invalidate the many techniques of Chapter 2 for calculating attenuation. Weak interface bond and the random presence of air molecules associated with the hydrophobic nature of the material are responsible for the differences in reflection coefficients observed during the experiments, causing all three assumptions under study to break down.

CHAPTER 5

NEW METHOD PROPOSED

After analyzing the results of Chapter 4 involving the Teflon specimens and the Polycarbonate Coated plate, it was shown how none of the techniques described in Chapter 2 are able to measure the attenuation coefficient since the assumptions they promote are not valid for those materials. This invites the development of a new method based on the ultrasonic pulse echo immersion technique that works with these materials as well as others. The new method desired can be seen as an extension of the existing techniques to incorporate the materials that cannot be measured at present. It should increase the reach of the ultrasonic immersion technique.

Before developing this new method, it is necessary to list the requirements it must fulfill. Primarily, it should be able to function without the need of any of the three assumptions discussed in this thesis. The phenomena observed in the experiments conducted were: unknown and different reflection coefficients on the faces of a single specimen and different reflection coefficients between tests. Therefore, the new method should achieve the following:

- To be able to measure reflection coefficients on both faces of the specimen during one immersion.

- To measure the attenuation coefficient during the same immersion process used to measure the reflection coefficients.

Indeed, the reflection coefficients are considered unknown and that is why they need to be measured. Also, they are different for each immersion. Therefore, measuring the attenuation coefficient during a different immersion process would be meaningless because the reflection coefficients for those two different immersions could likely be different.

The proposed method was partially introduced in Chapter 3 in the reflection coefficient measurement section. It uses a tank divided in half by a middle wall that isolates both sides and holds the specimen. Furthermore, only one transducer is required. The procedure consists on four simple steps. This can be seen in Figure 26. First, only side A of the tank is filled with water. The transducer is immersed on this side and is placed perpendicular to the specimen at a slightly greater distance than the nearfield (27 mm in our case). Signal $V^{(1)}$ is recorded. Then, side B is filled with water. Nothing is moved or modified in side A. Signal $V^{(2)}$ is recorded. After this, the transducer is carefully moved to the other side (side B) and it is placed aligned with respect to its previous position on side A. Signal $V^{(3)}$ is recorded. Finally, side A is emptied while nothing is moved or modified on side B. Signal $V^{(4)}$ is recorded.

In total, four full signals are recorded. Using signals $V^{(1)}$ and $V^{(2)}$ together with Equation (3.3) the reflection coefficient of face B of the specimen is obtained.

Likewise, using signals $V^{(3)}$ and $V^{(4)}$, the reflection coefficient of face A of the specimen is obtained. Next, any of the four signals can be used to calculate the attenuation coefficient using the proper reflection coefficients.

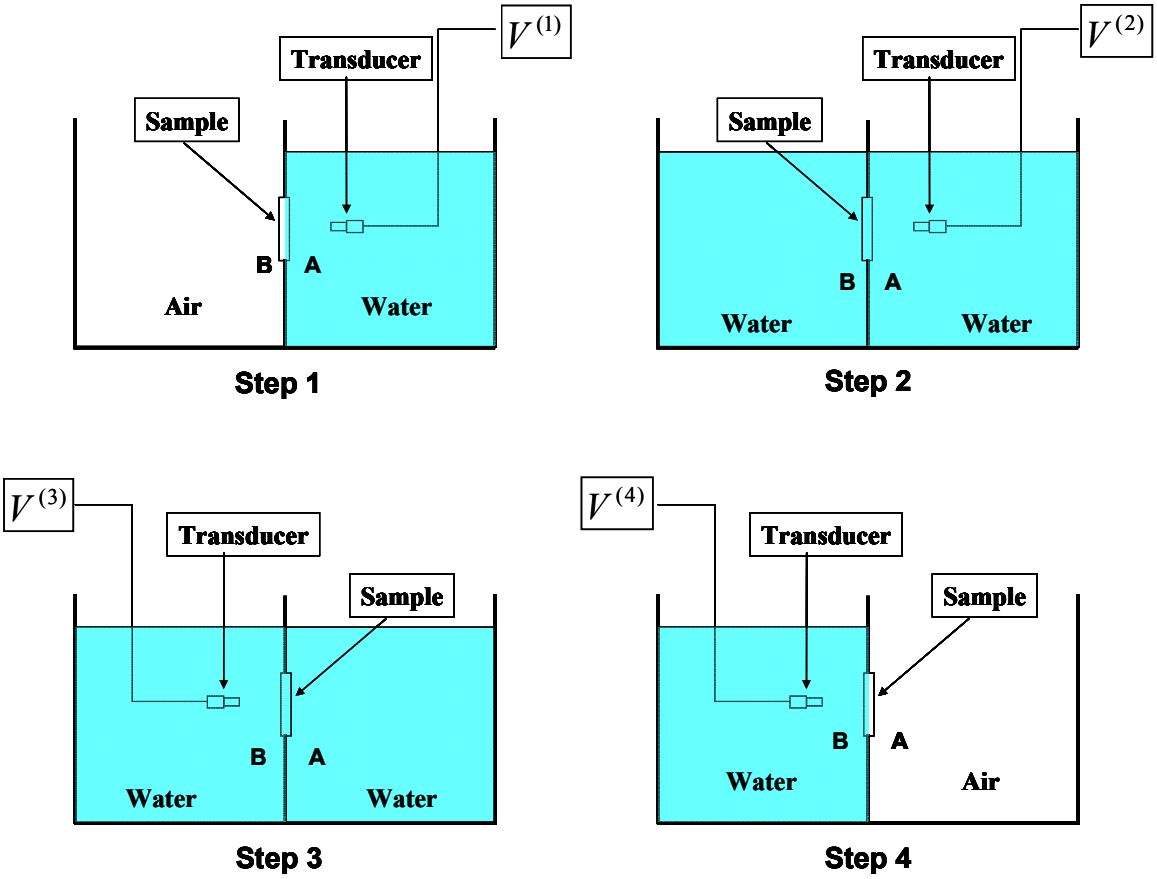

Figure 27. Procedure for the new method proposed to measure attenuation coefficients.

So,

- If signal $V^{(1)}$ is used: R_A = measured value with Steps 3 and 4, R_B = 1.
- If signal $V^{(2)}$ is used: R_A = measured value with Steps 3 and 4, R_B = measured value with Steps 1 and 2.
- If signal $V^{(3)}$ is used: R_A = measured value with Steps 3 and 4, R_B = measured value with Steps 1 and 2.
- If signal $V^{(4)}$ is used: R_A = 1, R_B = measured value with Steps 1 and 2.

Note that a specimen-air interface implies in practice a full reflection of the wave and that is why the reflection coefficients at those interfaces are taken equal to 1. Also, it must be noted that the method satisfies the stated requirements, i.e., both reflection coefficients belonging to a particular immersion are measured and the attenuation coefficient is calculated with a signal that depends on the measured reflection coefficients obtained from that same immersion. For instance, if signal $V^{(2)}$ is used both water-specimen interface reflection coefficients are needed for Equation (2.19) (shown below).

Recall:
$$\alpha = \frac{1}{2h} \cdot \ln\left(\frac{V_1}{V_2} \cdot R_A \cdot R_B \cdot \frac{D(s_2)}{D(s_1)} \right) \tag{2.19}$$

The method must be able to provide these two reflection coefficients specific to that unique immersion. Indeed, those two reflection coefficients are measured by this method. First the R_B present in step 2 is obviously measured. Then, the R_A measured during steps 3 and 4 is actually the R_A present in step 2, since from this step on, the side A interface remains untouched until R_A is measured. The same logic can be

applied to any of the other signals used to calculate attenuation. Thus, all variables needed for substitution into the requisite equations are measured directly within this method.

In order to experimentally prove the validity of this method, all four specimens used to test the three well discussed assumptions, that is the Teflon and Polycarbonate specimens, will be retested. It was seen how the Teflon specimens presented different values for the reflection coefficients. This proposed method should be able to overcome those drawbacks and provide the same result for both Teflon specimens since they are made from the same material. In a similar manner, both Polycarbonate plates should generate the same attenuation coefficient even though they present large differences at their interface behaviors. Note that the attenuation within the coating layer is negligible due to its very small thickness. Following these expectations all four specimens were tested using the new method. Fifteen and five tests were performed for the Teflon and Polycarbonate specimens, respectively. After this, the attenuation coefficients obtained from all tests were averaged for each specimen. Figures 27 and 28 show the final result for the attenuation coefficient measured for each specimen, along with the linear regression equation of the attenuation coefficients as a function of frequency, as well as the standard deviation corresponding to the tests that were averaged. Specimens made from the same material have been grouped in a single plot in order to compare the attenuation coefficients, which evidently should be the same.

Teflon case

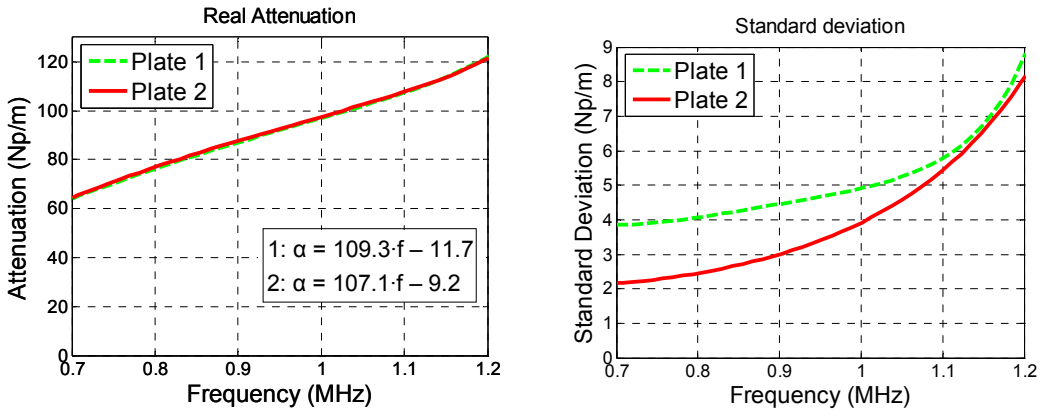

Figure 28. Attenuation coefficient for Teflon specimens (left) and standard deviation from the measurements (right).

Polycarbonate case

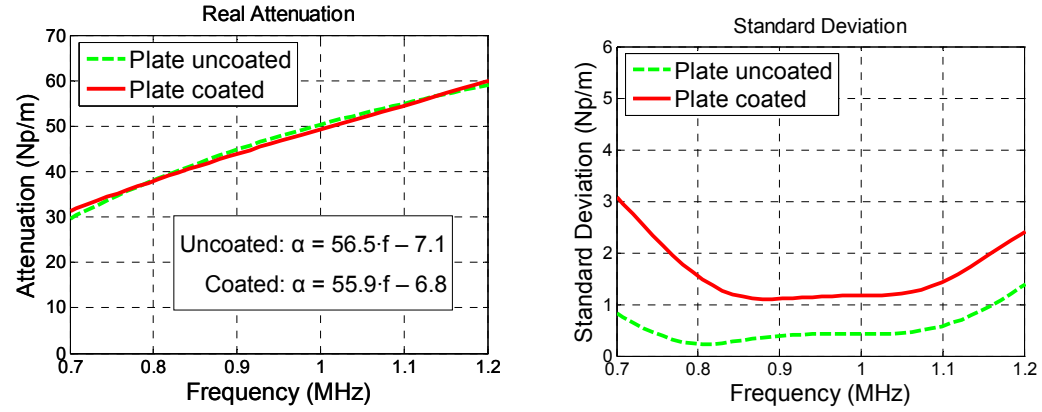

Figure 29. Attenuation coefficient for Polycarbonate specimens (left) and standard deviation from the measurements (right).

It is clearly observed that the new method provides the same attenuation coefficient for each material even though the reflection coefficients were very different from one specimen to the other and from one test to another, as shown in Chapter 4. These results can be compared to others found in literature to check the

accuracy and proper operation of the new method proposed. Mobley, *et al.*, [1] studied the attenuation of Polycarbonate (Lexan) by means of two different methods, obtaining values of 50.8 Np/m at 1 MHz for the attenuation coefficient, and 56.8 Np/m/MHz for the slope of the linear regression curve describing variation of attenuation with frequency. These values are very similar to the ones obtained in this study. In addition, Selfridge [2] and Kaye and Laby [3] provided values of approximately 267 Np/m and 240 Np/m at 5 MHz respectively for the attenuation coefficient in Polycarbonate. Considering a linear relationship between attenuation and frequency, the quoted values would correspond to 53.4 Np/m and 48 Np/m for attenuation at 1 MHz, respectively. This is done by simply dividing the values corresponding to the 5 MHz frequency by 5. Once again, these values are very similar and within the range of the attenuation measured in this study for Polycarbonate. Regarding the Teflon specimens, this case will be discussed later in Chapter 7 since a curious situation was encountered.

The results obtained with the new method proposed gain more relevance when they are compared to those that would have been obtained if the classical approach were to have been followed by accepting Assumption 1 as true. Below, Figures 29 and 30 show a comparison between the 2 methods: the classical or conventional approach on the left and the new proposed method on the right.

Teflon case

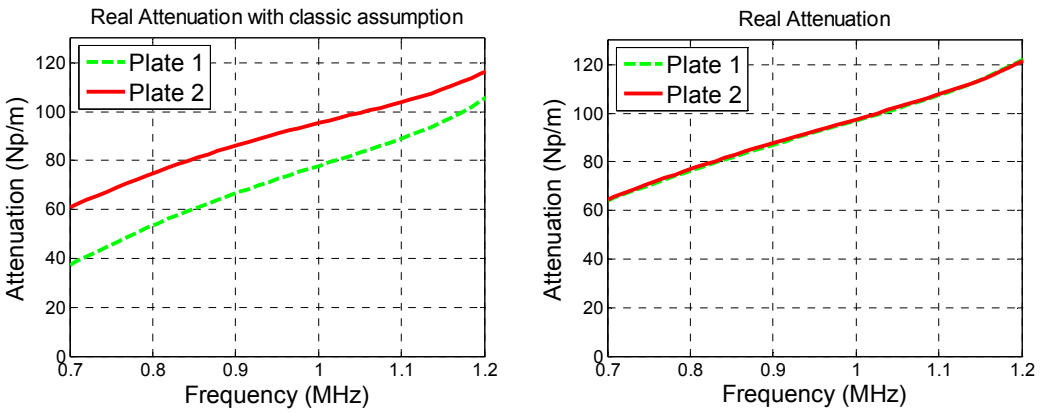

Figure 30. Comparison between Teflon attenuation coefficients provided by classical approach (left) and new method proposed (right).

Polycarbonate case

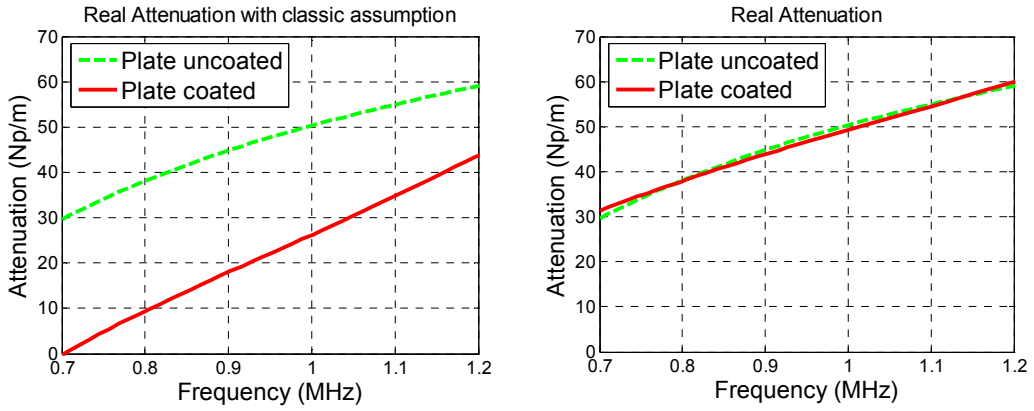

Figure 31. Comparison between Polycarbonate attenuation coefficients provided by classical approach (left) and new method proposed (right).

The robustness of the new method becomes more evident after showing how it corrects the large errors generated by using the classical approach.

In conclusion, a new method has been developed and is proposed here to overcome the errors introduced by current techniques of attenuation coefficient measurement for materials that violate three fundamental assumptions adopted by these current techniques. The new method proposed is not based on any of these three assumptions and therefore, it expands the range of applicability of the ultrasonic pulse echo immersion technique to a very wide variety of materials. Some of its principal advantages are that:

- Reflection coefficients can be unknown.
- Reflection coefficients can be different on each face of a single specimen.
- Reflection coefficients can be inconsistent and change from one immersion to another.
- Only one transducer is required.
- It is simple, robust and easy to apply.

The validity of this method has been experimentally proven by testing specimens that do not satisfy any of the three assumptions used by current techniques and providing the same attenuation coefficient for those specimens made from the same material even though their immersion conditions were often very different.

References

[1] Mobley, J., Vo-Dinh, T. “Photoacoustic method for the simultaneous acquisition of optical and ultrasonic spectra.” *The Journal of the Acoustical Society of America.* ARLO Vol. 4, (3) pp. 89-94 (2003).

[2] Selfridge, A. R. "Approximate Material Properties in Isotropic Materials." *Sonics and Ultrasonics, IEEE Transactions on.* Vol. 32, (3) pp. 381-394. (1985).

[3] Kaye, G. W. C. and Laby, T. H. *Tables of Physical and Chemical Constants.* Longmans, 1995.

CHAPTER 6

ATTENUATION IN PARTICULATE COMPOSITES

As mentioned in Chapter 1, one of the goals of this study was to contribute to the research on wave propagation in particulate composites. It was described how there have been many theoretical models developed, which tend to agree very well with experimental measurements for low particle concentrations, but face more difficulties predicting the behavior of waves propagating in high particle concentration composites. Because of this, the main effort recently has been placed on improving models for cases of high particle concentration. All these newly developed models will need experimental data for validation, thus, the impetus for conducting experiments on some particulate composites, and measuring the wave speeds and the attenuation coefficient with the method proposed in Chapter 5.

The most important parameters involved in wave propagation from an engineering point of view are wave speeds and attenuation. For the case of particulate composites, the attenuation coefficient has two distinct components: absorption and scattering. The absorption component is related to the conversion of energy carried by waves into heat within the material whereas the scattering component is related to wave interference caused by the interaction of the waves with the particles as well as reflections trapped among several particles.

The particulate composites tested consisted of solid glass microspheres embedded in an epoxy matrix. There were two types of glass microspheres used: one type was denoted 2530 and the other 3000. The 2530 type had an average diameter of 60-70 microns while the 3000 type had an average diameter of 30-50 microns. Four specimens were manufactured with the 2530 glass microspheres with 5, 10, 20 and 30% of particle volume fraction, respectively. Similarly, four specimens were made with the 3000 glass microspheres and also containing 5, 10, 20 and 30% particle volume fraction, respectively.

Once the specimens were manufactured, they were properly machined to a disk shape and the densities were calculated by weighing the samples using a high accuracy scale and measuring the dimensions to compute the volume. Figures 31 and 32 contain the density measurements for the 2530 and 3000 type specimens respectively.

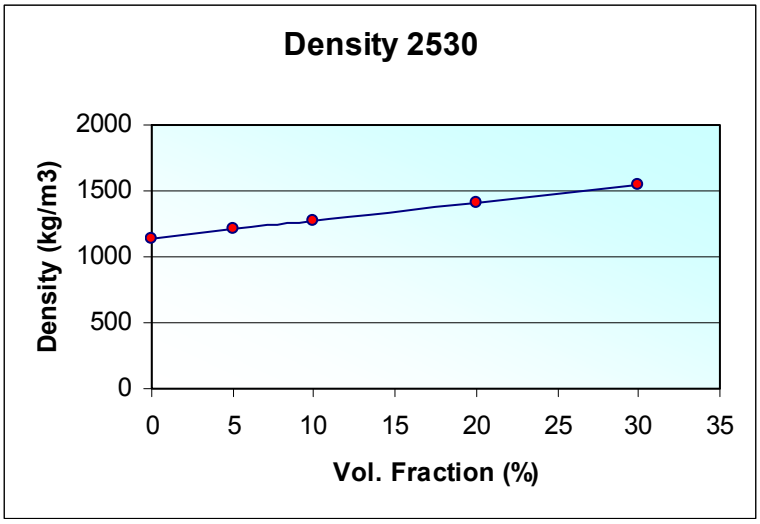

Figure 32. Density of the 2530 particulate composite type with respect to volume fraction.

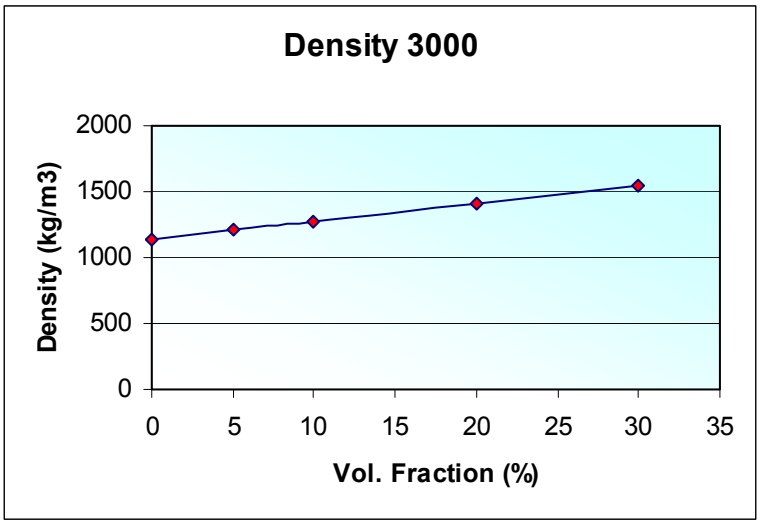

Figure 33. Density of the 3000 particulate composite type with respect to volume fraction.

It can be clearly appreciated that density increases linearly with the volume fraction as expected, since the density of the composites is given by

$$\rho_{pc} = X\left(\rho_p - \rho_{ep}\right) + \rho_{ep} \tag{6.1}$$

where X is the particle volume fraction, ρ is density and subscripts pc, p, ep stand for particulate composites, particles and epoxy, respectively.

Once the densities are known the next parameters of interest were longitudinal wave speed and attenuation coefficient. Both parameters are calculated using the method proposed in Chapter 5 based on the ultrasonic pulse echo immersion technique. Even though this thesis has been entirely focus on attenuation measurement, the ultrasonic pulse echo immersion technique can also measure the longitudinal wave speed in any material. This can be simply calculated using the following expression:

$$c = \frac{2h}{\Delta t} \tag{6.2}$$

where h is the thickness of the specimen and Δt is the time lapse between the first and second echoes.

Longitudinal wave speed measurements are plotted in Figures 33 and 34 for the 2530 and 3000 type specimens, respectively.

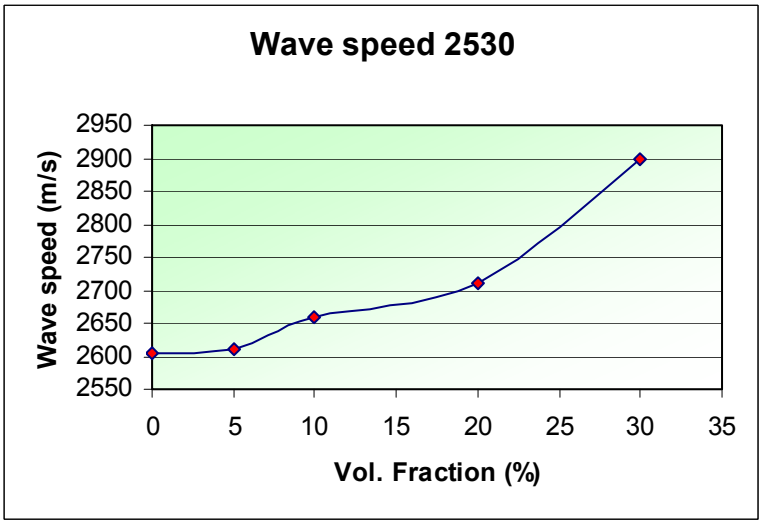

Figure 34. Longitudinal wave speed with volume fraction for the 2530 type particulate composites.

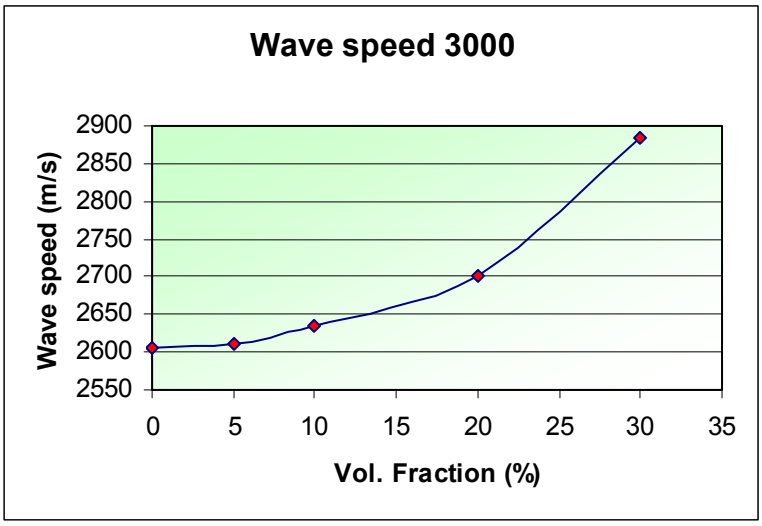

Figure 35. Longitudinal wave speed with volume fraction for the 3000 type particulate composites.

It is observed that the longitudinal wave speed increases monotonically with increasing glass microspheres volume fraction. This is not surprising because of the already established higher wave speed offered by glass in comparison to the epoxy matrix.

Regarding attenuation, it is very interesting to take a look at the reflection coefficients measured for this material. A priori it is very reasonable to think that the reflection coefficients should match the theoretical ones based on Assumption 1 since this type of particulate composite does not present hydrophobicity. The measurements however do not show the expected results, as seen in Figure 35 in which several measured reflection coefficients from different specimens are compared to the values provided by Equation (2.12).

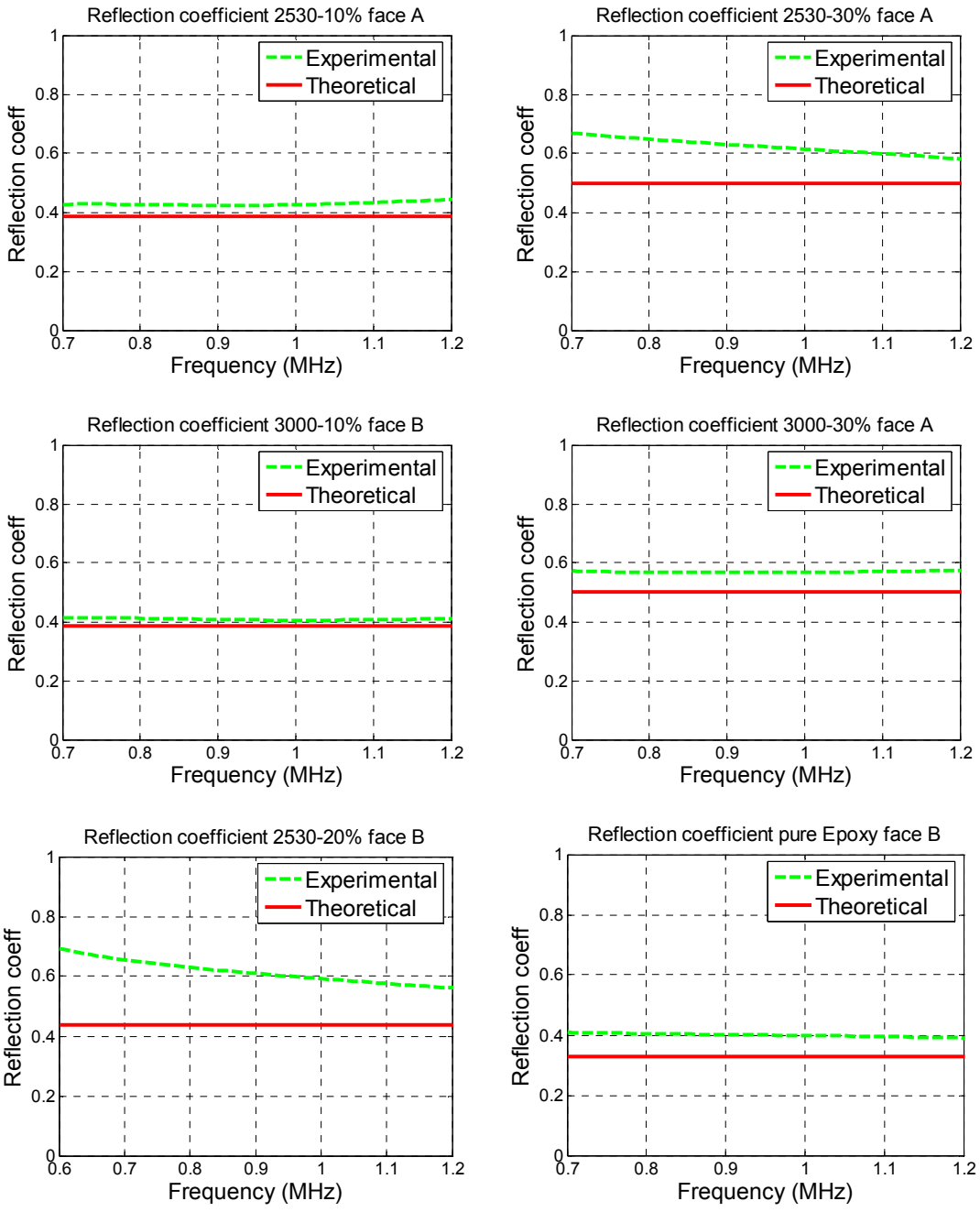

Figure 36. Measured reflection coefficients for different particulate composites and pure epoxy.

In the first place, it was a propitious to use the new method proposed in Chapter 5 to measure the attenuation coefficient since otherwise large errors in the attenuation calculation would have been introduced. Indeed, as it happened with the Teflon specimens Assumption 1 is violated with these particulate composite specimens. In the second place, it is unavoidable to wonder why this is happening. This phenomenon could be explained by studying the surface profile of the specimens. It is realistic to surmise that when the specimens are machined and sanded, some of the glass microspheres could debond from the matrix leaving semispherical voids on the surface and others could remain attached to the matrix and stand out above the surface plane. This could cause inadvertent trapping of air molecules when the specimen is immersed. Besides this, there could also exist a weak bond between water and epoxy since the reflection coefficients for pure epoxy do not correspond to a perfectly bonded interface. This weak bond with epoxy coupled with the presence of air due to the surface profile at the microscale level created by the glass particles could explain the behavior observed in relation to the reflection coefficients when the glass particle volume fraction increases.

Taking these various reflection coefficients into account, the attenuation coefficients of the different specimens were calculated. In order to explicitly observe the effect of the glass microspheres on attenuation, the attenuation coefficients of all composites were divided by the attenuation coefficient of the matrix. The attenuation coefficient of the epoxy matrix was measured as 31.3 Np/m for 20 ˚C room temperature during the curing process. Figures 36 and 37 present the results for the

normalized attenuation coefficients corresponding to a 1 MHz frequency of the 2530 and 3000 type specimens respectively.

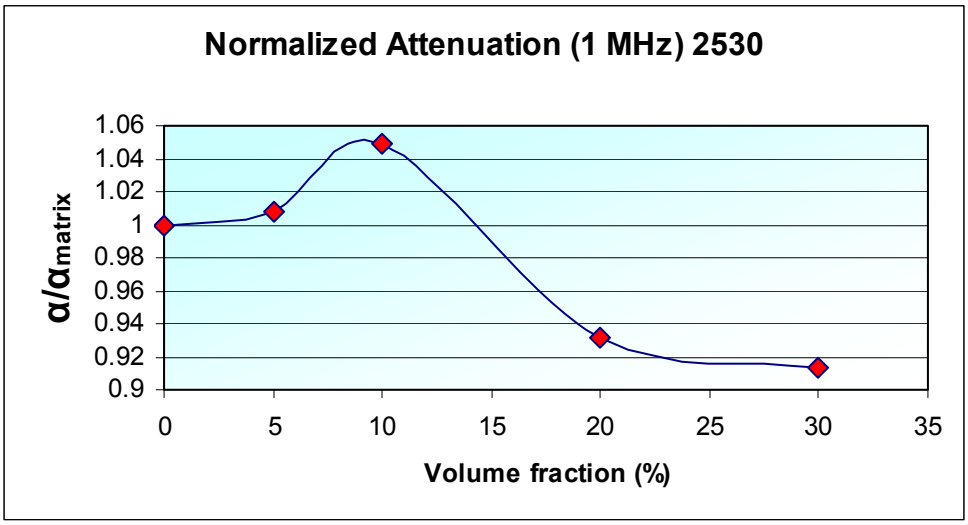

Figure 37. Normalized attenuation coefficient with volume fraction for the 2530 type particulate composites.

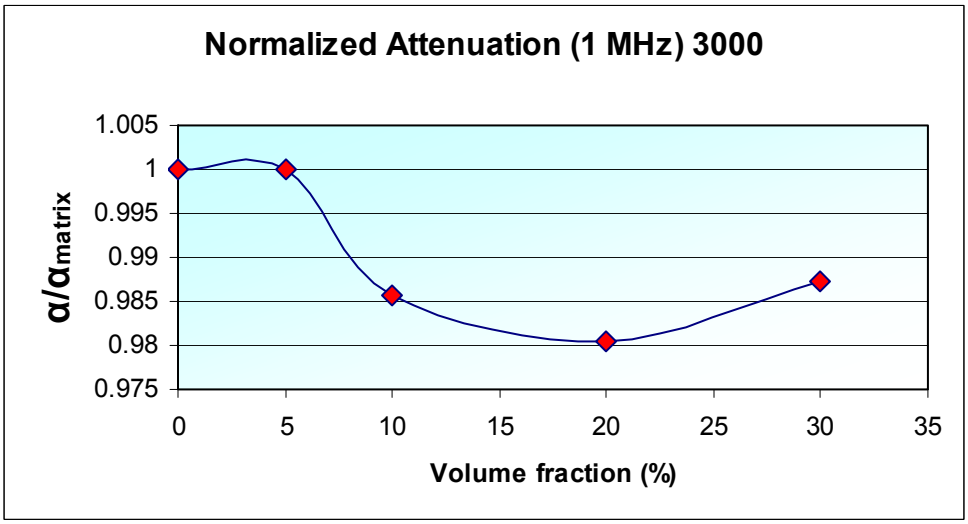

Figure 38. Normalized attenuation coefficient with volume fraction for the 3000 type particulate composites.

Characteristic trends for these specimens are clear. With respect to the 2530 type, the attenuation coefficient increases slightly with respect to that of the matrix for the low volume fractions (0-15 %) and after this starts decreasing, ending up reaching a lower value than that of pure epoxy. Thus, if the goal for adding glass microspheres into epoxy is to increase the attenuation of the matrix, it fails for moderate to high particle volume fractions. Even for the low volume fractions (0-15 %), the attenuation coefficient of the composite does not improve much with respect to the matrix material. Regarding the 3000 type specimens the addition of solid glass microspheres diminishes the attenuation coefficient of the matrix for volume fractions higher than 5%. For low volume fractions, the effect of the glass particles is not clear since the attenuation coefficient seems to be very similar to that of the epoxy matrix.

Remarkably similar trends were obtained by Layman, *et al*., [1] from the experiments they conducted on glass/epoxy particulate composites in which the average diameter of the glass microspheres was 45 μm. Even though these specimens look very similar to the 3000 type presented in this study, the epoxy matrix seems to be a different material. This would explain the different attenuation coefficient values obtained by them in comparison to the values presented in this thesis. Assuming linear frequency dependence, the attenuation coefficient of the epoxy used by Layman, *et al*., [1] was approximately 57 Np/m, which is significantly higher than that of the epoxy used in this work (31.3 Np/m). Nevertheless, the behavior of the attenuation coefficient in relation to the glass particle volume fractions was almost identical. Kinra, *et al*., [2] also performed some experiments on glass/epoxy particulate

composites. In this case, the glass microspheres used had an average diameter of 150 μm, which is much larger than that of the 2530 and 3000 type microspheres used in this work. The measurements carried out by Kinra, *et al*., [2] showed a slight increase in the attenuation coefficient with glass volume fraction. It is vain to mention the magnitude of the attenuation coefficients since the epoxy used in this case was different from that used in this and other works.

The reasons for these behaviors could be related to the glass microspheres size as well as the concept of attenuation. It is necessary to remember that the attenuation coefficient is composed of an absorption part and scattering part. In this case, the absorption mechanism only takes place in the matrix due to its polymeric nature. On the other hand, glass, similarly to metals, manifests a very low attenuation coefficient via absorption. Indeed, the glass embedded in these composites acts as a counterforce against epoxy when it comes to attenuation via absorption since all the space occupied by the glass microspheres annuls the attenuation that would have taken place if that space was filled with epoxy. Therefore, from an absorption point of view adding glass to epoxy will decrease the attenuation coefficient of the final composite. Nevertheless, the glass microspheres could potentially compensate for the absorption reduction via scattering. This compensation seems to take place in a positive manner for the 2530 specimens. At low volume fractions where there is ample space between particles, the larger size of the 2530 microspheres creates enough scattering to improve the attenuation coefficient of the matrix. For the 3000 microspheres, their smaller size does not seem to have a positive influence on wave scattering and in the end the

absorption reduction is not compensated by the scattering. This results in an undesirable decrease of the attenuation coefficient. In both cases, the more prominent presence of glass at high volume fractions (>30 %) drops the absorption mechanism of the composite to a point where the scattering effect cannot compensate by any means.

In conclusion, the effect of the microparticles on attenuation is not as strong as would be desired. For most of the configurations tested, the addition of glass microparticles decreased the attenuation coefficient with respect to the matrix. This effect is a consequence of a negative trade, in which the scattering phenomenon cannot overcome the reduction of attenuation via absorption introduced by the glass material in the epoxy matrix. In other words, the amount subtracted by the glass particles within the epoxy is not compensated by the amount added by the scattering effect provided by those same glass particles. However, some clues can guide the designer in the right direction in order to increase attenuation. It appears that a combination of low volume fractions and larger size microspheres could provide better results due to a more effective scattering effect, while maintaining most of the absorption provided by the matrix.

References

[1] Layman, C., Murthy, N. S., Yang, R., and Wu, J. "The Interaction of Ultrasound with Particulate Composites." *The Journal of the Acoustical Society of America.* Vol. 119, (3) pp. 1449-1456. (2006).

[2] Kinra, V. K., Petraitis, M. S., and Datta, S. K. "Ultrasonic Wave Propagation in a Random Particulate Composite." *International Journal of Solids and Structures.* Vol. 16, (4) pp. 301-312. (1980).

CHAPTER 7

CONCLUSIONS

There have been two differentiated studies carried out in this thesis. The first and main one consisted in a deep examination of the ultrasonic pulse echo immersion technique as used to measure attenuation in longitudinal waves. The examination analyzed the validity of the fundamental assumptions adopted by a variety of techniques ranging from the classical or conventional approach to more modern versions developed recently. The second study investigated some critical wave propagation parameters in engineering, namely, wave speeds and attenuation coefficient in glass/epoxy particulate composites. This investigation was purely experimental and it was conducted by means of a method developed in this thesis.

In the following section, the most important conclusions extracted from the studies mentioned above will be presented. Following the scheme of this thesis, first the conclusion pertaining to the ultrasonic pulse echo immersion technique examination will be exposed and after this the conclusions derived from the particulate composites study will be presented.

7.1 Conclusions on the Ultrasonic pulse echo immersion technique.

Several approaches pertaining to the use of the ultrasonic immersion technique to measure attenuation were described. One of them was called the classical or conventional approach and was based on an assumption designated as Assumption 1 that claimed a perfectly bonded interface between specimen and the immersion liquid, which in this case was water. The remaining techniques were grouped under the designation of modern versions and were based on two assumptions referred to here as Assumptions 2a and 2b. On the one hand, Assumption 2a required consistency of reflection coefficients for every test. On the other hand, Assumption 2b required equal reflection coefficients at both faces of a single specimen in a given test. After conducting numerous experiments that measured the reflection coefficients of different materials it was concluded that:

-**For some materials:**

- Assumption 1 is satisfied and therefore a perfectly bonded interface with water exists.
- In consequence, Assumptions 2a and 2b are also satisfied.
- Then, any of the approaches described during this thesis are valid and capable of providing a correct measurement of the attenuation coefficient of these materials.

-**<u>However, for other materials</u>:**

- Assumption 1 can be clearly violated. Consequently, the classical or conventional approach of the ultrasonic pulse echo immersion technique is not valid, since it will introduce large errors in the attenuation coefficient it provides.
- Assumptions 2a and 2b are also violated. Therefore, any of the modern versions of the technique are invalid as they will introduce errors in the calculations.
- This phenomenon is closely related to materials presenting hydrophobicity, though not exclusively.
- The reflection coefficients between these materials and water are unknown and can vary from one instance of immersion to another.
- A new method that takes into account this behavior is necessary to measure the attenuation coefficient of these materials.

The violation of these assumptions can be explained as follows: 1) the weak bond between water and these materials can be broken by the tensile component of the ultrasonic pulse; 2) the presence of air molecules at the surface roughness scale is already conjectured to break the condition for a perfectly bonded interface during experimental set up. The random distribution of the air molecules over the surface of the solid can explain the different reflection coefficients at the two faces of a single specimen as well as the different reflection coefficients at the interfaces when the

specimen undergoes future immersions. For cases in which there are enough air molecules to form relatively thick air pockets spreading over the surface, the reflection coefficient shows a clear dependence with frequency. Materials presenting hydrophobic surfaces are the most appropriate to show this type of behavior. However, they do not exclusively display this behavior since it was observed also during the particulate composites attenuation study. Indeed, the glass/epoxy particulate composites did violate Assumptions 1, 2a and 2b.

Since none of the techniques found and described in Chapters 1 and 2 can be used for these special cases where all three assumptions are not satisfied, a new method that could overcome these drawbacks needed to be developed. This was done in Chapter 5 where a proposed method was experimentally proven to be capable of measuring the attenuation coefficient correctly for these and any other materials. The method proposed can achieve correct results by measuring the reflection coefficient at both faces of the specimen during a single immersion and using signals that involve the measured reflection coefficients to calculate the attenuation coefficient.

Curious case.

There is a curious case that can be found in literature and that seems to be closely related to the behavior observed here with the Teflon specimens. In 1985 Selfridge [1] published, among many other data, the attenuation coefficient of various materials. One of them was Teflon, and according to Selfridge the attenuation coefficient at 5 MHz was 44.9 Np/m. A decade later, in 1995, Kaye and Laby [2] published a small

book containing multiple tables of physical and chemical constants. They also included the attenuation coefficient of Teflon and according to them it was 430 Np/m for the same frequency of 5 MHz frequency. The difference between the two values is remarkably large. In our study, the attenuation coefficient was measured for a 1 MHz frequency providing a value of approximately 95 Np/m. Assuming a linear dependence with frequency this value would yield an attenuation coefficient of 475 Np/m for a 5 MHz frequency. The surprisingly low value provided by Selfridge is very likely the consequence of using the classical approach of the ultrasonic immersion technique with very high reflection coefficients. In other words, if the real reflection coefficients are much higher than the theoretical values (Eq. 2.12) used by the classical approach, the signal used to calculate the attenuation will be overcorrected and this will result in an underestimation of the attenuation coefficient. The fact that the real reflection coefficients can be much higher than the theoretical ones is possible and it can be seen in one of the cases of Figure 17. As an example, if a Teflon specimen is sanded with a 240 grit sanding paper (commonly used in the laboratory) the reflection coefficient of that face will be very high. An analogous reasoning can be applied to explain the result given by Kaye and Laby, with the difference that in their case the reflection coefficients could have been slightly higher than the theoretical one and that is why their attenuation coefficient is not as underestimated. Figure 18 shows that it is possible for the real reflection coefficient to be slightly higher than the theoretical one provided by Equation (2.12). In conclusion, what happened in this curious case is identical to what Figure 29 shows when the

classical approach is used with Teflon specimens: if erroneous reflection coefficients are used, the attenuation coefficients will also be erroneous.

7.2 Conclusions on the glass/epoxy particulate composites.

The experimental measurements conducted with the new method proposed in this study revealed that:

- The longitudinal wave speed increases with glass microspheres volume fraction for both types of specimens (2530 and 3000 types).
- The attenuation coefficient shows a slight increase with respect to the matrix for the 2530 specimens at low volume fractions, then decreases for higher volume fractions until it reaches a lower value than that of the matrix for volume fractions greater than 20%.
- The attenuation coefficient presented by the 3000 specimens does not seem to increase for any volume fraction, and appears to be consistently lower than that of the matrix

The increase in wave speed with volume fraction is logical due to the higher wave speed offered by glass that contributes to faster wave propagation through the material.

Regarding the attenuation coefficient, several effects should be counted simultaneously in order to explain the results. In the first place, it is essential to realize

that introducing solid glass microspheres will degrade the absorptive capability of the epoxy matrix since glass, similar to metals, has a very low attenuation coefficient. Therefore, from an absorption point of view the composite will always present lower attenuation than the matrix itself. Hence, the only way to improve the attenuation coefficient of the matrix is through a large scattering effect caused by the glass microspheres. In this sense, the bigger size microspheres of the 2530 specimens seem to generate a stronger scattering effect than the 3000 type microspheres. It could be deduced that larger size inclusions perform a more effective scattering mechanism than small size inclusions in cases where low particle volume fractions are concerned. For high volume fractions, the scattering effect seems to lose effectiveness and the reduction of matrix absorption introduced by the glass generates a negative balance that results in a lower attenuation coefficient than that of the epoxy matrix. In this case, the loss of effectiveness in the scattering effect could be due to a greater number of glass microspheres clustered to form a channel for waves to travel without suffering much attenuation.

7.3 Future work.

There is at least one alternative to the use of ultrasonic immersion techniques to measure the attenuation coefficient of any material. This alternative consists in the use of contact transducers. There exists a method developed in 2009 by Treiber, *et al*., [3] that can perform correct measurements of longitudinal and shear wave speeds and attenuation coefficients. However, contact transducers also present the problem of an unknown reflection coefficient that is needed to calculate attenuation. This unknown

reflection coefficient corresponds to the interface formed by the transducer, the coupling agent and the specimen. Since it is very difficult to control the thickness of the coupling agent Equation (3.8) becomes ineffective in calculating the reflection coefficient. Nevertheless, the method developed by Treiber, *et al*., [3] can measure that reflection coefficient with the use of another transducer on the other side of the specimen and finally calculate correctly the attenuation coefficient. Unfortunately, the problem with contact transducers is that they are much less reliable than immersion transducers. As was expressed by the manufacturer (Panametrics) [4], contact transducers are only designed to provide a valid first echo. Therefore it is difficult to find contact transducers for which the second echo is not distorted. Consequently, improving the quality of contact transducers could provide a powerful alternative to the ultrasonic pulse echo immersion technique for measuring the attenuation coefficient of materials.

With respect to particulate composites from an attenuation point of view, the goal should be to find the optimum particle size and its volume fraction that maximize the final attenuation coefficient for given matrix and particle materials. In the case of glass/epoxy particulate composites, it appears that particles with diameter size larger than 70 microns can provide acceptable scattering and an improved attenuation coefficient for low volume fractions. Experimenting with larger size particles and low volume fractions as well as developing computer models based on FEM could probably bring success at considerably increasing the attenuation coefficient of the composite matrix material.

References

[1] Selfridge, A. R. "Approximate Material Properties in Isotropic Materials." *Sonics and Ultrasonics, IEEE Transactions on.* Vol. 32, (3) pp. 381-394. (1985).

[2] Kaye, G. W. C. and Laby, T. H. *Tables of Physical and Chemical Constants.* Longmans, 1995.

[3] Treiber, M., Kim, J., Jacobs, L. J., and Qu, J. "Correction for Partial Reflection in Ultrasonic Attenuation Measurements using Contact Transducers." *The Journal of the Acoustical Society of America.* Vol. 125, (5) pp. 2946-2953. (2009).

[4] Olympus NDT (Panametrics). Private communications. August 2012.

Template of the code used to calculate attenuation coefficients from the New Method Proposed.

```
clear all; clc;

%Signal V(1)

%First echo

inc1=0.01;
[x1]=xlsread('Time domain spreadsheet', 'FirstEchoIni:FirstEchoEnd');
N1=8192;
F1=[-N1/2:N1/2-1]/(N1*inc1);
X1=abs(fft(x1,N1));
X1=fftshift(X1);

%Second echo

inc2=0.01;
[x2]=xlsread('Time domain spreadsheet', 'SecondEchoIni:SecondEchoEnd');
N2=8192;
F2=[-N2/2:N2/2-1]/(N2*inc2);
X2=abs(fft(x2,N2));
X2=fftshift(X2);


%Beam spreading parameters for D(s) function

a=7.14375; %(mm)
c=2607; %(m/s)
L=31.08; %(mm)
h=0.3678*25.4; %(mm)
z1=2*h+L;
z2=4*h+L;

cw=1490; %(m/s)

f=F1(length(F1)/2:N1);
for i=1:length(f)
   lambda(i)=c*1000/(f(i)*1E6); %(mm)
   lambdaw(i)=cw*1000/(f(i)*1E6); %(mm)
end
```

```
s1=(1/a^2)*(2*h)*lambda+(1/a^2)*(2*L)*lambdaw;
s2=(1/a^2)*(4*h)*lambda+(1/a^2)*(2*L)*lambdaw;

for i=1:length(s1)
   D1(i)=sqrt((cos(2*pi/s1(i))-besselj(0, 2*pi/s1(i)))^2+(sin(2*pi/s1(i))-
besselj(1, 2*pi/s1(i)))^2);
   D2(i)=sqrt((cos(2*pi/s2(i))-besselj(0, 2*pi/s2(i)))^2+(sin(2*pi/s2(i))-
besselj(1, 2*pi/s2(i)))^2);

   RbRa1(i)=(X1(i+length(F1)/2-1)/X2(i+length(F1)/2-1))*(D2(i)/D1(i));

end


%Measured Reflection coefficient Face A

%First Echo full immersion

inc1=0.01;
[x1]=xlsread('Time domain spreadsheet', 'FirstEchoIni:FirstEchoEnd');
N1=8192;
F1=[-N1/2:N1/2-1]/(N1*inc1);
X1=abs(fft(x1,N1));
X1=fftshift(X1);

%First echo partial immersion

inc1p=0.01;
[x1p]=xlsread('Time domain spreadsheet', 'FirstEchoIni:FirstEchoEnd');
N1p=8192;
F1p=[-N1p/2:N1p/2-1]/(N1p*inc1p);
X1p=abs(fft(x1p,N1p));
X1p=fftshift(X1p);

fr=F1(length(F1)/2:N1);

%Reflection coefficient calculation

for i=1:length(fr)
   Ra(i)=X1(i+length(F1)/2-1)/X1p(i+length(F1)/2-1);
end

%Attenuation calculation

for i=1:length(f)
```

```
   alphaonA(i)=log(RbRa1(i)*Ra(i)*1)*1000/(2*h);
end


%Signal V(4)

%First echo

inc1=0.01;
[x1]=xlsread('Time domain spreadsheet', 'FirstEchoIni:FirstEchoEnd');
N1=8192;
F1=[-N1/2:N1/2-1]/(N1*inc1);
X1=abs(fft(x1,N1));
X1=fftshift(X1);

%Second echo

inc2=0.01;
[x2]=xlsread('Time domain spreadsheet', 'SecondEchoIni:SecondEchoEnd');
N2=8192;
F2=[-N2/2:N2/2-1]/(N2*inc2);
X2=abs(fft(x2,N2));
X2=fftshift(X2);


%Beam spreading parameters for D(s) function

a=7.14375; %(mm)
c=2607; %(m/s)
L=27.95; %(mm)
h=0.3678*25.4; %(mm)
z1=2*h+L;
z2=4*h+L;

cw=1490; %(m/s)

f=F1(length(F1)/2:N1);
for i=1:length(f)
   lambda(i)=c*1000/(f(i)*1E6); %(mm)
   lambdaw(i)=cw*1000/(f(i)*1E6); %(mm)
end

s1=(1/a^2)*(2*h)*lambda+(1/a^2)*(2*L)*lambdaw;
s2=(1/a^2)*(4*h)*lambda+(1/a^2)*(2*L)*lambdaw;

for i=1:length(s1)
```

```
   D1(i)=sqrt((cos(2*pi/s1(i))-besselj(0, 2*pi/s1(i)))^2+(sin(2*pi/s1(i))-
besselj(1, 2*pi/s1(i)))^2);
   D2(i)=sqrt((cos(2*pi/s2(i))-besselj(0, 2*pi/s2(i)))^2+(sin(2*pi/s2(i))-
besselj(1, 2*pi/s2(i)))^2);

   RbRa1(i)=(X1(i+length(F1)/2-1)/X2(i+length(F1)/2-1))*(D2(i)/D1(i));

end


%Measured Reflection coefficient Face B


%First echo full immersion

inc1=0.01;
[x1]=xlsread('Time domain spreadsheet', 'FirstEchoIni:FirstEchoEnd');
N1=8192;
F1=[-N1/2:N1/2-1]/(N1*inc1);
X1=abs(fft(x1,N1));
X1=fftshift(X1);

%First echo partial immersion

inc1p=0.01;
[x1p]=xlsread('Time domain spreadsheet', 'FirstEchoIni:FirstEchoEnd');
N1p=8192;
F1p=[-N1p/2:N1p/2-1]/(N1p*inc1p);
X1p=abs(fft(x1p,N1p));
X1p=fftshift(X1p);

%Reflection coeffiecient calculation

for i=1:length(fr)
   Rb(i)=X1(i+length(F1)/2-1)/X1p(i+length(F1)/2-1);
end

%Attenuation calculation


for i=1:length(f)
   alphaonB(i)=log(RbRa1(i)*Rb(i)*1)*1000/(2*h);
end
```

```
%Plots


figure(1)

plot(f, alphaonA, 'b', 'linewidth',2); grid on;hold on;
plot(f, alphaonB, 'r', 'linewidth',2)
xlim([0.7 1.2])
title('Real Attenuation')
xlabel('Frequency (MHz)')
ylabel('Np/m')
legend('on A','on B','Location','NorthWest')


figure(2)
plot(f, alphaonA, 'b', 'linewidth',2); grid on;hold on;
plot(f, alphaonB, 'r', 'linewidth',2)
xlim([0.7 1.2])
title('Real Attenuation')
xlabel('Frequency (MHz)')
ylabel('Np/m')
legend('on A','on B','Location','NorthWest')
```

RESIN PROPERTIES

SECTION 1 – CHEMICAL PRODUCT AND COMPANY IDENTIFICATION

PRODUCT NAME: Buehler Epothin Resin

IDENTIFICATION NUMBER: 20-8140-032 & 20-8140-128

PRODUCT USE/CLASS: Epoxy Resin

SUPPLIER:

BUEHLER, a division of Illinois Tool Works Inc.

41 WAUKEGAN ROAD

LAKE BLUFF, IL 60044

EMERGENCY: 800-424-9300

INFORMATION: 847-295-6500

PREPARER: Technical Department, 847-295-6500

PREPARE DATE: 6/08/2012, 08 June 2012

SECTION 2 – COMPOSITION/INFORMATION ON INGREDIENTS

ITEM	CHEMICAL NAME	CAS NUMBER	WT/WT%
01	Epoxy resin	25068-38-6	50 - 100
02	N-butyl glycidyl ether	2426-08-6	10 - 20
03	Trimethylolpropane triacrylate	15625-89-5	1 – 5
04	Neopentyl Glycol Diglycidyl	17557-23-2	1 - 5

SECTION 9 – PHYSICAL AND CHEMICAL PROPERTIES

BOILING RANGE:	No Data	VAPOR DENSITY:	Heavier than Air
ODOR:	Mild sweet	ODOR THRESHOLD:	No Data
APPEARANCE:	Clear pale yellow	EVAPORATION RATE:	Is slower than n-Butyl Acetate
SOLUBILITY IN H2O:	Insoluble		
FREEZE POINT:	No Data	SPECIFIC GRAVITY:	1.126
VAPOR PRESSURE:	No Data	pH @ 0.0%:	No Data
PHYSICAL STATE:	Thin liquid	VISCOSITY:	Low
COEFFICIENT OF WATER/OIL DISTRIBUTION:		No Data	

(SEE SECTION 16 FOR ABBREVIATION LEGEND)

HARDENER PROPERTIES

SECTION 1 – CHEMICAL PRODUCT AND COMPANY IDENTIFICATION

PRODUCT NAME: BUEHLER EPOTHIN HARDENER

IDENTIFICATION NUMBER: 20-8142-016, 20-8142-064, 20-8142-032

PRODUCT USE/CLASS: Epoxy hardener

SUPPLIER:

BUEHLER, a division of Illinois Tool Works Inc.

41 WAUKEGAN ROAD

LAKE BLUFF, IL 60044

EMERGENCY: 800-424-9300

INFORMATION: 847-295-6500

PREPARER: Technical Department, 847-295-6500

PREPARE DATE: 10/18/2011, 18 October 2011

SECTION 2 – COMPOSITION/INFORMATION ON INGREDIENTS

ITEM	CHEMICAL NAME	CAS NUMBER	WT/WT%
01	Polyoxyalkylamine blend	NONE - MIX	30.0-60.0
02	Nonyl phenol	25154-52-3	5.0-10.0
03	Benzene-1,3-dimethaneamine	1477-55-0	10.0-30.0
04	Substituted phenol	TRADE SECRET	10.0-30.0
05	Triethylenetetramine	112-24-3	1.0-5.0
06	Trimethylhexanediamine	3236-53-1	10.0-30.0

SECTION 9 – PHYSICAL AND CHEMICAL PROPERTIES

BOILING RANGE:	278 - 500 F	VAPOR DENSITY:	Is heavier than air
ODOR:	Ammonia-like	ODOR THRESHOLD:	No data
APPEARANCE:	Clear thin	EVAPORATION RATE:	Is slower than Butyl Acetate
SOLUBILITY IN H_2O:	Appreciable		
FREEZE POINT:	No data	SPECIFIC GRAVITY:	0.97
VAPOR PRESSURE:	No data	pH @ 0.0%:	N.A.
PHYSICAL STATE:	Liquid	VISCOSITY:	Low
COEFFICIENT OF WATER/OIL DISTRIBUTION:		No data	

(SEE SECTION 16 FOR ABBREVIATION LEGEND)

GLASS MICROSPHERES PROPERTIES

General Product Information						
	Particle Size Distribution*			Bulk Density* (lbs/cu. ft.) ASTM D-3101-78		Oil Absorption* (g oil/100g. spheres) ASTM D-1483
Product	Mean Value (microns)	Range (microns)	US Mesh Size	Untapped	Tapped	
A-GLASS						
1922	-	150 – 250	60 – 100	91	98	18
2024	-	106 – 212	70 – 140	91	98	18
2429	70 – 100	53 – 106	140 – 270	91	98	18
2530	60 – 70	45 – 90	170 – 325	91	98	18
3000	30 – 50	-	- 325	90	99	18
5000	7 – 10	-	-	80	101	20
E-GLASS						
3000E	30 – 50	-	- 325	82	100	19

*Typical Values

	A Glass Soda-Lime	E Glass Boro-Silicate
Physical:		
Specific Gravity	2.5	2.54
Refractive Index	1.51	1.55
Free Iron Content, % max	0.1	0.1
Mechanical:		
Young's Modulus, 10^6 psi	10.0	10.5
Rigidity Modulus, 10^6 psi	4.3	
Hardness (Moh)	6.0	6.5
Coefficient of Friction	0.9-1.0	1.0
Electrical:		
Dielectric Constant, 22°C, 10^6 Hz	6.9	5.8
Loss Tangent, 22°C 10^6 Hz	0.0085	0.0010
Vol. Resistivity, 25°C, ohm-cm	6.5×10^{12}	10^{13}-10^{16}
Thermal:		
Softening Point, °C	704	846
Expansion Coefficient, in/in/°C$X10^{-7}$	90	28
Thermal Conductivity (cal/(sec)(cm^2)(°C/cm)at 500°C)	0.0036	
Composition %:	A-Glass	E-Glass
SiO_2*	72.5	52.5
Na_2O	13.7	0.3
CaO	9.8	22.5
MgO	3.3	1.2
Al_2O_3	0.4	14.5
FeO/Fe_2O_3	0.2	0.2
K_2O	0.1	0.2
B_2O_3	0.0	8.6

*** No measurable free crystalline silica content as tested by ASTM C-169**

Mold Photograph.

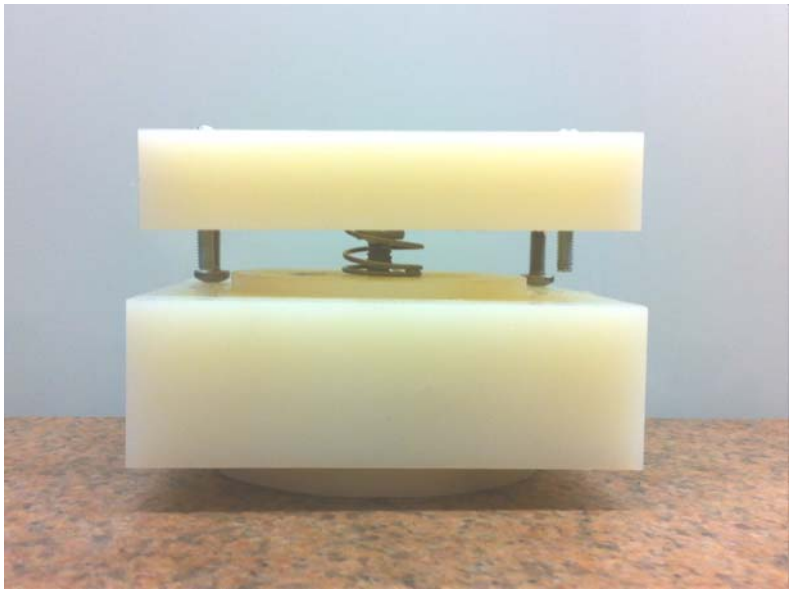

Mold rotating apparatus.

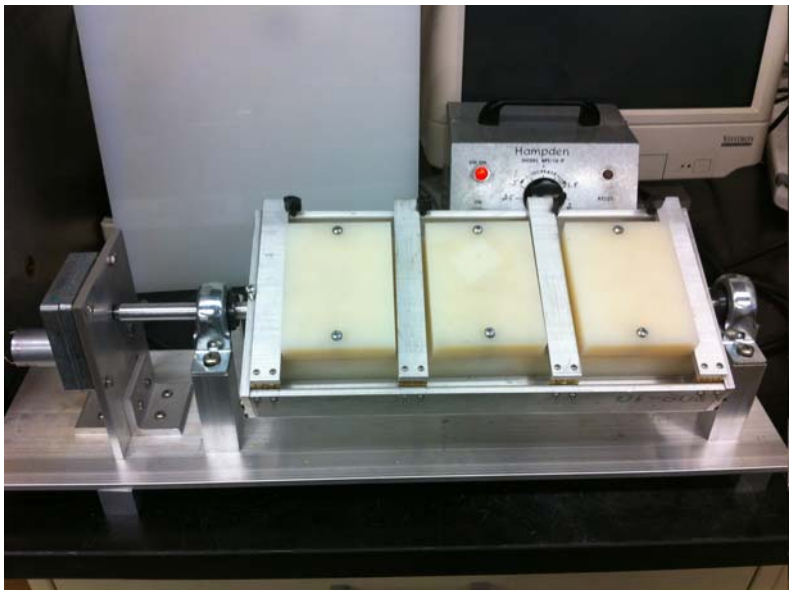

BIBLIOGRAPHY

"46876 the Pulsed Ultrasonic Velocity Method for Determining Material Dynamic Elastic Moduli : Blessing, G.V. Dynamic Elastic Modulus Measurements in Materials, ASTM STP 1045. Edited by A. Wolfenden. Pp. 47–57. American Society for Testing and Materials, Philadelphia, Pennsylvania (United States)." *NDT & E International.* Vol. 27, (1) pp. 50. (1994).

"52971 Determination of the Elastic Constants of Composite Materials from Ultrasonic Group Velocity Measurements : Niu, Lin Dissertation Abstracts International, Vol. 53, no. 7, p. 3584 (Jan. 1993) (DA9236006)." *NDT & E International.* Vol. 27, (1) pp. 45. (1994).

American Society for Nondestructive Testing.,Society for Nondestructive Testing.,. "Materials Evaluation : ME." *Materials evaluation : ME.* (1964).

Batra, N. K., and Chaskelis, H. H. "Determination of Minimum Flaw Size Detectable by Ultrasonics in Titanium Alloy Plates." *NDT International.* Vol. 18, (5) pp. 261-264. (1985).

Beltzer, A. I., and Brauner, N. "Acoustic Waves in Random Discrete Media Via a Differential Scheme." *Journal of Applied Physics.* Vol. 60, (2) pp. 538-540. (1986).

Beltzer, A. I., Bert, C. W., and Striz, A. G. "On Wave Propagation in Random Particulate Composites." *International Journal of Solids and Structures.* Vol. 19, (9) pp. 785-791. (1983).

Beltzer, A. I., and Brauner, N. "The Dynamic Response of Random Composites by a Causal Differential Method." *Mechanics of Materials.* Vol. 6, (4) pp. 337-345. (1987).

Biwa, S. "Independent Scattering and Wave Attenuation in Viscoelastic Composites." *Mechanics of Materials.* Vol. 33, (11) pp. 635-647. (2001).

Biwa, S., Idekoba, S., and Ohno, N. "Wave Attenuation in Particulate Polymer Composites: Independent scattering/absorption Analysis and Comparison to Measurements." *Mechanics of Materials.* Vol. 34, (10) pp. 671-682. (2002).

Biwa, S., Ito, N., and Ohno, N. "Elastic Properties of Rubber Particles in Toughened PMMA: Ultrasonic and Micromechanical Evaluation." *Mechanics of Materials.* Vol. 33, (12) pp. 717-728. (2001).

Biwa, S., Watanabe, Y., Motogi, S., and Ohno, N. "Analysis of Ultrasonic Attenuation in Particle-Reinforced Plastics by a Differential Scheme." *Ultrasonics.* Vol. 43, (1) pp. 5-12. (2004).

Brauner, N., and Beltzer, A. I. "High-Frequency Elastic Waves in Random Composites Via the Kramers--Kronig Relations." *Applied Physics Letters.* Vol. 46, (3) pp. 243-245. (1985).

Cerri, M., and Cusolito, R. "Experiences in Capability Assessment of Manual Ultrasonic Examination Techniques for Planar Flaw Detection and Sizing in Austenitic Stainless Steel Joints." *NDT International.* Vol. 22, (4) pp. 229-239. (1989).

Datta, S. K., ed. *Scattering by a Random Distribution of Inclusions and Effective Elastic Properties,* J. W. Proban ed. University of Waterloo press, 1978.

Davis, Julian L. *Mathematics of Wave Propagation.* Princeton University Press, 1997.

Freitas, V. L. d. A., Albuquerque, V. H. C. d., Silva, E. d. M., Silva, A. A., and Tavares, J. M. R. S. "Nondestructive Characterization of Microstructures and Determination of Elastic Properties in Plain Carbon Steel using Ultrasonic Measurements." *Materials Science and Engineering: A.* Vol. 527, (16–17) pp. 4431-4437. (2010).

Graff, Karl F. *Wave Motion in Elastic Solids.* Dover Publications, 1991.

He, P., and Zheng, J. "Acoustic Dispersion and Attenuation Measurement using both Transmitted and Reflected Pulses." *Ultrasonics.* Vol. 39, (1) pp. 27-32. (2001).

Hislop, J. D. "Flaw Size Evaluation in Immersed Ultrasonic Testing." *Non-Destructive Testing.* Vol. 2, (3) pp. 183-192. (1969).

Kanaun, S., Levin, V., and Pervago, E. "Acoustical and Optical Branches of Wave Propagation in Random Particulate Composites." *International Journal of Engineering Science.* Vol. 46, (4) pp. 352-373. (2008).

Kaye, G. W. C. and Laby, T. H. *Tables of Physical and Chemical Constants.* Longmans, 1995.

Kim, J., Ih, J., and Lee, B. "Dispersion of Elastic Waves in Random Particulate Composites." *The Journal of the Acoustical Society of America.* Vol. 97, (3) pp. 1380-1388. (1995).

Kinra, V. K., Petraitis, M. S., and Datta, S. K. "Ultrasonic Wave Propagation in a Random Particulate Composite." *International Journal of Solids and Structures.* Vol. 16, (4) pp. 301-312. (1980).

Kline, R. A. "Measurement of Attenuation and Dispersion using an Ultrasonic Spectroscopy Technique." *The Journal of the Acoustical Society of America.* Vol. 76, (2) pp. 498-504. (1984).

Kolsky, H. *Stress Waves in Solids.* Dover Publications, 1963.

Lakes, Roderic S. *Viscoelastic Solids.* CRC Press, 1998.

Lavender, J. D. "Methods for Non-Destructive Testing of Steel Forgings Part 1.—Ultrasonic Flaw Detection: British Standard BS 4124 (Part 1)." *Non-Destructive Testing.* Vol. 1, (4) pp. 251. (1968).

Layman, C., Murthy, N. S., Yang, R., and Wu, J. "The Interaction of Ultrasound with Particulate Composites." *The Journal of the Acoustical Society of America.* Vol. 119, (3) pp. 1449-1456. (2006).

Liu, Z., Oswald, J., and Belytschko, T. "XFEM Modeling of Ultrasonic Wave Propagation in Polymer Matrix particulate/fibrous Composites." *Wave Motion.* Vol. 50, (3) pp. 389-401. (2013).

Marianeschi, E., and Tili, T. "A Note on the Smallest Defect that can be Detected using Ultrasonics." *NDT International.* Vol. 16, (2) pp. 75-77. (1983).

McSkimin, H. J. *Physical Acoustics: Principles and Methods.* Academic Press, 1964.

Mobley, J., Vo-Dinh, T. "Photoacoustic method for the simultaneous acquisition of optical and ultrasonic spectra." *The Journal of the Acoustical Society of America.* ARLO Vol. 4, (3) pp. 89-94 (2003).

Mylavarapu, P., and Woldesenbet, E. "A Predictive Model for Ultrasonic Attenuation Coefficient in Particulate Composites." *Composites Part B: Engineering.* Vol. 41, (1) pp. 42-47. (2010).

Mylavarapu, P., and Woldesenbet, E. "Ultrasonic Characterization of Sandwich Core Materials." *Journal of Sandwich Structures and Materials.* Vol. 10, (5) pp. 413-428. (2008).

Nolle, A. W. "Measurement of Ultrasonic Bulk-Wave Propagation in High Polymers." *The Journal of the Acoustical Society of America.* Vol. 20, (4) pp. 587. (1948).

Papadakis, E. P., Patton, T., Tsai, Y., Thompson, D. O., and Thompson, R. B. "The Elastic Moduli of a Thick Composite as Measured by Ultrasonic Bulk Wave

Pulse Velocity." *The Journal of the Acoustical Society of America.* Vol. 89, (6) pp. 2753-2757. (1991).

Rodríguez, M. A., Ramos, A., and San Emeterio, J. L. "Location of Multiple Proximate Flaws using Perpendicular NDT Ultrasonic Arrays." *Ultrasonics.* Vol. 44, Supplement, (0) pp. e1105-e1109. (2006).

Rogers, P. H., and Van Buren, A. L. "An Exact Expression for the Lommel-Diffraction Correction Integral." *The Journal of the Acoustical Society of America.* Vol. 55, (4) pp. 724-728. (1974).

Rokhlin, S. I., and Wang, W. "Double through-Transmission Bulk Wave Method for Ultrasonic Phase Velocity Measurement and Determination of Elastic Constants of Composite Materials." *The Journal of the Acoustical Society of America.* Vol. 91, (6) pp. 3303-3312. (1992).

Rose, J. L., and Meyer, P. A. "Ultrasonic Signal Processing Concepts for Measuring the Thickness of Thin Layers." *Materials evaluation : ME.* Vol. 32, (12) pp. 249-258. (1974).

Ruiz-Reyes, N., Vera-Candeas, P., Curpián-Alonso, J., Cuevas-Martínez, J. C., and Blanco-Claraco, J. L. "High-Resolution Pursuit for Detecting Flaw Echoes Close to the Material Surface in Ultrasonic NDT." *NDT & E International.* Vol. 39, (6) pp. 487-492. (2006).

Sadd, Martin H. *Elasticity: Theory, Applications and Numerics.* Academic Press, 2009.

Scott, W. R., and Gordon, P. F. "Ultrasonic Spectrum Analysis for Nondestructive Testing of Layered Composite Materials." *The Journal of the Acoustical Society of America.* Vol. 62, (1) pp. 108-116. (1977).

Selfridge, A. R. "Approximate Material Properties in Isotropic Materials." *Sonics and Ultrasonics, IEEE Transactions on.* Vol. 32, (3) pp. 381-394. (1985).

Smith, R. E. "Ultrasonic Elastic Constants of Carbon Fibers and their Composites." *Journal of Applied Physics.* Vol. 43, (6) pp. 2555-2561. (1972).

Tauchert, T. R., and Güzelsu, A. N. "Measurements of the Elastic Moduli of Laminated Composites using an Ultrasonic Technique." *Journal of Composite Materials.* Vol. 5, (4) pp. 549-552. (1971).

Treiber, M., Kim, J., Jacobs, L. J., and Qu, J. "Correction for Partial Reflection in Ultrasonic Attenuation Measurements using Contact Transducers." *The Journal of the Acoustical Society of America.* Vol. 125, (5) pp. 2946-2953. (2009).

Turó, A., Chávez, J. A., García-Hernández, M. J., Bulkai, A., Tomek, P., Tóth, G., Gironés, A., and Salazar, J. "Ultrasonic Inspection System for Powder Metallurgy Parts." *Measurement.* Vol. 46, (3) pp. 1101-1108. (2013).

Umchid, S. "Frequency Dependent Ultrasonic Attenuation Coefficient Measurement." *The 3rd International Symposium on Biomedical Engineering.* pp. 234-238. (2008).

Vincent, A. "Influence of Wearplate and Coupling Layer Thickness on Ultrasonic Velocity Measurement." *Ultrasonics.* Vol. 25, (4) pp. 237-243. (1987).

Waterman, P. C., and Truell, R. "Multiple Scattering of Waves." *Journal of Mathematical Physics.* Vol. 2, (4) pp. 512-537. (1961).

Yamakawa, N. "Scattering and Attenuation of Elastic Waves." *Geophysical Magazine (Tokyo).* Vol. 31, pp. 63-103. (1962).

Yang, R. -. "A Dynamic Generalized Self-Consistent Model for Wave Propagation in Particulate Composites." *Journal of Applied Mechanics.* Vol. 70, (4) pp. 575-582. (2003).

Youssef, M. H., and Gobran, N. K. "Modified Treatment of Ultrasonic Pulse-Echo Immersion Technique." *Ultrasonics.* Vol. 39, (7) pp. 473-477. (2002).

Zimmer, J. E., and Cost, J. R. "Determination of the Elastic Constants of a Unidirectional Fiber Composite using Ultrasonic Velocity Measurements." *The Journal of the Acoustical Society of America.* Vol. 47, (3B) pp. 795-803. (1970).